International Pyrheliometer Comparison

pmod wrc

WORLD METEOROLOGICAL ORGANIZATION

IPC-XII

28. Sep - 16. Oct 2015

Davos, Switzerland

WMO IOM Report No. 124

2016

FOREWORD

The World Meteorological Organization (WMO) through its Members recognizes in this era of Big Data that its Members and the organization must not forget that a weather datum is the result of the processes of a measurement, and that traceable measurements are fit-for-purpose in both weather and climate work and provide environmental intelligence for government and business sector decision makers.

The Commission for Instrument and Method of Observation (CIMO) as one of the eight Technical Commission in WMO focuses its work on accurate weather measurements by promoting and facilitating international standardization and compatibility of meteorological measurement systems used by Members within the WMO Integrated Global Observing System to improve quality of products and services of Members. The CIMO mission is achieved by supporting initiatives which by coordinating collective actions by Members with respect to observing systems produce results that exceed what each Member could produce unilaterally to meet their critical needs. CIMO supports development of new measuring methods and equipment critical to Member's needs, collaborates with meteorological instrument manufacturers, the scientific community and other developers to facilitate a production of reliable instruments that are adequately tested before use, and supports capacity and capability building in developing and least developed countries to close the gap between them and the developed countries.

The organization and hosting of the WMO International Pyrheliometer Comparisons (IPCs) at the Physikalisch-Meteorologisches Observatorium Davos/World Radiation Centre (PMOD/WRC) has a long and important history. It aims at ensuring the traceability of solar radiation measurements around the world using the World Radiometric Reference (WRR) and defining suitable working references to WMO Members and instrument manufacturers. This work involves CIMO experts and is one of the core activities in which the Commission is directly involved.

The regularity of IPCs is a key to traceability of solar radiation measurements around the world using the WRR, and this report summarizes the outcomes of the 12^{th} IPC. The report demonstrates the stability of the WRR in providing a world-wide metrological reference. However, comparisons held over the last decade, and particularly since IPC-XI, have indicated that there may be a 0.3% bias between the International System of Units (SI) and WRR. As a result CIMO has established a Task Team on Radiation References to advise on whether the WRR needs to be replaced with a revised reference with zero bias to SI. The Task Team will report to CIMO in 2018, and based on that report, a recommendation may be made to the following WMO Congress. But more work is required to ensure a small but significant change is really required, as it will not only impact on future measurements but the historical record. The last significant change in the historical record was done with the introduction of the WRR on 1 January 1980 as the measurement reference for solar exposure and irradiance data records. For the 12^{th} IPC in autumn 2015, there were fewer clear sky days than in 2010 but still more than sufficient to provide a statistically significant sample of solar irradiance data.

A key serendipitous outcome of IPC-XII was through MeteoSwiss making a video with help of PMOD and the IPC participants. The video focuses on the reasons why an IPC is so important, both as a means of providing traceability, as well as information sharing amongst solar and longwave radiation measurement experts and capability building for newcomers to this form of metrology. I recommend that you view the video on the following link: https://vimeo.com/164968933. Furthermore I have heard from IPC-XII participants that they believe it was a very successful IPC, and also provided the excellent opportunity to host the 4^{th} Filter Radiometer Comparison, and the 3^{rd} Infrared Pyrgeometer Comparison. Reports of those comparisons are to be released shortly.

IPC-XII also demonstrated the continuing importance of the World Radiation Centre at PMOD in ensuring the artefacts currently required to define the WRR in the form of cavity radiometers. While it is unfortunate that two of the radiometers that are used to define the WRR will need to be restored, the progress demonstrated in developing new instruments, including the cryogenic radiometer as a method of direct traceability to SI is encouraging. However, with the help of Dr John Hickey, a veteran of solar radiation metrology and IPCs, the initial repair of the WRR HF was accomplished, and provided participating experts with significant insight into the workings of absolute radiometers.

I wish to express my sincere appreciation to all the major players during the preparation of the IPC-XII, during the intercomparisons, and when analyzing and reporting the final results. Particularly to all PMOD/WRC staff as well as the members of the Ad-hoc committee.

Prof. B. Calpini
President Commission for Instruments and Methods of Observation

WMO International Pyrheliometer Comparison
IPC-XII
28 September - 16 October 2015
Davos, Switzerland

Final Report

Wolfgang Finsterle

PMOD/WRC, Davos, June 2016
WMO IOM Report No. 124

Contents

Chapter 1 Organization and Procedures

1.1 Introduction

The 12^{th} International Pyrheliometer Comparison (IPC-XII) was held together with Regional Pyrheliometer Comparisons (RPCs) of all WMO Regional Associations (RA I to RA VI) from 28 September through 16 October 2015 at the Physikalisch-Meteorologisches Observatorium Davos/World Radiation Centre (PMOD/WRC) in Davos, Switzerland. Concurrent with the IPC-XII were held the fourth Filter Radiometer Comparisons (FRC-IV) and the second International Pyrgeometer Comparisons (IPgC-II). Results from the FRC-IV and IPgC-II will be presented in separate reports.

The results presented in this report are based on the measurements carried out during the three weeks assigned to the IPC-XII. The favorable weather conditions allowed to acquire a large number of calibration points for most participating instruments. Seminar presentations were given on days when the weather conditions did not allow taking measurements.

1.2 Participation

Representatives from 15 Regional and 15 National Radiation Centers as well as 25 manufacturers and other institutions took part in the comparison. They were represented by 111 participants from 33 countries who operated 134 pyrheliometers. The six World Standard Group (WSG) and 18 additional pyrheliometers, including the Cryogenic Solar Absolute Radiometer (CSAR), were operated by the WRC staff. See Tables 1.1 and 1.2 for a complete list of all participating centres and institutions. A representative of WMO was attending during the first couple of days of IPC-XII.

1.3 Relevance to Other International Organizations

The IPC-XII were also held as Euramet supplementary comparisons (EURAMET.PR-S6) and were open to calibration laboratories which have current CMCs for solar irradiance listed in the BIPM key comparison database (BIPM-KCDB). PMOD/WRC served as *coordinating institute* for this supplementary comparison with METAS (Switzerland) and NPL (United Kingdom) as *participating partners*. *Further partners* were VNIIOFI (Russian Federation) and NIM (China).

Table 1.1: IPC-XII Participation: *World, Regional and National Radiation Centers*

Country	*Type*	*Institution*	*Operator(s)*	*Instrument(s)*
World Radiation Center				
Switzerland	WRC	Physikalisch-Meteorologisches Observatorium Davos, World Radiation Centre, Davos	Wolfgang Finsterle Nathan Mingard Benjamin Walter Christian Thomann Ricco Soder Markus Suter Julian Gröbner Stelios Kazadzis Natalia Kouremeti André Gauderon Patrik Caspar Werner Schmutz	**PMO2** **PMO5** **CROM2L** **PAC3** **HF18748** **MK67814** NIP-31144E6 DARA A, B, C EPAC11402 CH1-970147 PMO6-79-122 PMO6-80022 AHF32455 CSAR PMO6-0401 PMO6-0801 PMO6-0803 PMO6-1105 PMO6-1106 PMO6-1107 PMO6-1111 PMO6-1112 SIAR-2A SIAR-2B PMO6-7 (on behalf of Meteoswiss, Payerene)
RA I (Africa)				
Egypt	RRC	Egyptian Meteorolgical Auth., Cairo	Mohamed Korany	AHF-31103
Nigeria	RRC	Nigerian Meteorolical Agency, Abuja, FCT	Olatokunbo Ouklaja	Å 576 CHP1-150291
South Africa	NRC	South African Weather Service, Pretoria, Gauteng	Lucky Ntsangwane Katlego Ncogwane Brighton Mabasa	AHF 31109 PMO6-850404 Linke-700198

Table 1.1: (continued)

Country	*Type*	*Institution*	*Operator(s)*	*Instrument(s)*
RA II (Asia)				
China	NRC	CMA, Beijing	Yang Yun Ding Lei Chong Wei Ren Zhihua Jin Qi	PMO6-850406 PMO6-0808 AHF 36011
India	RRC	Indian Meteorological Dept., Central Radiation Laboratory, Pune, Maharashtra	Anjit Anjan	AHF 18742
Japan	RRC	JMA, Tokyo	Nozomu Ohkawara Osamu Ijima	PMO6-0403 AHF-37815
Republic of Korea	NRC	Korea Meteorological Administration, Seoul	Yong-June Park Il-sung Zo	AHF-36014
Saudi Arabia	NRC	K.A.CARE, Riyadh	Hussain Shibli Naif Alsaheel	AHF-30110 AHF-31107
Thailand	NRC	Thai Meteorological Department, Bangkok	Pisood Promsut	HF 27796
RA III (South America)				
Argentina	RRC	Servicio Meteorologico Nacional, Buenos Aires	Gerardo Carbajal Benítez	AHF-30112
Chile	RRC	Dirección Meteorológica Chile, Santiago	Luis Valdés	PMO6-850410
RA IV (North America, Central America and the Caribbean)				
Mexico	RRC	Instituto de Geofísica, UNAM México, DF	David Riveros Hector Estevez	HF 29223 PMO6-1102
USA	RRC	NOAA/ESRL/GMD, Boulder	Donald Nelson Jim Wendell Emiel Hall	HF 28553 AHF 14917 AWX-32448 AWX-31114 AHF 30710 AHF 28553 TMI 67502 sNIP-37881 sNIP-37909

Table 1.1: (continued)

Country	*Type*	*Institution*	*Operator(s)*	*Instrument(s)*
RA V (South-West Pacific)				
Australia	RRC	Bureau of Meteorology, Melbourne	Bruce Forgan Michael Milner	HF 27160 TMI 69137
RA VI (Europe)				
Austria	NRC	ZAMG, Vienna	Martin Mair Marc Olefs	A15192 TMI 68025 CHP1 100245
Belgium	RRC	Royal Meteorological Institute, Uccle	André Chevalier Steven Dewitte Christian Conscience Stijn Nevens	CR05R
Croatia	NRC	DHMZ, Zagreb	Krunoslav Premec	CH1 940072 CHP1 100288 PMO6-1109
Czech Republic	NRC	Czech. Hydromet. Institute, Hradec Kralove	Jiri Pokorny	AHF 30497
Estonia	NRC	Estonian Environment Agency, Toravere	Kristjan Nurmela	PMO6-850405
France	RRC	Météo-France-Centre Radiométrique, Carpentras, Vaucluse	Thierry Duprat	PMO6-0810
Germany	RRC	DWD Met. Obs. Lindenberg, Tauche OT Lindenberg	Klaus Behrens Ralf Becker	HF 27157 PMO6-5 PMO6-0405
Hungary	RRC	Hungarian Met. Service, Budapest	Zlotàn Tòth	HF 19746
Israel	NRC	Israel Meteorological Service, Bet Dagan	Alexander Baskis	HF 27162
Lithuania	NRC	Lithuanian HMS, Vilnius	Darius Mikalajunas	PMO6-0804
Russian Federation	RRC WRDC	Voeikov MGO, St. Petersburg	Alexander Pavlov Dmitrii Frolov	PMO6-0817
Slovakia	NRC	SHMI, Poprad-Ganovce	Anna Pribullova	AHF-37814 A13439

Table 1.1: (continued)

Country	*Type*	*Institution*	*Operator(s)*	*Instrument(s)*
Spain	NRC	AEMET, Madrid	Irene Melero-Asensio Ana Díaz-Rodríguez Juan Moreta-González	PMO6-0105 PMO6-0404
Sweden	RRC	SMHI, Norrköping	Thomas Carlund	PMO6-811108 AWX 33393
The Netherlands	NRC	KNMI, De Bilt	Wouter Knap Cor van Oort Tiemo Mathijssen	HF-27159 CH1-040380 CH1-020283
United Kingdom of Great Britain and Northern Ireland	NRC	Met Office, Exeter, Devon	Jonathan Tamlyn Thomas Dent-Jones Sarah Fotheringham	AHF-31110 AHF-37813

Table 1.2: IPC-XII Participation: *Various Institutions and Manufacturers*

Country	*Institution*	*Participant(s)*	*Instrument(s)*
Argentina	Universidad Nacional de Luján	Adrián Jorge Roldán	TMI-67605
Chile	Fundacion Fraunhofer Chile Res, Santiago	Alan Pino Rodrigo Escobar Cristián Cortés Marcelo Selgado	CHP1-100378 CHP1-100384 CHP1-100385
China	CIOMP, Changchun, Jilin	Wei Fang Yupeng Wang Hongrui Wang Yang Luo	SIAR-2C SIAR-4A SIAR-4B SIAR-4D
Canada	COFOVO Energy, Ottawa, ON	Viktar Tatsiankou	SolarSIM-D1-SN102 SolarSIM-D1-SN103 SolarSIM-D1-SN112 SolarSIM-D1-SN113
Germany	PTB, Braunschweig	Stefan Winter Dirk Friedrich	PMO6-1104 CMP22-140007 CMP22-140044 CMS-849335 SHP1V-130042
Germany	Black Photon Instrument, Freiburg	Joachim Jaus	MS56-P13027

Table 1.2: (continued)

Country	*Institution*	*Participant(s)*	*Instrument(s)*
Germany	PV Performance Labs, Freiburg	Anton Driesse	-
Italy	European Commission JRC, Ispra, Varese	Willem Zaaiman Roberto Galleano Germana Trentadue	PMO6-81109 PMO6-911204 NIP-21451E6 NIP-23927E6 NIP-25738E6 NIP-26626E5 CH1-060460 CH1-930018 CH1-040370 CHP1-110533 MS56-12036 MS56-12039 TMI 68835
India	NIWE, Chennai, Tamil Nadu	Karthik Ramanathan	PMO6-1110 AHF-36766
Japan	EKO Instruments CO., Ltd., Tokyo	Akihito Akiyama William Beuttell Kazunori Shibayama Kees Hoogendijk	PMO6-850402 PMO6-0816 MS56-P12023
Japan	Ishikawa Trading Co., Ltd., Tokyo	Kazuhiko Ohkubo Kotaro Makino Keiji Ishikawa Yanqun Xue	IRS02-1504 AHF-33396
Russian Federation	VNIIOFI, Moscow	Svetlana Morozova Mariia Pavlovich	MAR-1-3 MAR-1-4
Sweden	SP Swedish National Testing and Research Institute, Borås	Stefan Källberg Anne Andersson	HF 15744
South Africa	GeoSUN Africa, Stellenbosch	Anro le Roux Sophie Mulaudzi	AHF-31117
Spain	CIEMAT, Madrid	Jose Balenzategui	AHF 28486 PMO6-0301 NIP-35356E6
Taiwan POC	National Central University, Taoyuan City	Sheng-Hsiang Wang	CHP1-100304 AHF-31102

Table 1.2: (continued)

Country	*Institution*	*Participant(s)*	*Instrument(s)*
Thailand	Silpakorn University, Nakhon Pathom	Serm Janjai Somchit Janjai Somjet Pattarapanitchai Sumaman Buntoung Pranomkorn Choosri	AHF 36013
The Netherlands	Hukseflux Thermal Sensors, Delft	Kees van den Bos Dorine van der Vlies Eric Hoeksema Bart van der Meer	DR01-8348 DR01-8377 DR02-9191 DR02-9210 DR02-9212 DR04-13001 DR04-13002 CP
The Netherlands	Kipp & Zonen BV, Delft	Ilja Staupe Marc Korevaar Joop Mees	PMO6-0103 CHP1-090127 CHP1-121042 CHP1-REF2 SHP1-110005
USA	Argonne National Lab, Billings OK	Craig Webb	AHF-28968
USA	ATLAS-DSET Laboratories, Phoenix AZ	Duncan Maciver	AHF 17142 AHF-28556
USA	NASA Langley, Hampton VA	Fred Denn	AHF 31041 AHF 31105
USA	National Renewable Energy Lab., Golden CO	Ibrahim Reda Afshin Andreas	AHF 23734 AHF 28968 AHF 29220 AHF 30713 TMI 68018
USA	The Eppley Laboratory Inc., Newport RI	John Hickey Tom Kirk	AHF 14915 AHF 27798 sNIP-37441E6
USA	ISO-CAL North America, LCC, Phoenix AZ	Erik Naranen	AHF-37816 AHF-28560
USA	Campbell Scientific, Inc., Logan UT	Matthew Perry Ajay Singh	-

1.4 Data Acquisition and Evaluation

The signals from the WSG instruments and additional WRC radiometers were acquired by a data acquisition system based on 18 National Instruments PXI-4065 6.5-digit digital multimeters with NI PXI-2501 24-channel multiplexers. The system was controlled by a LabView application ("DAQ2010") running on an industrial PC and operated flawlessly. A separate LabView application triggered the aural and visual timing signals on the measurement field as well as the initialization and readout of the data entry forms for manually operated instruments (see below). This system is very robust and flexible, allowing to add/remove pyrheliometers without need to re-initialize the software and to analyze and visualize the measurements in near-real-time.

The participating pyrheliometers were operated with their standard pointing and data acquisition equipment, either manually or automated.

The data from the manually operated instruments were typed into a java based web interface by the operator. WLAN connections were used to initialize the web interface and to upload its content to the central data acquisition computer at end of each measurement series. Laptop computers have been provided by the WRC, if needed. Written records were kept for backup purposes and to double-check for typing errors in the web interface.

Computer controlled data acquisition systems had to run on CET (Central European Standard Time) and be synchronized to the basic measurement cadence (see below). A dedicated directory on the FTP server was provided for uploading the measurements. The prescribed file naming and format convention with three columns corresponding to date, time, and irradiance was observed by most participants. All data were ingested into the data acquisition and evaluation system at the end of each measurement day.

1.4.1 Timing of the Measurements

The measurements were taken in series of 21 minutes with a basic cadence of 90 seconds. The starting time of each series was either on the full hour or the minute xx:30. Where needed, electrical calibrations and/or zero readings were completed *before* the starting time[1]. Voice announcements and acoustic signals together with a visual indicator on the measurement field informed the participants about the starting times and progress of the measurement series'. A network time server or a digital reference clock on the measurement field could be used to synchronize all data acquisition systems. The time until the next measurement was also indicated on the web interface for manual operators. The timing for the each type of instrument was as follows[2]:

- Ångström pyrheliometers: Before the start and after the end of the run the zero of the instrument was established. Alternating right and left strip readings were performed, starting with the right hand strip exposed to the sun. The following readings were paired as L-R, R-L, etc., yielding a total of 12 irradiance values per series.

- PAC3: the calibration phase started with the shutter closed and the electrical heater[3] switched on for 40 seconds (this was introduced after IPC-III in order to have a well defined thermal state of the instrument independent of the operation sequence before the run). The zero of the thermopile was read 90 seconds after the heater had been switched off again. Then the heater was switched on for another 90 seconds before the heater voltage, current and the thermopile

[1]Manually operated radiometers which were using the web interface for submitting the data started their calibration sequence and/or zero reading on the starting time of the series. Hence they acquired slightly fewer irradiance readings per series.

[2]This timing scheme applies to all WRC radiometers and radiometers that were connected to the WRC data acquisition system. Radiometers which were controlled by their own computer may have deviated partly from this scheme.

[3]The heater voltage was manually selected before each series to match the expected level of solar irradiance.

signal were read. The calibration sequence ends with the shutter open command 90 seconds before the starting time of the series. Each series produced 14 irradiance readings at 90-second cadence. After the last reading the shutter was closed.

- HF- and TMI-type pyrheliometers: the calibration phase started with the shutter closed, after 90 seconds the thermopile zero was read and the electrical heater[3] turned on during 90 seconds. At the end of the heating phase the heater voltage, current and thermopile signal were read. The calibration sequence ends with the shutter open command, 90 seconds before the starting time of the series. Each series produced 14 irradiance readings at 90-second cadence (11 irradiance readings via the web interface). After the last reading the shutter was closed.

- PMO-, SIAR- and CROM-type pyrheliometers: The measurements started with a reference phase (shutter closed) of 90 seconds, followed by a measurement phase (shutter open) of 90 seconds. The closed and open heater voltage and current are read at the end of each reference or measurement phase. This reference/measurement sequence was repeated seven times, followed by an additional reference phase, yielding 7 open and 8 closed readings during each run (6 open and 7 closed via the web interface). PMO2 was read at twice that pace, with a reference phase of 45 seconds and a measurement phase of 45 seconds, producing 13 irradiance values per series. Note that for PMO2 the *open* heater current and voltage were read 6 times in rapid succession (200 ms cadence) to assess the atmospheric stability.

- Field pyrheliometers with thermopile sensor (NIP, CHP1, MS56, DR0x, etc.): These pyrheliometers started with a zero reading 90 seconds before the starting time of the series, followed by the shutter open command. The thermopile signal was then recorded every 90 seconds, yielding 14 irradiance readings (13 irradiance readings via web interface).

- Other pyrheliometers: Prototype instruments (e.g. CSAR) were using various modes of operation which are specific to their design but were synchronized to the 90-seconds base cadence.

1.4.2 Data Evaluation

For each instrument the irradiance was calculated according to the appropriate evaluation procedure as listed below. After each day a graphical print-out of the ratios to PMO2 was put on display in the "Carl Dorno" room at Hotel Seehof to be reviewed by the participants. This simple but effective measure of quality control revealed instrumental problems in several cases which subsequently could be fixed quickly.

"Quick-look" print-outs were also produced at any time during the measurement day when an instrument was suspected to malfunction.

The procedure used to calculate the irradiance *S* of each instrument type is described below. The notations are:

V_{th}	output of the thermopile
U_h, U_i	voltage across the heater (index h) or across the standard resistor (index i)
R_n	standard resistor (For PMOx-type radiometers R_n is often included in C_1.)
C_1	calibration factor (see Table 2.2)
C_2	correction factor for lead heating (see Table 2.2)
P	electrical power in the active cavities

- Ångström-pyrheliometers: the current through the right or left strip was measured as voltage drop across a standard resistor and the irradiance was obtained as:

$$S = C_1 \frac{U_i(\text{left}) U_i(\text{right})}{R_n^2}$$

This corresponds to the geometric mean of the irradiances at the time of right and left readings. Thus, the ratio to WRR was calculated using the geometric mean of the WSG irradiances at the corresponding instances.

- PAC3, HF, and TMI type pyrheliometers: the irradiance was calculated from the thermopile output V_{th}(irrad) when the receiver was irradiated. The sensitivity was determined by the calibration during which the cavity was shaded and electrically heated and U_h and U_i were measured together with the corresponding thermopile output V_{th}(cal). Furthermore, the zero of the thermopile V_{th}(zero) was measured and subtracted from all thermopile readings.

$$S = C_1 \frac{V_{th}(\text{irrad}) - V_{th}(\text{zero})}{V_{th}(\text{cal}) - V_{th}(\text{zero})} \frac{U_i}{R_n} \left(U_h - \frac{U_i}{R_n} C_2 \right)$$

- PMO-, SIAR- and CROM-type pyrheliometers: the irradiance was obtained from P(closed) averaged from the closed values before and after the open reading P(open).

$$S = C_1(P(\text{closed}) - P(\text{open}))$$

The power calculation was done according to the prescription of the instrument type with

$$P = U_h^2 \qquad \text{or} \qquad P = U_h U_i \qquad \text{or} \qquad P = U_h \frac{U_i}{R_n}$$

The SIAR-type radiometers slightly deviate from this scheme in that they subtract the open power from the *preceding* closed power rather than the average of the preceding and successive closed reading.

- Field Pyrheliometers with thermoplie sensor: the thermopile reading was divided by the calibration factor after subtraction of the zero point reading[4].

- PMO2: As during preceding IPCs, PMO2 was used as the reference instrument for the daily summaries because it can be operated fast enough to provide an irradiance value every 90 seconds. The values of PMO2 were obtained with the algorithm for PMO-type pyrheliometers. At the end of the open phase, 6 readings were taken in rapid succession within 1 second. The standard deviation of the 6 readings was used during the final evaluation as a quality control parameter to assess the atmospheric stability during each acquisition sequence (see Sect. 2.1).

1.4.3 Auxiliary Data

The meteorological parameters (air temperature, relative humidity, atmospheric pressure) were obtained from the MeteoSwiss' automated weather station SwissMetNet located at PMOD/WRC (see Sect. 4.5). Wind speed and direction sensors were set up at the south and west corners of the measuring field as well as at the WSG tracker.

A cloud sensor flagged all data points when clouds were within 15 degrees of the Sun. The flagged points were not used to evaluate Ångström type pyrheliometers.

Precision Filter Radiometers (PFR) were used to determine Aerosol Optical Depth (AOD) at four wavelengths (367.6 nm, 412.0 nm, 501.2 nm, and 862.4 nm, see Sect. 4.2).

[4]Some operators assumed a vanishing zero signal. They did not perform zero readings.

1.5 Approvement and Dissemination of the Results

According to Resolution 1 of CIMO-XI an Ad-hoc Group was established to discuss the preliminary results of the IPC-XII, based upon criteria defined by the WRC, evaluate the above reference and recommend the updating of the calibration factors of the participating instruments. It was chaired by Bruce W. Forgan, (Australia, RA V) and composed as follows: Lucky Ntsangwane (South Africa, RA I), Anjit Anjan (India, RA II), Nozomu Ohkawara (Japan, RA II), Gerardo Crabajal Benítez (Argentina, RA III), David Riveros (Mexico, RA IV), Don Nelson (USA, RA IV), Thomas Carlund (Sweden, RA VI), Klaus Behrens (Germany, RA VI). The WRC was represented by Wolfgang Finsterle.

The procedures used to compute the new WRR factors of the WSG and participating instruments are explained in Section 2.2.

Chapter 2 Irradiance Measurements and Results

Measurements were taken on 11 days (2015 September 28 - 30, October 1 - 3, 5, 9, 10, 12, and 14). October 8^{th} and 12^{th} were the most productive days, each yielding 17 series' of 21 minutes duration. In total 164 series' were acquired. All data from October 2^{nd} and 5^{th} were rejected due to bad or unstable weather conditions on those days. Of the remaining 9 days all data points that satisfy the following data selection criteria were considered in the final evaluation, resulting in 578 valid irradiance readings for the WRR.

2.1 Data Selection Criteria for the Final Evaluation

The Ad-hoc Group responsible for the approval of the final evaluation procedure (c.f. Sect. 1.5) agreed on the following criteria for the acceptance of IPC-XII data:

1. Any series or part there-of in which the field of view of Ångström pyrheliometers is obscured by local topographic features (e.g. mountain sides) shall not be considered as valid data for the evaluation of the affected instruments.
2. That no measurements be used for Ångström pyrheliometers if a cloud is within 15 degrees of the sun. No measurements will be used for the absolute cavity radiometers (field of view = 5 degrees) if a cloud is within 8 degrees of the sun.
3. That no measurements be used if the wind speed is greater than 2.5 m/s.
4. That no data be used if the 500 nm AOD is greater than 0.120.
5. That an individual point be excluded from the series if the standard deviation of the solar irradiance in a 1-second period is greater than 1 Wm^{-2} (based on the 6 fast readings by PMO2).
6. That an individual point be excluded if it is not in a contiguous stretch of 6 valid points.
7. That the minimum number of acceptable data points be 150 for the PMO2 taken over a minimum of three days during the comparison period.
8. The temporal derivative of the circumsolar measurements (provided by Black Photon) must not exceed 2 mV/s, which corresponds to ≈ 0.6 Wm^{-2}/s.

2.2 Computation of the New WRR Factors

2.2.1 WSG Instruments

The WRR factor $WRR_{i,IPC}$ for the WSG instrument i, $i \in \{$PMO2, CROM2L, MK67814, HF18748, PAC3, PMO5$\}$, by definition is the ratio of the WRR to the WSG instrument i averaged over the duration of the IPC:

$$WRR_{i,IPC} = \left\langle \frac{WRR(t)}{WSG_i(t)} \right\rangle_t ,$$

where $WRR(t)$ is the reference irradiance and $WSG_i(t)$ irradiance measured by WSG instrument i at the time t, and $\langle x(t)\rangle_t$ denotes the temporal average of $x(t)$. The reference irradiance (WRR) is defined as the mean value of the simultaneous readings of at least four WSG instruments, multiplied by their corresponding WRR factors from the previous IPC. Because the ratios of MK67814 and HF18748 with respect to the WRR were unstable during the past five years these two instruments were not used to compute the reference irradiance during IPC-XII. With the help from the manufacturer (Eplab) and other experts HF18748 and MK67814 could be cleaned and fixed and will be considered to transfer the WRR for the coming inter-IPC period. With $j \in \{$PMO2, CROM2L, PAC3, PMO5$\}$ we calculate the reference irradiance as

$$WRR(t) = \langle WSG_j(t) * WRR_{j,\mathsf{IPC-XI}}\rangle_j \,.$$

We thus get

$$WRR_{i,\mathsf{IPC-XII}} = \left\langle \frac{\langle WSG_j(t) * WRR_{j,\mathsf{IPC-XI}}\rangle_j}{WSG_i(t)} \right\rangle_t ,$$

where $i \in \{$PMO2, CROM2L, MK67814, HF18748, PAC3, PMO5$\}$ and $j \in \{$PMO2, CROM2L, PAC3, PMO5$\}$.

2.2.2 Participating Instruments

For each participating instrument k the new WRR factor is calculated according to

$$WRR_{k,\mathsf{IPC-XII}} = \left\langle \frac{WRR(t)}{Irr_k(t)} \right\rangle_t ,$$

where $Irr_k(t)$ is the irradiance measured by the instrument k at the time t and $WRR(t)$ the reference irradiance at time t.

Temporal averaging is done by fitting a gaussian to the distribution of WRR-to-instrument ratios. Outliers are sucessively removed until the ratios are normally distributed with a probability higher than 90%, or until all ratios are within a certain range of their arithmetic mean value[1].

The new WRR factors for the WSG and all participating instruments are listed in Table 2.2.

2.3 Status of the WSG and Transfer of the WRR

The main objective of the periodic IPCs is the dissemination of the World Radiometric Reference (WRR) in order to ensure worldwide homogeneity of solar radiation measurements. The WRR is realized by the World Standard Group (WSG) at PMOD/WRC, which is frequently inter-compared to detect possible deviations of individual WSG-radiometers with respect to the group average and to ensure the stability of the WRR. In addition to this *internal* stability check the stability of the WRR is assessed during IPCs by comparing the WSG to other pyrheliometers that have participated in previous IPCs.

Since IPC-XI, which was held in 2010, two member instruments of the WSG failed in internal stability checks. The instrument HF18748 produced unstable irradiance readings throughout most of the last inter-IPC period. The sensitivity of MK67814 also dropped gradually starting in 2014. Non-intrusive checks of both instruments did not reveal any contamination in their cavities. However, during IPC-XII both instruments were opened by the manufacturer (Eplab) and other experts and

[1] This threshold range ususally is ± 0.002 for cavity pyrheliometers. However, for most Ångströms, NIP's and some cavities a different range had to be chosen manually in order to make the most plausible selection of data points.

Table 2.1: New WRR-factors for the WSG instruments computed using PMO2, PMO5, CROM2L, and PAC3 and the IPC-XI WRR-factors.

Instrument	*WRR factor IPC-XI*	**WRR Factor IPC-XII**	*Standard Uncertainty* $\frac{\sigma}{\sqrt{N-1}}$ *[ppm]*	*# of points N*	*Relative Change of WRR Factor [ppm]*
PMO2	0.998623	**0.998189**	33	576	-435
PMO5	0.999052	**0.999395**	22	578	343
CROM2L	1.003157	**1.003118**	21	578	-39
MK67814	1.000458	**1.001702**	76	566	1244
PAC3	1.002117	**1.002190**	23	576	73
HF18748	0.997138	**0.998258**	47	578	1120

thoroughly cleaned, including the cavities. After the cleaning, both instruments appeared to have recovered and performed reasonably stable over the remaining two days of the IPC-XII. Nevertheless, they were not considered for the calculation of the new WRR but will hopefully help to transfer the WRR to the next IPC.

The remaining four WSG instruments (PMO2, PMO5, CROM2L, PAC3) did not show any irregularities and are thus considered stable over the past five years. The new WRR is calculated based on the average readings of these four radiometers.

Table 2.2: The new WRR factors for the participating instruments

Instrument	C_1	C_2	R_n Ω	**WRR Factor**	σ ppm	*N*	*Country/ Owner*
A13439	4426.32		1000	**1.003456**	1356	272	Slovakia
A-15192	4494.95			**1.030413**	6019	497	Austria
A576	5885.13		1000	**0.990848**	5360	70	Nigeria
ADARA-B	5000			**1.072267**	5064	527	WRC
ADARA-C	5000			**1.105435**	7244	519	WRC
AHF-0000	2.0355			**1.000307**	863	516	JRC Italy
AHF-14915	20010			**0.999542**	942	474	Eppley USA
AHF-14917	2			**0.997900**	684	507	NOAA USA
AHF-17142	19982	0.06648		**0.997946**	676	370	ATLAS-DSET USA
AHF18742	20089.26	0.066	10000	**1.004506**	2801	310	India
AHF-23734	2.002			**0.998187**	608	523	NREL USA
AHF-27798	20020			**0.998654**	1037	473	Eppley USA
AHF-28486	2.001			**0.997318**	629	280	Spain
AHF-28553	19986			**0.997739**	630	498	NOAA USA
AHF-28556	1.999	0.066		**0.995408**	913	327	ATLAS-DSET USA
AHF-28560	2.0028	0.06648		**0.999283**	1855	346	ISO-Cal North America USA
AHF-28968	19980.2			**0.997629**	630	519	ARM/SGP USA
AHF-29220	19999			**0.997485**	619	523	NREL USA
AHF-29223	19998			**1.003219**	768	198	Mexico
AHF-30110	1.9999			**1.063471**	801	346	KACARE Saudi Arabia

Table 2.2: (continued)

Instrument	C_1	C_2	R_n Ω	**WRR Factor**	σ ppm	N	*Country/ Owner*
AHF-30112	19936.7			**1.010501**	2428	173	Argentina
AHF-30710	19999			**1.000970**	874	512	NOAA USA
AHF-30713	19989			**0.997231**	637	525	NREL USA
AHF-31041	19999.2			**0.996394**	689	484	NASA Langley USA
AHF31102	1.99992	0.066	1000	**1.046871**	2278	222	Taiwan
AHF31103	19989	0.066	10000	**0.999345**	1056	353	Egypt
AHF-31105	1.9989			**0.998657**	732	486	NASA Langley USA
AHF-31107	1.99892			**1.047428**	796	254	KACARE Saudi Arabia
AHF-31109	1.9989	0.066	10000	**0.997798**	1035	282	South Africa
AHF-31110	19989	0.066		**0.997038**	668	495	United Kingdom of Great Britain and Northern Ireland
AHF-31117	1.9989			**0.999042**	706	489	GeoSUN South Africa
AHF32455	20009.2			**1.001380**	641	574	WRC
AHF-33396	1.9988			**0.997184**	947	487	AIST Japan
AHF-36011	1.99737			**1.000005**	597	436	China
AHF-36013	1.9925			**0.999802**	738	326	Silpakorn University Thailand
AHF-36014	1.99452			**1.001494**	647	446	Republic of Korea
AHF-37813	1.9979			**1.000461**	689	490	United Kingdom of Great Britain and Northern Ireland
AHF-37814	2.013			**1.001054**	605	282	Slovakia
AHF-37815	20011	0.066		**0.998679**	697	500	Japan
AHF-37816	1.9998	0.06648		**0.999458**	721	248	ISO-Cal North America USA
AWX-31114	1.99892			**1.001209**	691	488	NOAA USA
AWX-32448	1			**0.999986**	736	395	NOAA USA
AWX-33393	2.0009			**0.999885**	692	395	Sweden
CH1-020283	4.06			**0.993817**	1216	482	KNMI The Netherlands
CH1-040370	10.48			**0.998163**	2080	559	JRC Italy
CH1-040380	10.35			**0.995440**	1768	491	KNMI The Netherlands
CH1-050392	9.62			**1.010948**	981	561	ISAC-CNR Italy
CH1-060460	10.07			**1.004748**	1382	556	JRC Italy
CH1-930018	10.85			**1.001234**	2348	562	JRC Italy
CH1-940072	10330			**1.009321**	1932	433	Croatia
CHP1-090127	7.68			**1.001437**	1257	155	K&Z The Netherlands
CHP1-100245	7.83			**1.001156**	1281	513	Austria
CHP1-100304	7.79			**0.998409**	1511	356	Taiwan
CHP1-100378	7.89			**1.012082**	1859	458	Fraunhofer Chile
CHP1-100384	7.79			**1.007443**	2683	496	Fraunhofer Chile

Table 2.2: (continued)

Instrument	C_1	C_2	R_n Ω	**WRR Factor**	σ ppm	N	*Country/ Owner*
CHP1-100385	8.17			**1.013669**	1574	457	Fraunhofer Chile
CHP1-110533	7.8			**0.998562**	2315	563	JRC Italy
CHP1-110597	8.02			**0.995972**	1714	460	Fraunhofer Chile
CHP1-121042	7.63			**1.000769**	1488	328	K&Z The Netherlands
CHP1-150291	7.64			**1.000044**	1366	181	Nigeria
CHP1-REF2	7.94			**1.004987**	871	326	K&Z The Netherlands
CMP-22-140007	1			**0.901274**	20575	323	PTB Germany
CMP-22-140044	1			**0.916539**	22764	410	PTB Germany
CMS-849335	1			**1.403575**	36626	139	PTB Germany
CP	1			**0.879740**	9846	34	Hukseflux The Netherlands
CR05R	1			**0.997946**	1975	135	Belgium
CROM2L	127.687			**1.003118**	532	578	WRC
CSAR	1			**1.002100**	1249	247	WRC
DARAAREFB	1			**1.002895**	1235	117	WRC
DR01-8348	1			**0.106812**	1697	357	Hukseflux The Netherlands
DR01-8377	1			**0.081904**	1311	356	Hukseflux The Netherlands
DR02-9191	1			**0.084729**	1127	354	Hukseflux The Netherlands
DR02-9210	1			**0.093140**	1789	358	Hukseflux The Netherlands
DR02-9212	11.46			**0.982034**	1153	304	Hukseflux The Netherlands
DR04-13001	1			**0.118583**	1146	351	Hukseflux The Netherlands
DR04-13002	1			**0.105306**	1701	357	Hukseflux The Netherlands
EPAC	10024			**1.036229**	11271	285	WRC
HF-15744	20020			**0.998201**	689	282	SP Sweden
HF18748	19989	0.07		**0.998258**	1139	578	WRC
HF19746	19991.5	0.066	1000	**1.000021**	1096	266	Hungary
HF-27157	20037.6			**0.999084**	936	456	Germany
HF-27159	20030			**0.999438**	634	477	KNMI The Netherlands
HF-27160	20030			**0.997425**	625	515	Australia
HF27162	20020	0.066	1000	**0.999543**	1287	191	Israel
HF27796	19986.1	0.066	1000	**0.996033**	1459	271	Thailand
HF-30497	19943.8			**0.999590**	600	483	Czech Republic
IRS02-1504	1			**0.991175**	5447	297	AIST Japan
LINKE-700198	51.214			**1.000992**	4795	287	South Africa
MAR-01-03	1			**0.999953**	595	394	VNIIOFI Russian Federation

Table 2.2: (continued)

Instrument	C_1	C_2	R_n Ω	**WRR Factor**	σ ppm	N	*Country/ Owner*
MAR-01-04	1			**0.999536**	761	395	VNIIOFI Russian Federation
MK67814	10007			**1.001702**	1796	566	WRC
MS56-12036	1			**0.982223**	7424	536	JRC Italy
MS56-12039	1			**0.998848**	5528	557	JRC Italy
MS56-P12023	1			**1.022350**	1429	547	EKO Japan
MS-56-P13027	8.486			**0.995881**	2123	264	Black Photon Germany
NIP-21451E6	8.42			**1.005957**	6949	559	JRC Italy
NIP-23927E6	1			**1.000885**	7207	554	JRC Italy
NIP-25738E6	7.92			**0.991889**	6275	540	JRC Italy
NIP-26626E6	1			**1.000334**	4504	550	JRC Italy
NIP-31144E6	8.04			**0.996836**	4753	561	WRC
NIP-35356E6	1			**1.011018**	2691	234	CIEMAT Spain
PAC3	9962.6	0.07		**1.002190**	552	576	WRC
PMO2	600.1634			**0.998189**	798	576	WRC
PMO5	2565.14			**0.999395**	518	578	WRC
PMO6-0103	51183.3			**0.997916**	583	177	Kipp and Zonen The Netherlands
PMO6-0105	51065.4			**1.001409**	642	323	AEMET Spain
PMO6-0105-90	51065.4			**1.001215**	670	107	AEMET Spain
PMO6-0301	51161.5			**1.000183**	792	381	Spain
PMO6-0401	50000			**1.020799**	465	563	WRC
PMO6-0403	50489.5			**0.999753**	597	414	Japan
PMO6-0404	51237			**0.998208**	650	307	AEMET Spain
PMO6-0404-90	51237			**0.998593**	562	101	AEMET Spain
PMO6-0405	50927			**0.999265**	635	469	Germany
PMO6-0801	1			**1.053402**	751	70	WRC
PMO6-0803	51221			**1.000335**	522	542	WRC
PMO6-0804	51397.2			**0.999908**	609	357	Lithuania
PMO6-0808	50479			**0.999421**	679	430	China
PMO6-0810	50950.9			**0.999918**	548	418	France
PMO6-0816	50989.1			**0.999947**	1688	338	EKO Japan
PMO6-0817	51106.3			**0.999516**	624	312	Russian Federation
PMO6-1102	51295.5			**0.999389**	1462	215	Mexico
PMO6-1104	51231.89			**1.000194**	575	441	PTB Germany
PMO6-1105	1			**1.025664**	517	565	WRC
PMO6-1106	1			**1.027588**	605	542	WRC
PMO6-1107	1			**1.024318**	596	549	WRC
PMO6-1109	51250.1			**0.998732**	990	277	Croatia
PMO6-1111	1			**1.023764**	516	561	WRC
PMO6-1112	1			**1.028274**	614	547	WRC
PMO6-5	50865.1			**0.998288**	690	466	Germany
PMO6-7	1			**0.999681**	845	474	Switzerland
PMO6-79-122	600			**1.000050**	649	563	WRC

Table 2.2: (continued)

Instrument	C_1	C_2	R_n Ω	**WRR Factor**	σ ppm	*N*	*Country/ Owner*
PMO6-80022	23.915			**0.997891**	514	575	WRC
PMO6-81109	600.035			**0.998317**	623	540	JRC Italy
PMO6-811108	24.101			**1.000083**	649	417	Sweden
PMO6-850404	1207.29			**0.998033**	735	307	South Africa
PMO6-850405	24.194			**0.998919**	569	324	Estonia
PMO6-850406	23.9922			**1.001992**	927	323	China
PMO6-850410	609.17			**0.990976**	2380	413	Chile
PMO6-911204	601.7356			**0.999446**	942	539	JRC Italy
SHP1-110005	1			**0.998586**	1511	328	K&Z The Netherlands
SHP1V-130042	7.94			**1.001614**	1790	466	PTB Germany
SIAR-2A	1			**0.991432**	2535	221	WRC
SIAR-2B	1			**1.000941**	2227	210	WRC
SIAR-2C	1			**0.998949**	753	392	CIOMP China
SIAR-4A	1			**0.998445**	807	405	CIOMP China
SIAR-4B	1			**0.996734**	882	395	CIOMP China
SIAR-4D	1			**0.995917**	966	392	CIOMP China
SNIP-37441	8.32			**0.998375**	2014	484	Eppley USA
SNIP-37881	1			**1.000939**	1288	532	NOAA USA
SNIP-37909	1			**1.000501**	1489	539	NOAA USA
SOLARSIM-D1-SN102	1			**0.999674**	1440	425	COFOVO Energy Canada
SOLARSIM-D1-SN103	1			**0.998951**	2206	424	COFOVO Energy Canada
SOLARSIM-D2-SN112	1			**0.994610**	1957	426	COFOVO Energy Canada
SOLARSIM-D2-SN113	1			**0.999494**	2534	430	COFOVO Energy Canada
TMI-67502	1.0039			**1.000999**	1102	487	NOAA USA
TMI67605	1.0025			**0.998546**	2140	116	Argentina
TMI-68018	1.0046			**0.996597**	667	522	NREL USA
TMI-68025	1.002			**0.998133**	960	453	Austria
TMI-68835	1.00383			**1.000714**	764	523	JRC Italy
TMI-69137	10020			**1.002150**	770	513	Australia

2.4 External stability check of the WSG

In Section 2.3 the stability of the WSG was checked by analyzing the trends of individual members of the WSG with respect to the group's average. Here we present an external assessment of the stability of the WSG with respect to all cavity radiometers which have participated in at least two IPCs since 1980 (c.f. Fig. 2.1). This analysis confirms the long-term stability of the WSG within the required uncertainty level of $3000\ \mathrm{ppm}$ (0.3%). Compared to IPC-XI (2010) the WRR factors of 63 cavity radiometers has changed by $167\ \mathrm{ppm}$ on average, with a statistical uncertainty of $352\ \mathrm{ppm}$

(1-σ). We thus conclude that the WSG has not significantly drifted over the past five years. For completeness the history of WRR factors since 1980 (IPC-V) is given in Table 2.3 for all participating instruments. Note that in this table the actual WRR factors are listed while normalized factors (with respect to C_1) were used for assessing the stability of the WSG. Normalization was necessary because some instruments changed their calibration factors C_1, which produces spurious changes in their WRR factors.

Table 2.3: The history of WRR factors. In this table the actual WRR factors are listed. They depend on the calibration constant C_1 which was used and which may have changed over time. In the WSG-stability analysis presented in Section 2.4 and Figure 2.1 these factors were re-normalized accordingly.

Instrument	*IPC-V*	*IPC-VI*	*IPC-VII*	*IPC-VIII*	*IPC-IX*	*IPC-X*	*IPC-XI*	*IPC-XII*
A576	1.020130	1.005233	1.001071	1.000460	0.997370	1.000050	0.990369	0.990848
A13439				1.022990	1.002370	1.003291	1.001350	1.003456
A15192			0.99913	1.00189	1.00157	1.002165		1.030413
CH1-050392							1.000250	1.010939
CH1-020283							0.997677	0.993817
CH1-060460							1.002330	1.004742
CH1-930018							1.000750	1.001242
CH1-940072						1.005958	1.007580	1.009321
CHP1-100245							1.000490	1.001156
NIP-21451E6							0.999193	1.005944
NIP-25738E6							0.998843	0.991885
NIP-31144E6							0.997184	0.996824
EPAC11402					0.999250	1.000560	1.000680	1.036265
HF15744	1.000640	1.000030	0.999650	0.999470	0.999160	0.998034	0.998085	0.998201
HF19746	0.999520	0.999940	1.001603	0.999190	0.999660	0.998782	0.998886	1.000021
HF27157				1.000380	0.999020	0.998722	0.999647	0.999084
HF27159			0.999271	0.998880		0.998004	1.000020	0.999438
HF27162			1.000370	1.000960	1.000820	1.000180	0.999212	0.999543
HF27796					0.996910	0.996979	0.997204	0.996033
AHF29223				0.997450	0.997470	0.996761	0.997352	1.003219
AHF14915	0.998751	0.998421	0.999980	1.000460	1.000260	0.999640	0.999682	0.999542
AHF17142	0.998801	0.997733	0.998901	0.998860	0.998930	0.999141	0.998358	0.997946
AHF18742						1.003773	1.002280	1.004506
AHF27160			0.997267	0.997090	0.996770	0.996910	0.996467	0.997424
AHF27798			0.998363	0.998980	0.999880	0.999410	0.999018	0.998654
AHF28486							0.997308	0.997318
AHF28553				0.997560	0.997330	0.996105	0.996842	0.997739
AHF28968				0.998720	0.998660	0.997765	0.997734	0.997627
AHF29220				0.998620	0.998460	0.997556	0.997691	0.997482
AHF30497					0.997740	0.999350	0.999623	0.999589
AHF30713					0.998610	0.997512	0.997548	0.997228
AHF31041					0.998130	0.996294	0.996286	0.996392
AHF31103					0.998990	0.999640		0.999345
AHF31105						1.001649	0.999964	0.998656
AHF31110					0.997890	0.997211	0.996431	0.997038

Table 2.3: (continued)

Instrument	*IPC-V*	*IPC-VI*	*IPC-VII*	*IPC-VIII*	*IPC-IX*	*IPC-X*	*IPC-XI*	*IPC-XII*
AHF31117							0.998861	0.999042
AHF32455						0.999090	1.000280	1.001380
AHF33396						0.997951	0.998079	0.997184
AHF36011							0.998226[2]	1.000005
AHF36013							1.058110	0.999802
AWX31114							1.001240	1.001209
AWX32448					1.00031	0.999874	0.999939	0.999986
AWX33393						0.997281	0.999362	0.999885
TMI67502	0.999290	0.998471	1.000390	0.998660	0.999660	0.999480	0.999294	1.000999
TMI68018			0.998692		0.998480	0.997138	0.996804	0.996601
TMI68025			0.999460	0.999860	1.000060	0.998135	0.998613	0.998133
TMI68835							1.000980	1.000723
MAR-1-3				0.999610			0.999991	0.999953
PMO6-5	1.006756	1.000100	0.998602	0.997980	1.000530	0.999960	0.999116	0.998288
PMO6-79-122			0.996890	0.999970	0.999860	1.000390	0.999401	1.000051
PMO6-80022		1.000230	0.996890	0.996130	0.996990	0.997944	1.003080	0.997891
PMO6-811108		0.999210	0.999970	1.000110	0.999970	0.998114	1.000660	1.000083
PMO6-811109					0.999460	0.998412	0.998577	0.998315
PMO6-850405				1.000370	0.999290	0.999191	1.000560	0.998919
PMO6-850406					1.000320	0.999440	1.000200	1.001992
PMO6-850410				1.001800	1.015280	0.987030	0.990890	0.990976
PMO6-911204					1.000810	0.999011	0.999711	0.999445
PMO6-0301							1.000588	1.000183
PMO6-0403							1.000160	0.999753
PMO6-0405							0.999684	0.999265
PMO6-0804							0.999914	0.999908
SIAR-2A						1.000623	0.991696	0.991360
SIAR-2B						0.998620	1.000290	1.000895
SIAR-2C						1.000087	0.999839	0.998949

[2] This WRR factor results from a re-evaluation of the IPC-XI data after excluding all measurements from October 3^{rd} and 7^{th}, 2010, because a wrong calibration factor was used on those days. The IPC-XI report erroneously included the affected data and states a WRR factor of 0.996933.

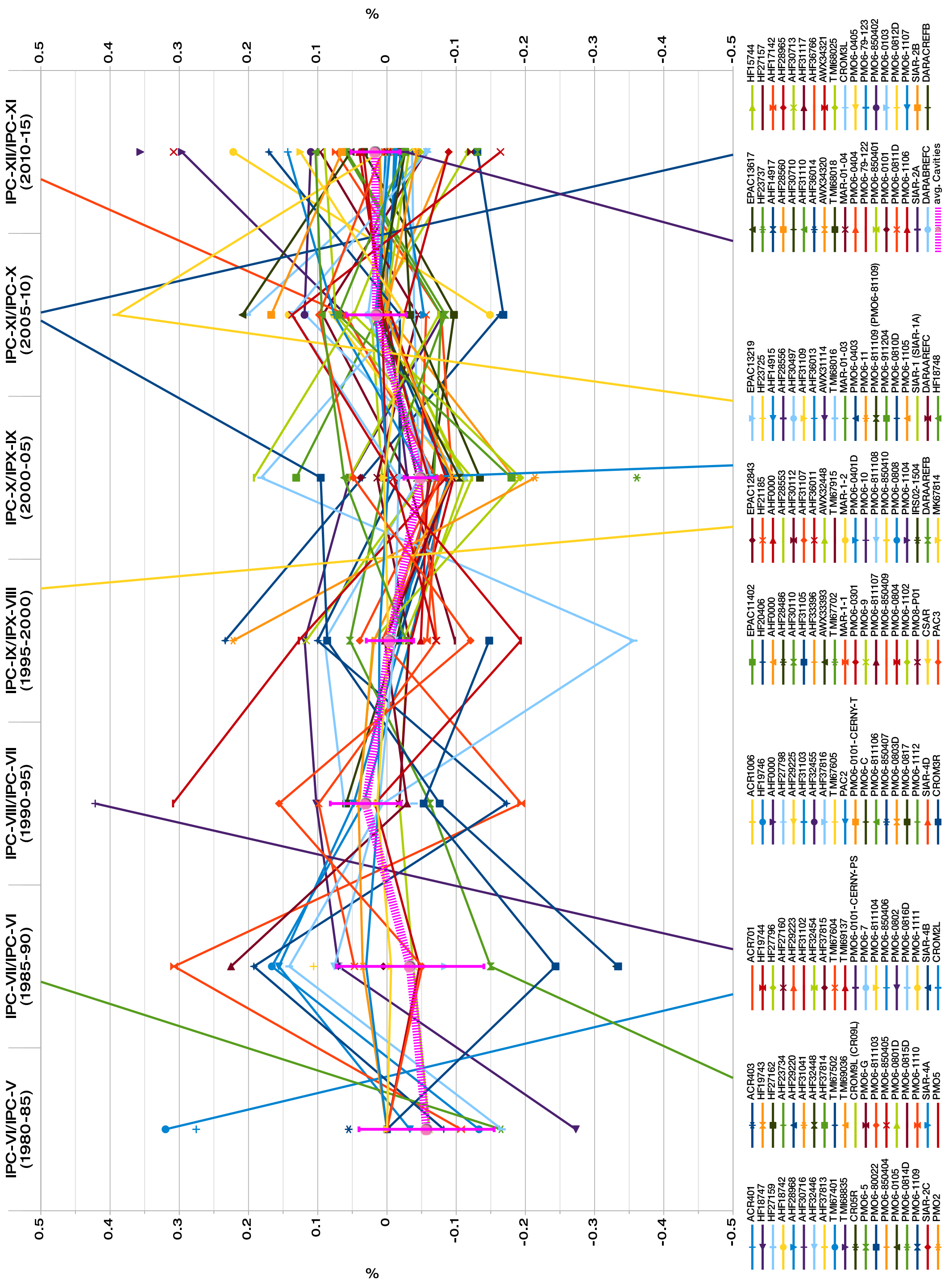

Figure 2.1: The historic evolution of the WRR factors of all cavity radiometers which have participated in at least two consecutive IPC's since 1980 (IPC-V). Note that in this analysis all WRR factors are normalized to the calibration constant C_1 which was used at the time. The thick magenta line is the average of all participating cavities. This line is interpreted as the inter-IPC stability of the WSG. In this metric any potential drift of the WSG between IPC-XI (2010) and IPC-XII (2015) was below the detection limit indicated by the $1-\sigma$ error bars. (The measured drift is $0.017 \pm 0.035\%$.)

Chapter 3 Conclusions and Recommendations

Despite the partial failure of two WSG instruments (MK67814 and HF18748, c.f. Sect. 2.4) the WRR is considered stable within the limits required by the WMO-CIMO Guide. The new WRR factors are calculated based on the average readings of PMO2, PMO5, CROM2L, and PAC3. Compared to IPC-XI most participating instruments show insignificant changes in their WRR factors, which confirms the stability of the WRR. The recommended WRR factors are listed in Table 2.2.

3.1 Graphical Representation of the Results

On the following pages are the data plots for each instrument. The deviation from WRR is plotted in percents. All the points which were used for the analysis (i.e. the points fulfilling the selection criteria listed in Sect. 2.1) have been plotted with a corresponding histogram on the side.

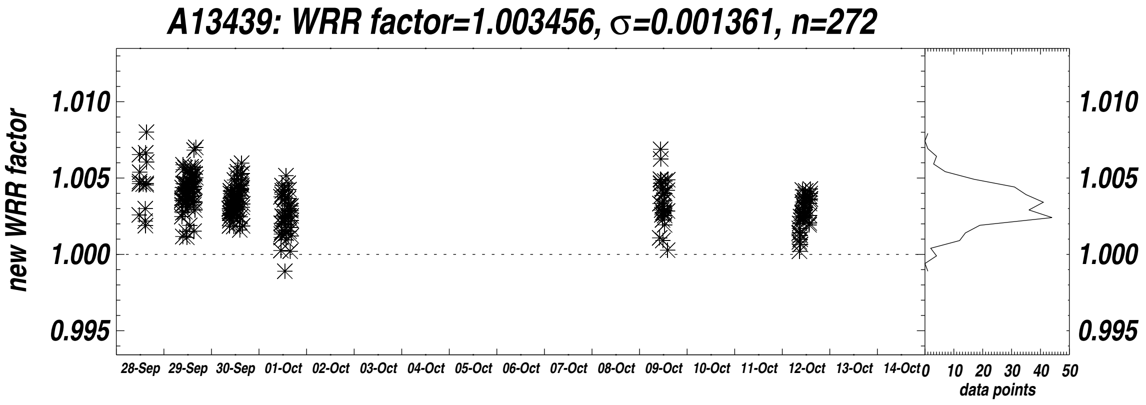
A13439: WRR factor=1.003456, σ=0.001361, n=272
new WRR factor
1.010
1.005
1.000
0.995
28-Sep 29-Sep 30-Sep 01-Oct 02-Oct 03-Oct 04-Oct 05-Oct 06-Oct 07-Oct 08-Oct 09-Oct 10-Oct 11-Oct 12-Oct 13-Oct 14-Oct
0 10 20 30 40 50
data points

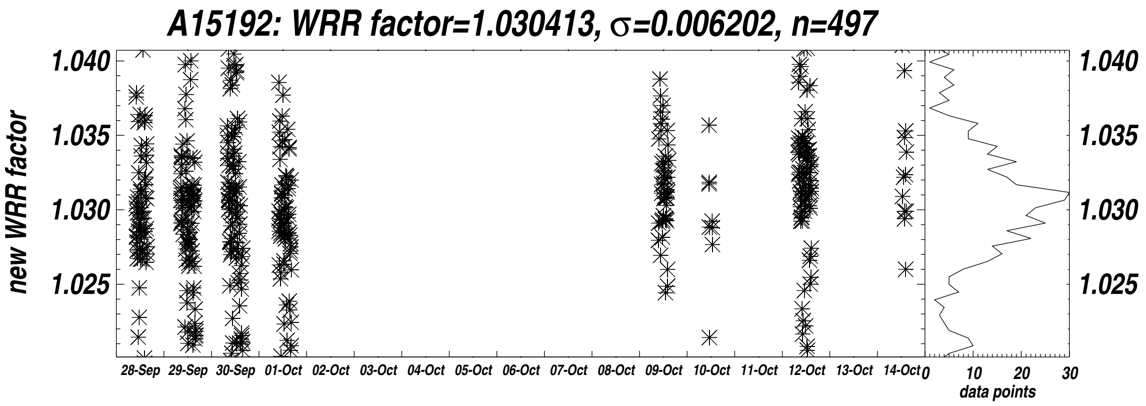
A15192: WRR factor=1.030413, σ=0.006202, n=497
new WRR factor
1.040
1.035
1.030
1.025
28-Sep 29-Sep 30-Sep 01-Oct 02-Oct 03-Oct 04-Oct 05-Oct 06-Oct 07-Oct 08-Oct 09-Oct 10-Oct 11-Oct 12-Oct 13-Oct 14-Oct
0 10 20 30
data points

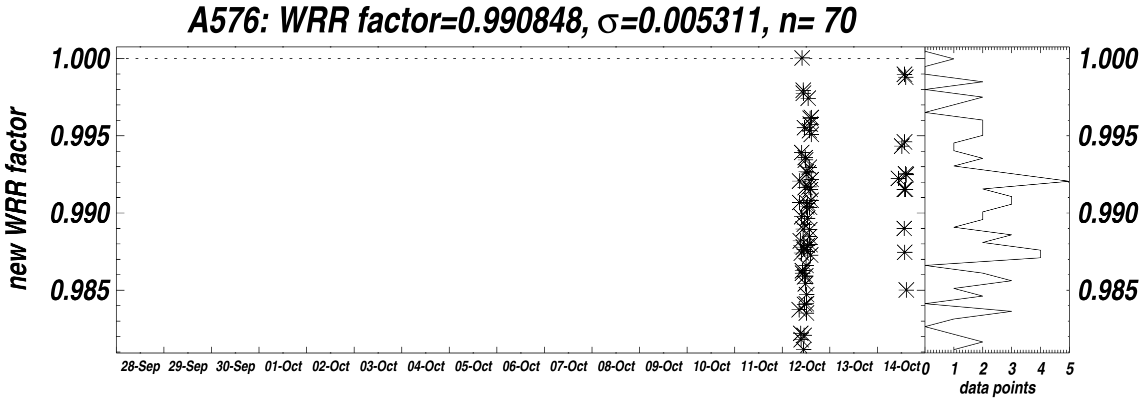
A576: WRR factor=0.990848, σ=0.005311, n= 70
new WRR factor
1.000
0.995
0.990
0.985
28-Sep 29-Sep 30-Sep 01-Oct 02-Oct 03-Oct 04-Oct 05-Oct 06-Oct 07-Oct 08-Oct 09-Oct 10-Oct 11-Oct 12-Oct 13-Oct 14-Oct
0 1 2 3 4 5
data points

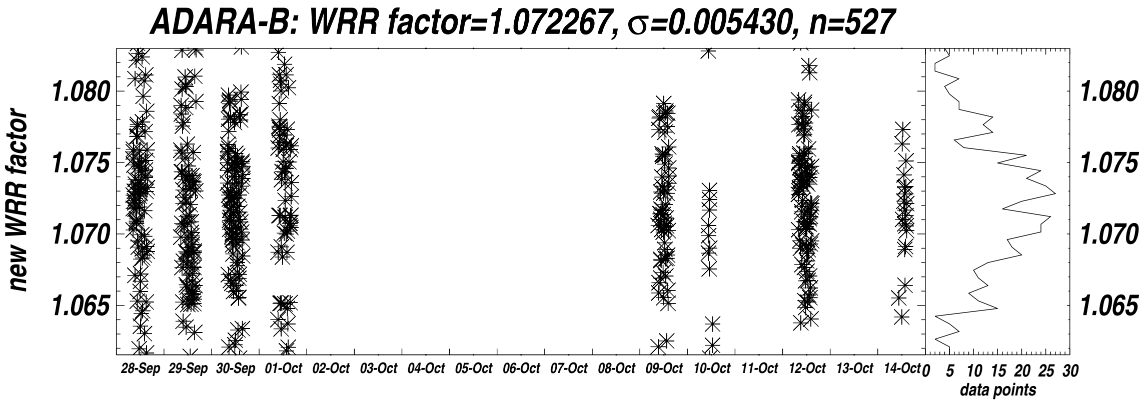
ADARA-B: WRR factor=1.072267, σ=0.005430, n=527
new WRR factor
1.080
1.075
1.070
1.065
28-Sep 29-Sep 30-Sep 01-Oct 02-Oct 03-Oct 04-Oct 05-Oct 06-Oct 07-Oct 08-Oct 09-Oct 10-Oct 11-Oct 12-Oct 13-Oct 14-Oct
0 5 10 15 20 25 30
data points

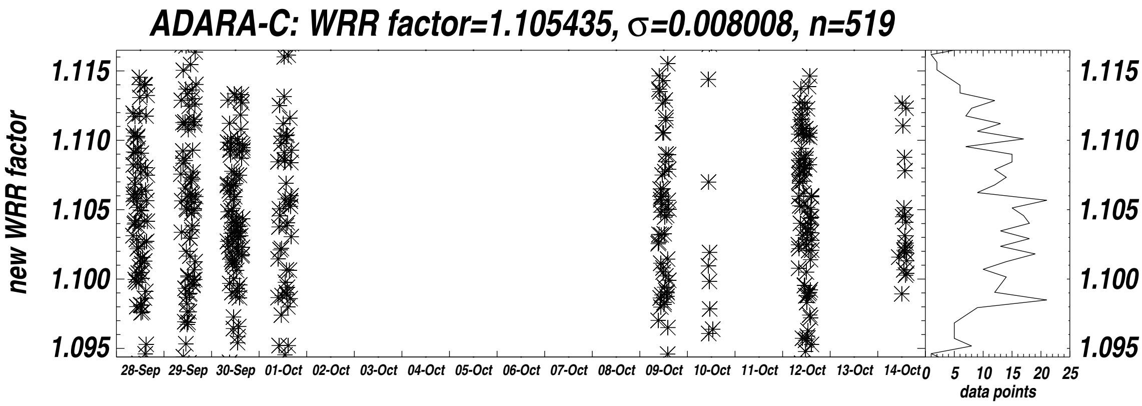
ADARA-C: WRR factor=1.105435, σ=0.008008, n=519
new WRR factor
1.115
1.110
1.105
1.100
1.095
28-Sep 29-Sep 30-Sep 01-Oct 02-Oct 03-Oct 04-Oct 05-Oct 06-Oct 07-Oct 08-Oct 09-Oct 10-Oct 11-Oct 12-Oct 13-Oct 14-Oct
0 5 10 15 20 25
data points

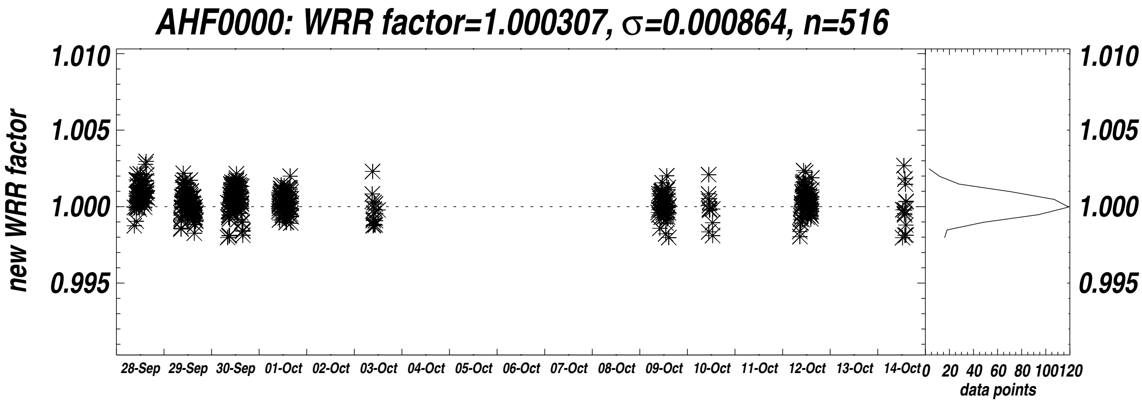
AHF0000: WRR factor=1.000307, σ=0.000864, n=516
new WRR factor
1.010
1.005
1.000
0.995
28-Sep 29-Sep 30-Sep 01-Oct 02-Oct 03-Oct 04-Oct 05-Oct 06-Oct 07-Oct 08-Oct 09-Oct 10-Oct 11-Oct 12-Oct 13-Oct 14-Oct
0 20 40 60 80 100 120
data points

AHF14915: WRR factor=0.999542, σ=0.000943, n=474

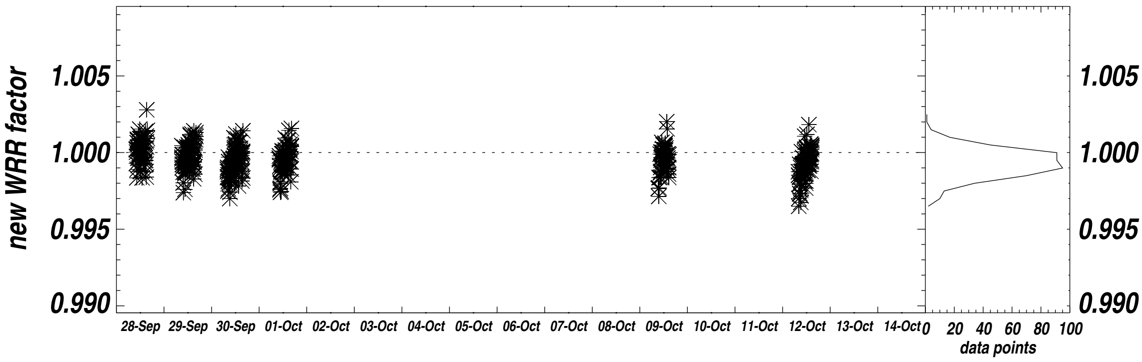

AHF14917: WRR factor=0.997900, σ=0.000683, n=507

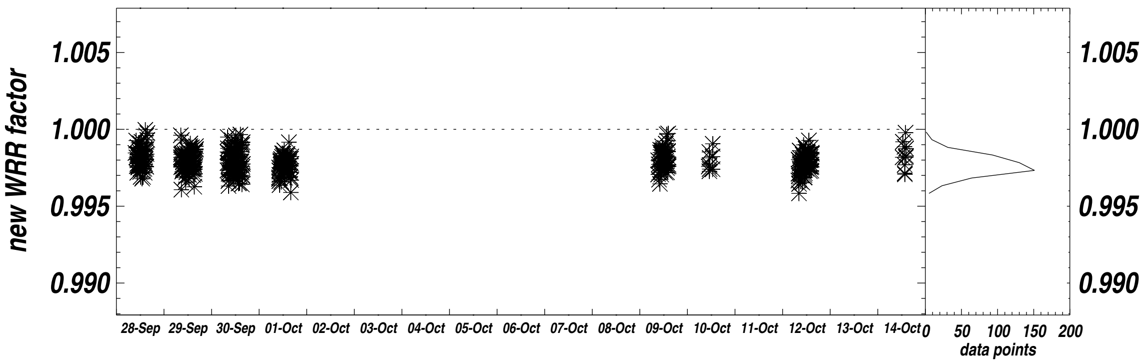

AHF17142: WRR factor=0.997946, σ=0.000675, n=370

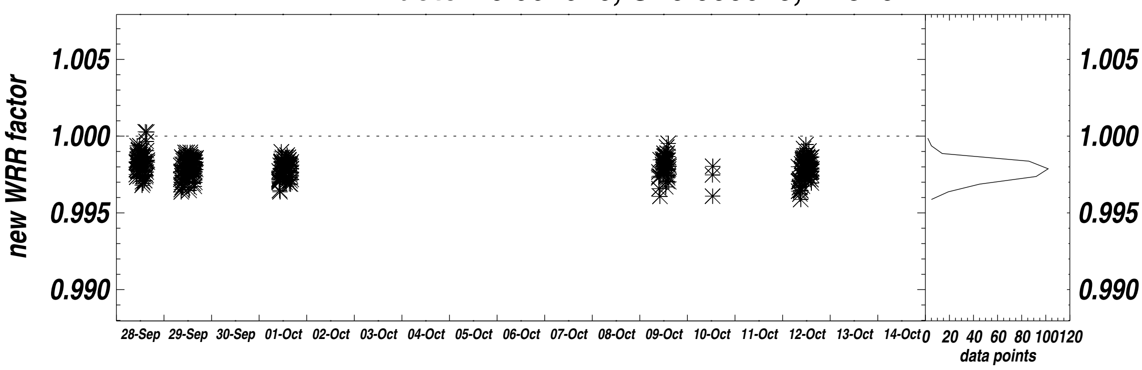

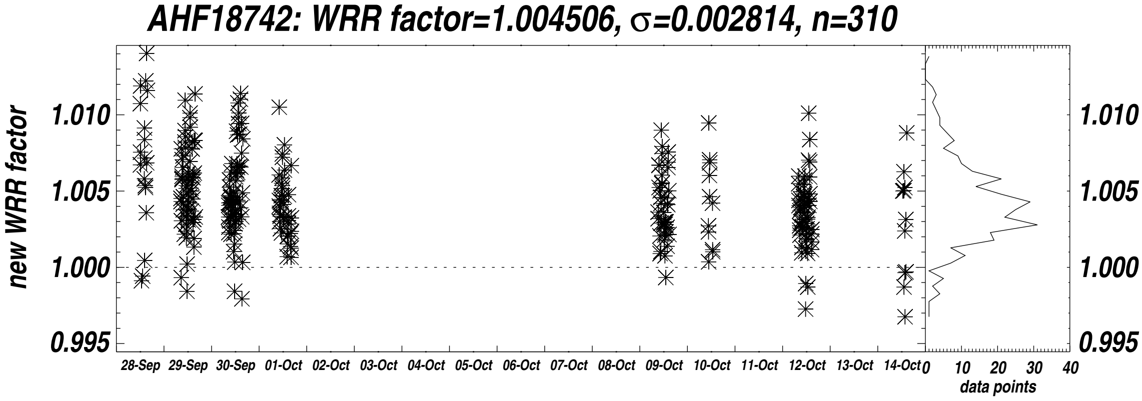
AHF18742: WRR factor=1.004506, σ=0.002814, n=310
new WRR factor
1.010
1.005
1.000
0.995
28-Sep 29-Sep 30-Sep 01-Oct 02-Oct 03-Oct 04-Oct 05-Oct 06-Oct 07-Oct 08-Oct 09-Oct 10-Oct 11-Oct 12-Oct 13-Oct 14-Oct
0 10 20 30 40
data points

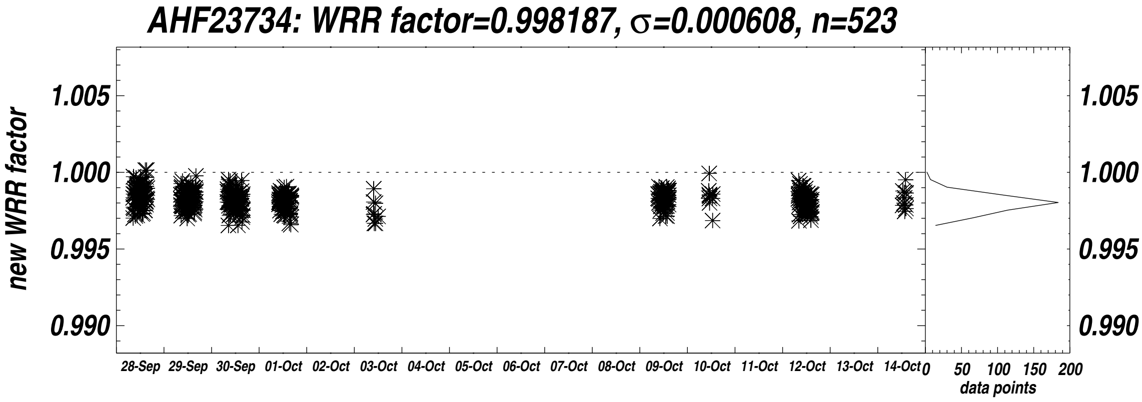
AHF23734: WRR factor=0.998187, σ=0.000608, n=523
new WRR factor
1.005
1.000
0.995
0.990
28-Sep 29-Sep 30-Sep 01-Oct 02-Oct 03-Oct 04-Oct 05-Oct 06-Oct 07-Oct 08-Oct 09-Oct 10-Oct 11-Oct 12-Oct 13-Oct 14-Oct
0 50 100 150 200
data points

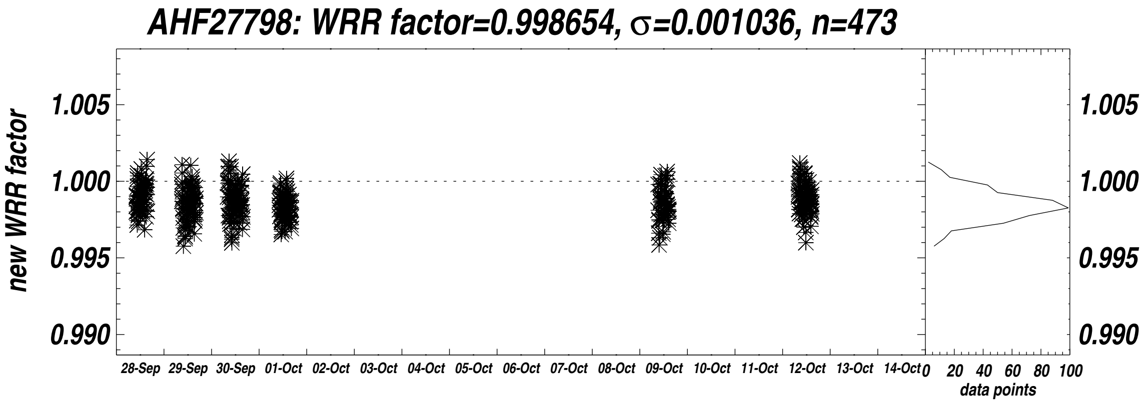
AHF27798: WRR factor=0.998654, σ=0.001036, n=473
new WRR factor
1.005
1.000
0.995
0.990
28-Sep 29-Sep 30-Sep 01-Oct 02-Oct 03-Oct 04-Oct 05-Oct 06-Oct 07-Oct 08-Oct 09-Oct 10-Oct 11-Oct 12-Oct 13-Oct 14-Oct
0 20 40 60 80 100
data points

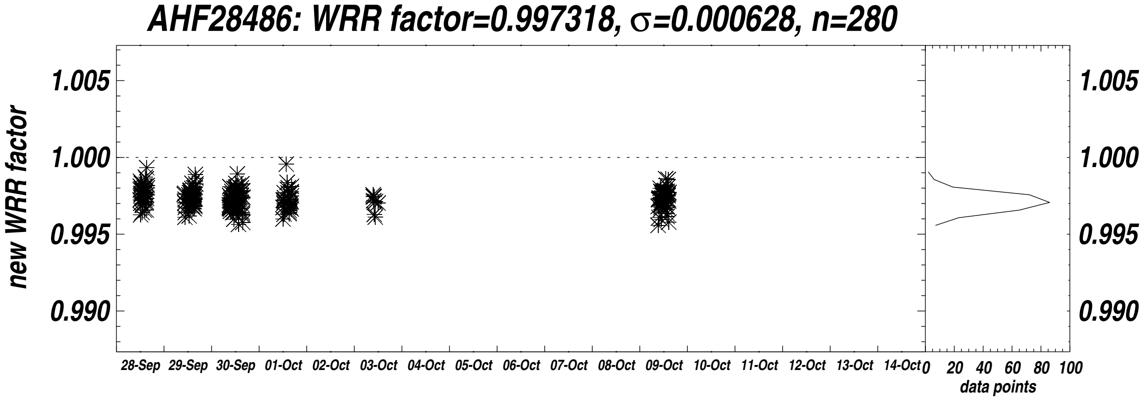
AHF28486: WRR factor=0.997318, σ=0.000628, n=280
new WRR factor
1.005
1.000
0.995
0.990
28-Sep 29-Sep 30-Sep 01-Oct 02-Oct 03-Oct 04-Oct 05-Oct 06-Oct 07-Oct 08-Oct 09-Oct 10-Oct 11-Oct 12-Oct 13-Oct 14-Oct
0 20 40 60 80 100
data points

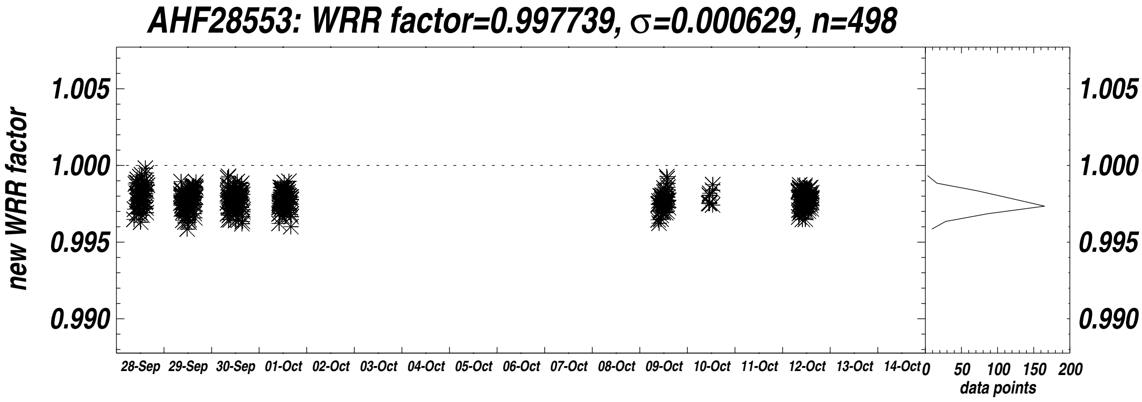
AHF28553: WRR factor=0.997739, σ=0.000629, n=498
new WRR factor
1.005
1.000
0.995
0.990
28-Sep 29-Sep 30-Sep 01-Oct 02-Oct 03-Oct 04-Oct 05-Oct 06-Oct 07-Oct 08-Oct 09-Oct 10-Oct 11-Oct 12-Oct 13-Oct 14-Oct
0 50 100 150 200
data points

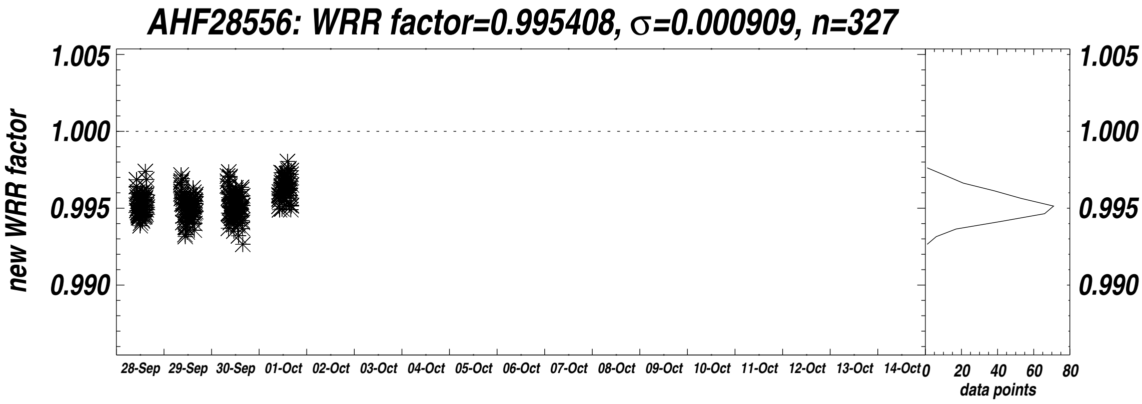
AHF28556: WRR factor=0.995408, σ=0.000909, n=327
new WRR factor
1.005
1.000
0.995
0.990
28-Sep 29-Sep 30-Sep 01-Oct 02-Oct 03-Oct 04-Oct 05-Oct 06-Oct 07-Oct 08-Oct 09-Oct 10-Oct 11-Oct 12-Oct 13-Oct 14-Oct
0 20 40 60 80
data points

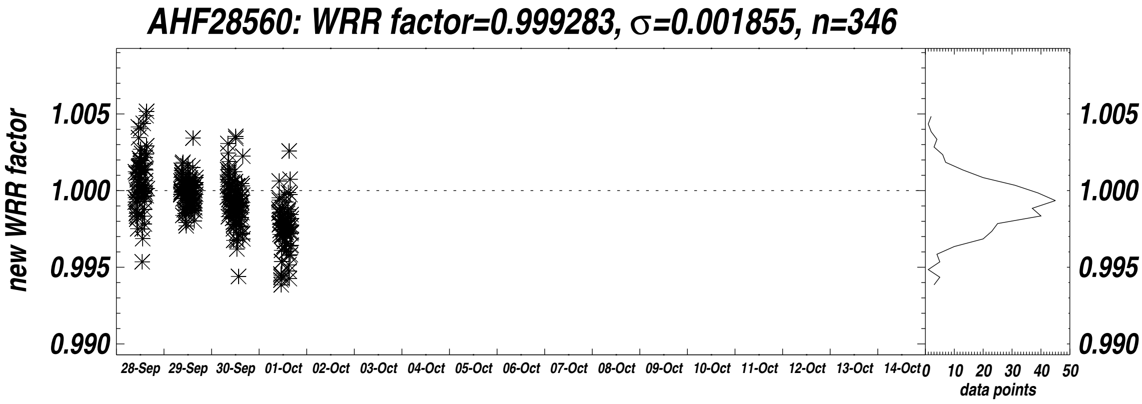
AHF28560: WRR factor=0.999283, σ=0.001855, n=346
new WRR factor
data points

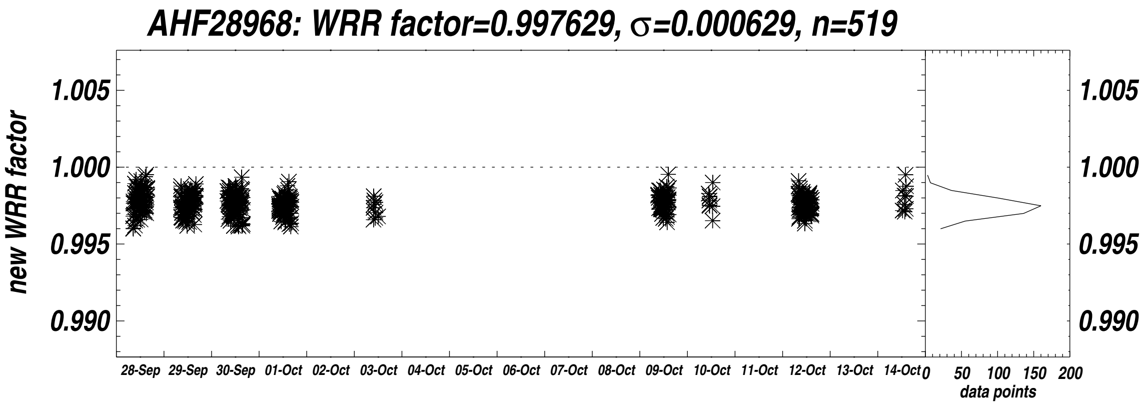
AHF28968: WRR factor=0.997629, σ=0.000629, n=519
new WRR factor
data points

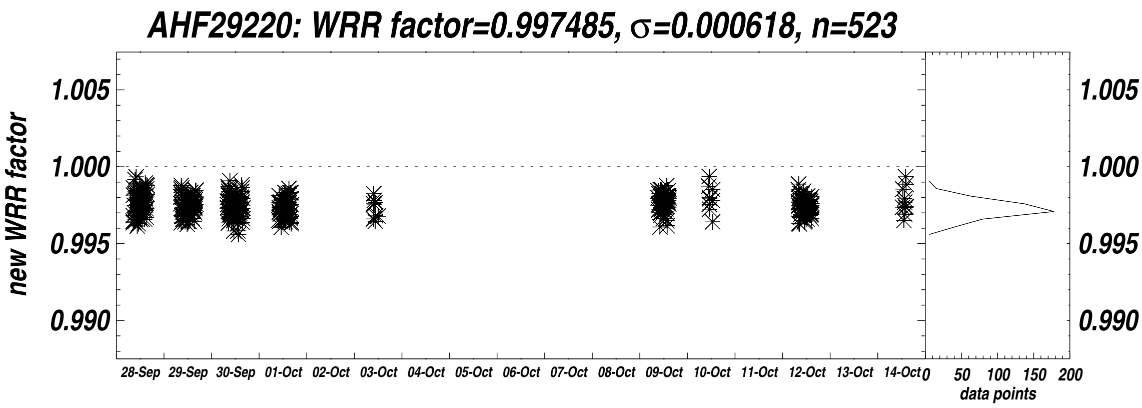
AHF29220: WRR factor=0.997485, σ=0.000618, n=523
new WRR factor
data points

AHF29223: WRR factor=1.003219, σ=0.000771, n=198

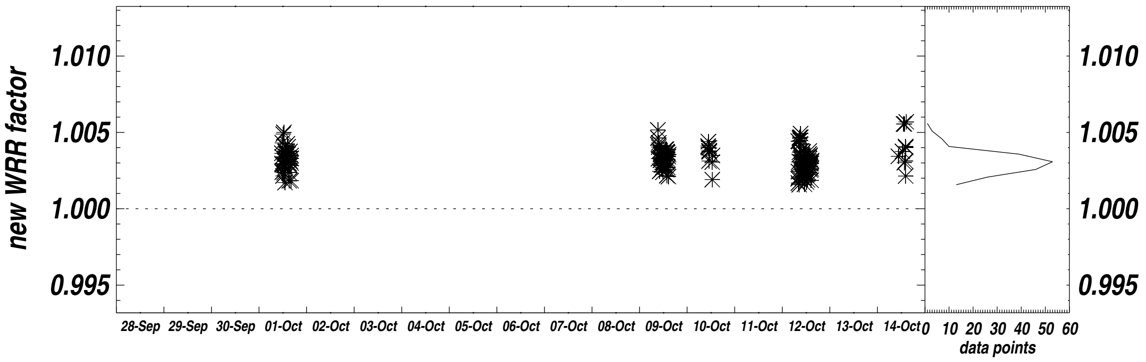

AHF30110: WRR factor=1.063471, σ=0.000852, n=346

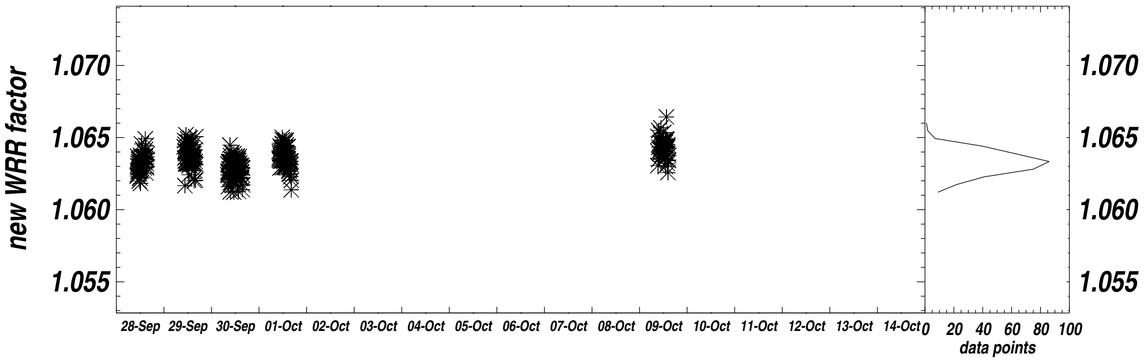

AHF30112: WRR factor=1.010501, σ=0.002454, n=173

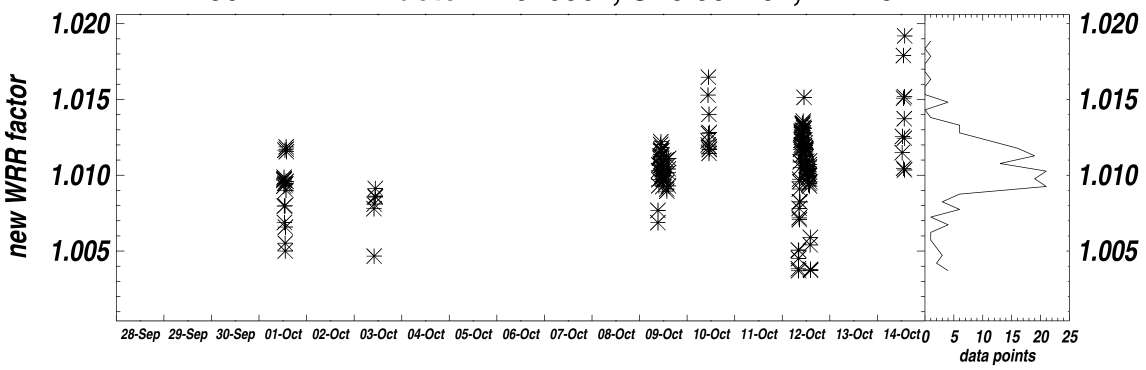

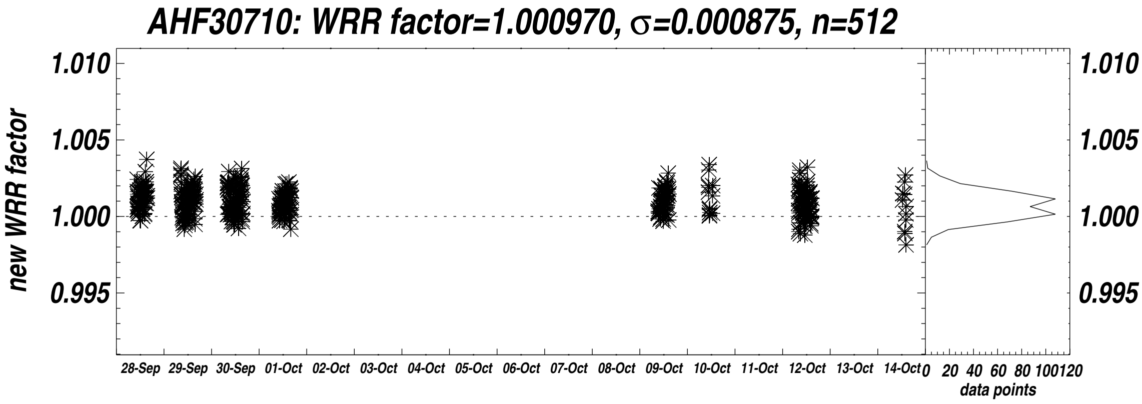
AHF30710: WRR factor=1.000970, σ=0.000875, n=512
new WRR factor
1.010
1.005
1.000
0.995
28-Sep 29-Sep 30-Sep 01-Oct 02-Oct 03-Oct 04-Oct 05-Oct 06-Oct 07-Oct 08-Oct 09-Oct 10-Oct 11-Oct 12-Oct 13-Oct 14-Oct
0 20 40 60 80 100120
data points

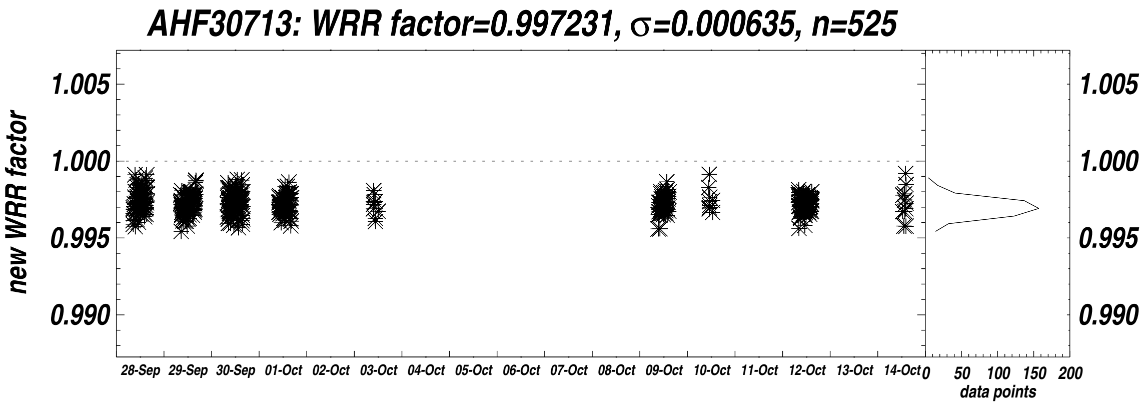
AHF30713: WRR factor=0.997231, σ=0.000635, n=525
new WRR factor
1.005
1.000
0.995
0.990
28-Sep 29-Sep 30-Sep 01-Oct 02-Oct 03-Oct 04-Oct 05-Oct 06-Oct 07-Oct 08-Oct 09-Oct 10-Oct 11-Oct 12-Oct 13-Oct 14-Oct
0 50 100 150 200
data points

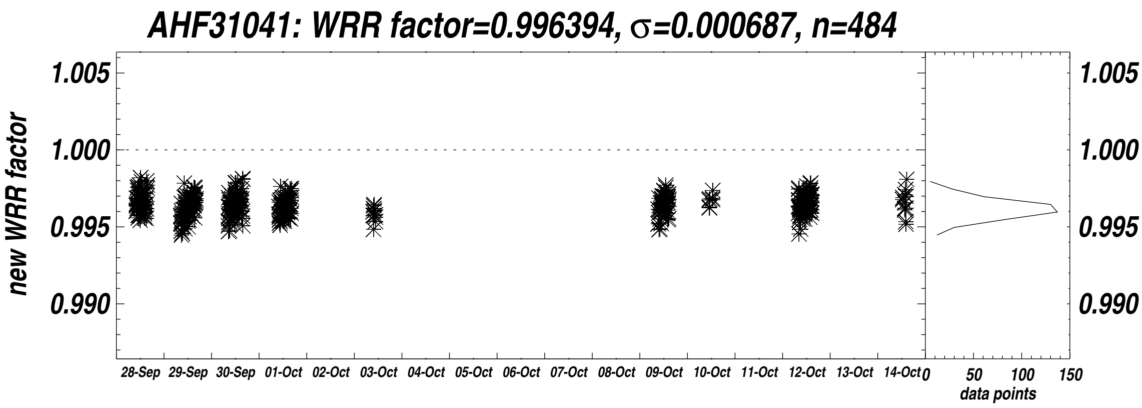
AHF31041: WRR factor=0.996394, σ=0.000687, n=484
new WRR factor
1.005
1.000
0.995
0.990
28-Sep 29-Sep 30-Sep 01-Oct 02-Oct 03-Oct 04-Oct 05-Oct 06-Oct 07-Oct 08-Oct 09-Oct 10-Oct 11-Oct 12-Oct 13-Oct 14-Oct
0 50 100 150
data points

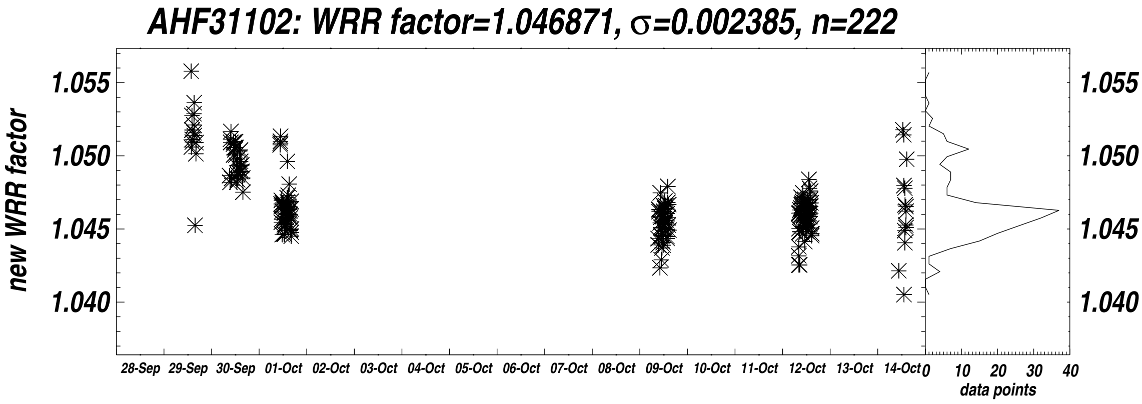
AHF31102: WRR factor=1.046871, σ=0.002385, n=222
new WRR factor
data points

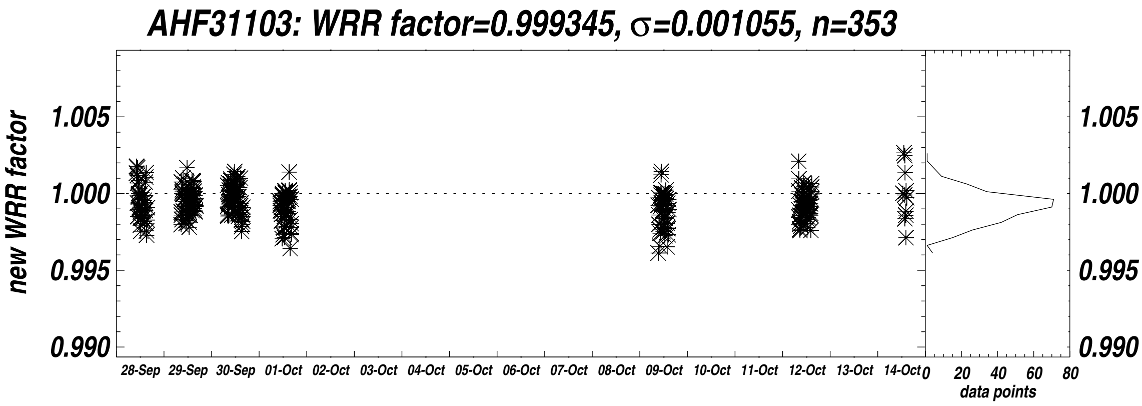
AHF31103: WRR factor=0.999345, σ=0.001055, n=353
new WRR factor
data points

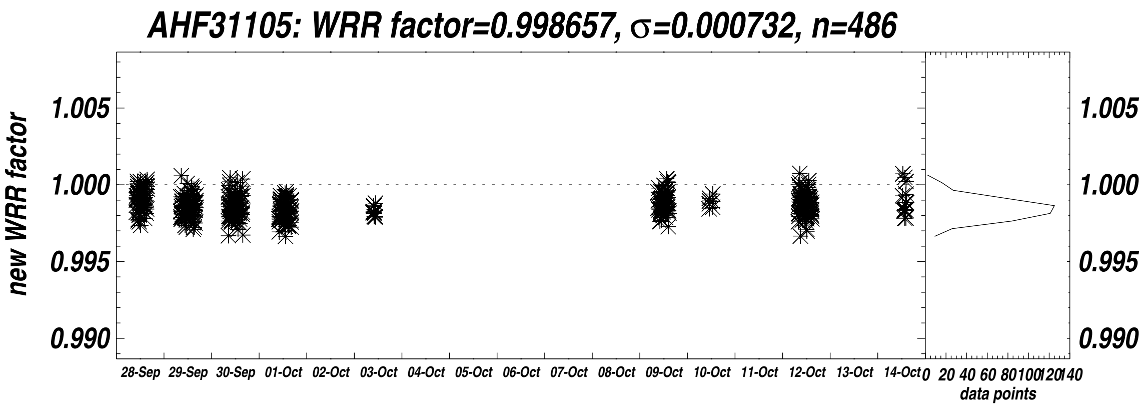
AHF31105: WRR factor=0.998657, σ=0.000732, n=486
new WRR factor
data points

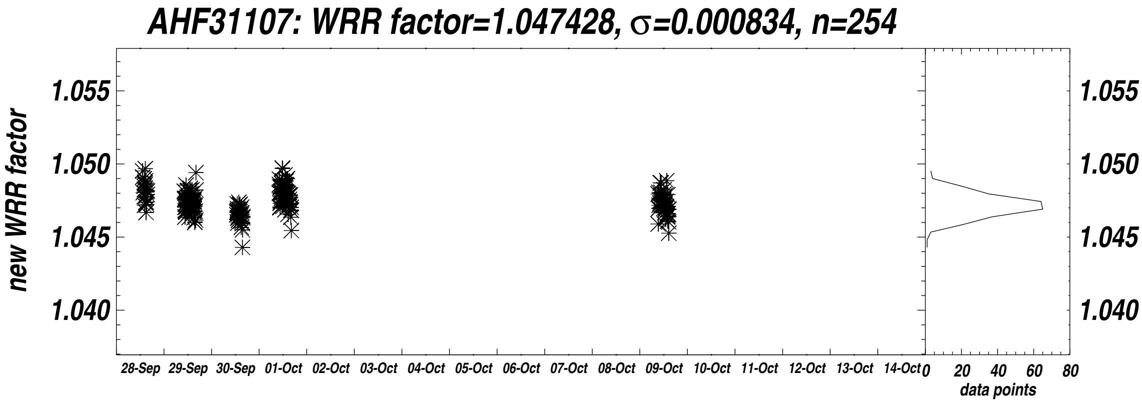
AHF31107: WRR factor=1.047428, σ=0.000834, n=254
new WRR factor
data points

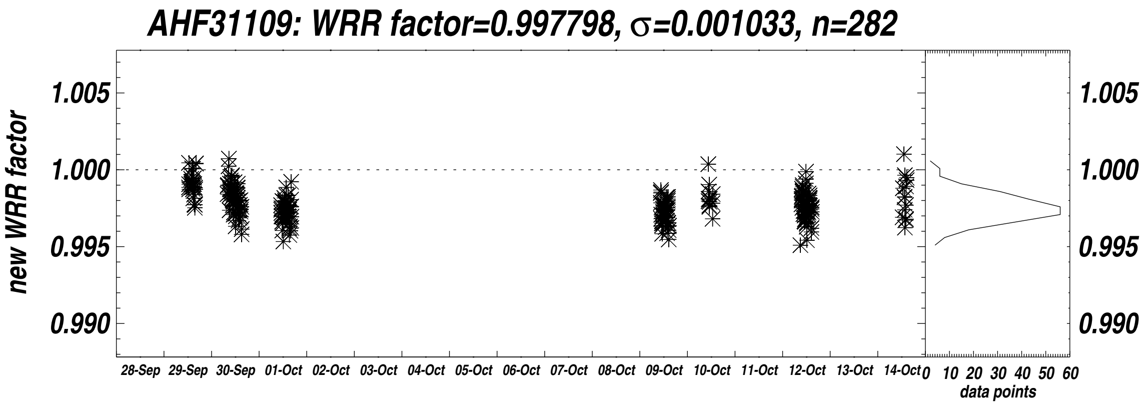
AHF31109: WRR factor=0.997798, σ=0.001033, n=282
new WRR factor
data points

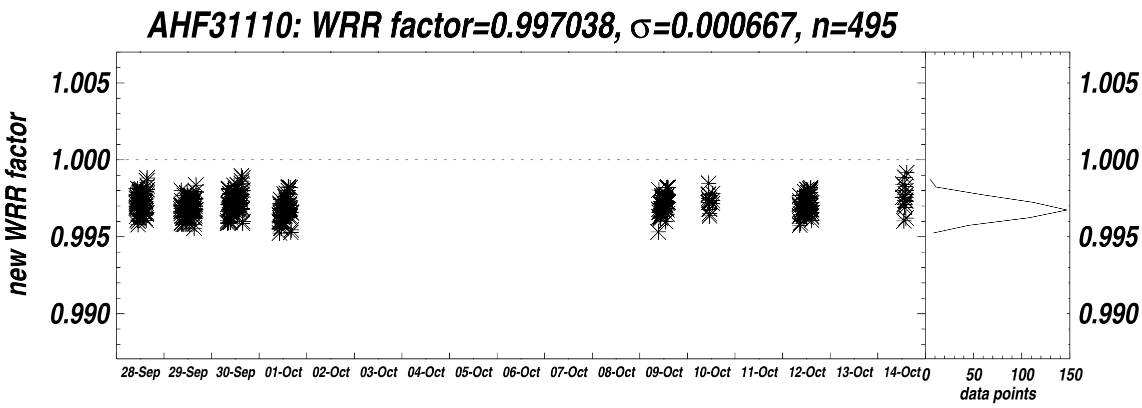
AHF31110: WRR factor=0.997038, σ=0.000667, n=495
new WRR factor
data points

AHF31117: WRR factor=0.999042, σ=0.000705, n=489

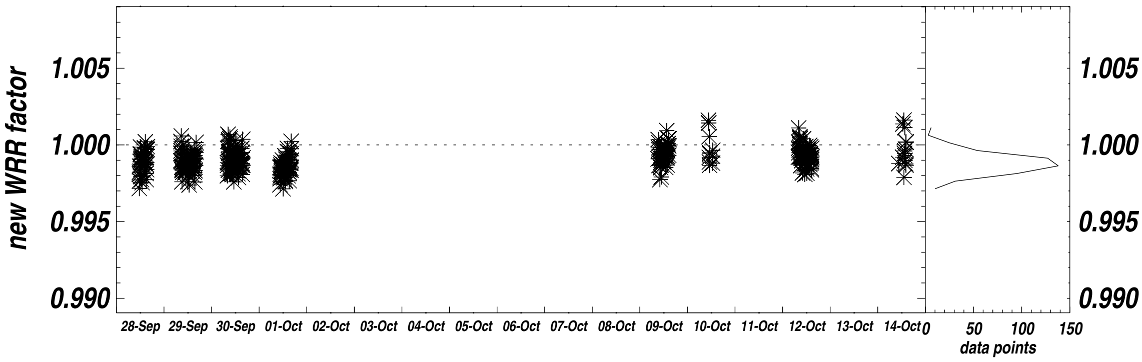

AHF32455: WRR factor=1.001380, σ=0.000642, n=574

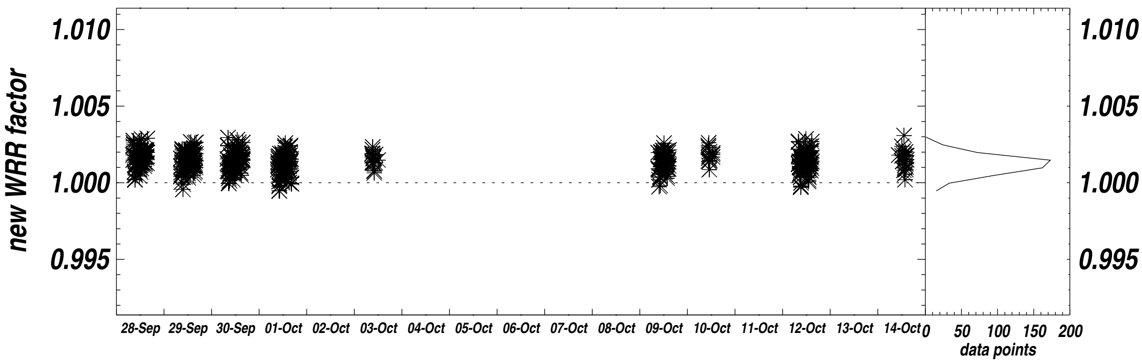

AHF33396: WRR factor=0.997184, σ=0.000945, n=487

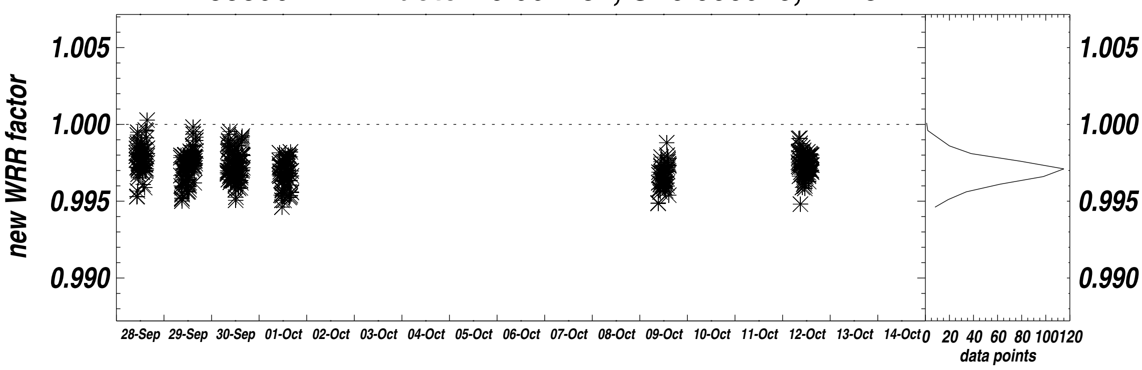

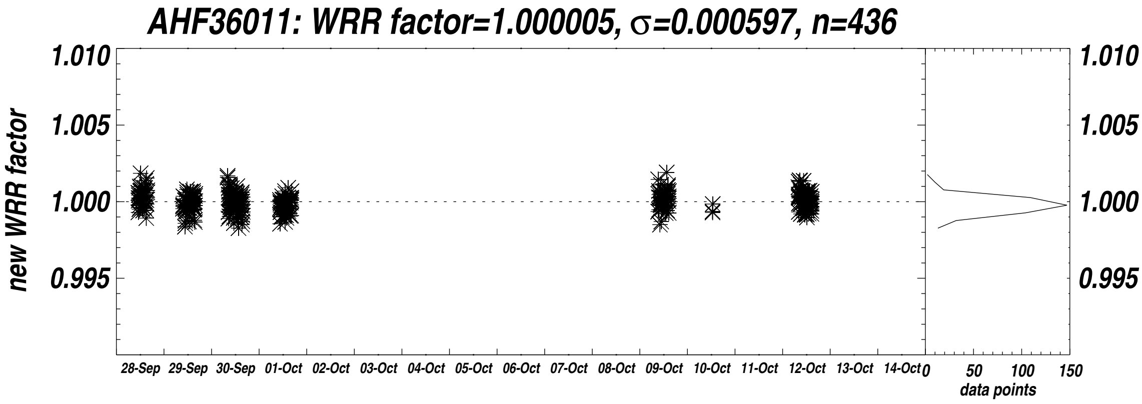
AHF36011: WRR factor=1.000005, σ=0.000597, n=436
new WRR factor
1.010
1.005
1.000
0.995
28-Sep 29-Sep 30-Sep 01-Oct 02-Oct 03-Oct 04-Oct 05-Oct 06-Oct 07-Oct 08-Oct 09-Oct 10-Oct 11-Oct 12-Oct 13-Oct 14-Oct
0 50 100 150
data points

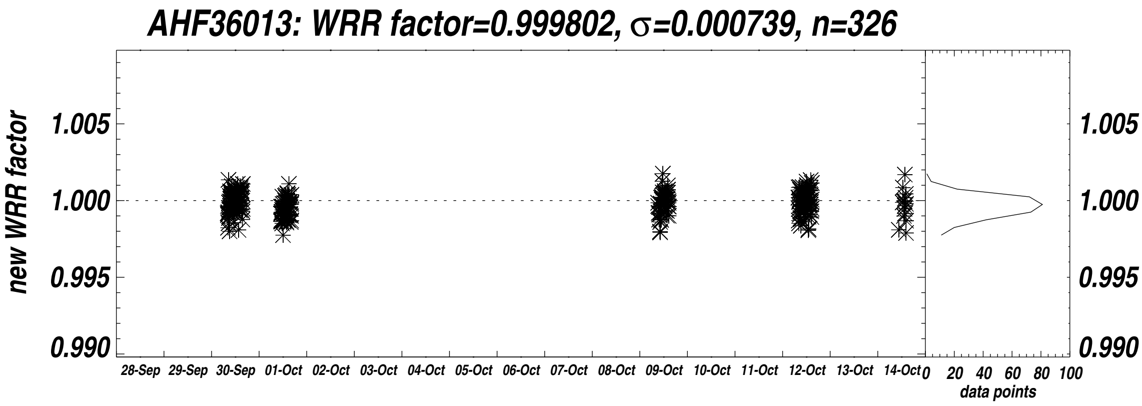
AHF36013: WRR factor=0.999802, σ=0.000739, n=326
new WRR factor
1.005
1.000
0.995
0.990
28-Sep 29-Sep 30-Sep 01-Oct 02-Oct 03-Oct 04-Oct 05-Oct 06-Oct 07-Oct 08-Oct 09-Oct 10-Oct 11-Oct 12-Oct 13-Oct 14-Oct
0 20 40 60 80 100
data points

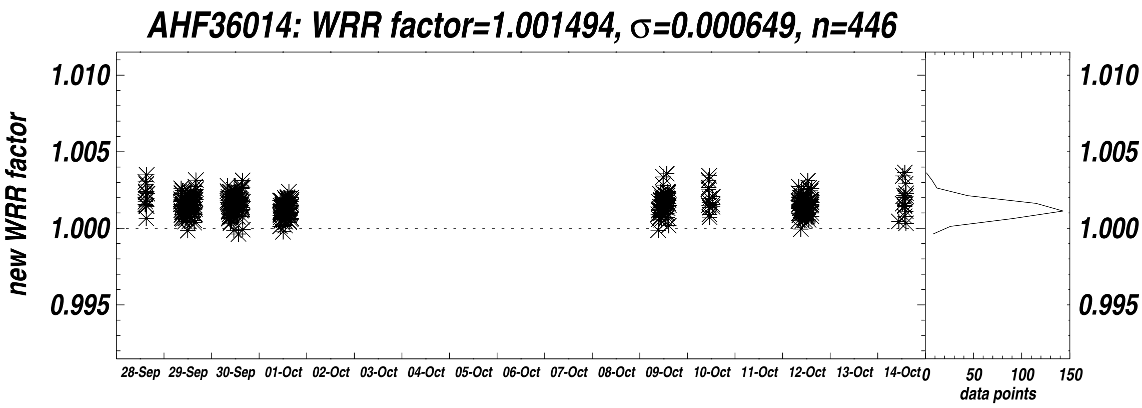
AHF36014: WRR factor=1.001494, σ=0.000649, n=446
new WRR factor
1.010
1.005
1.000
0.995
28-Sep 29-Sep 30-Sep 01-Oct 02-Oct 03-Oct 04-Oct 05-Oct 06-Oct 07-Oct 08-Oct 09-Oct 10-Oct 11-Oct 12-Oct 13-Oct 14-Oct
0 50 100 150
data points

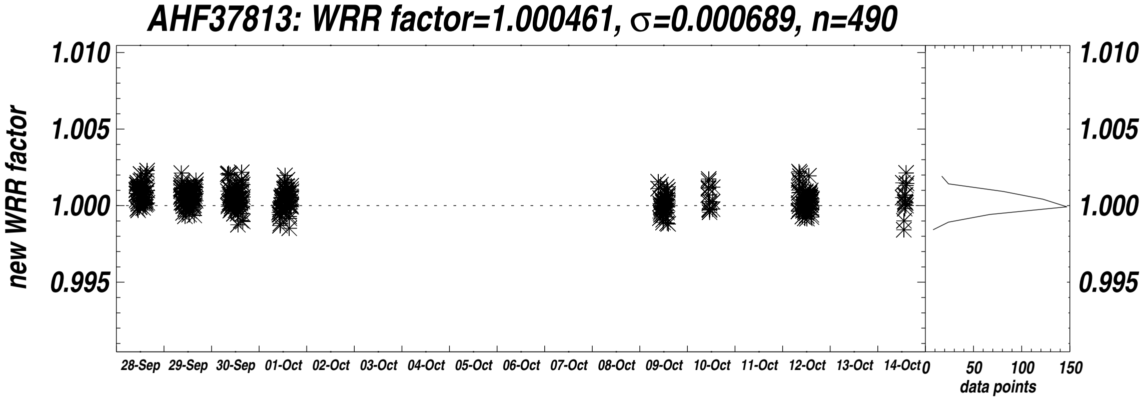
AHF37813: WRR factor=1.000461, σ=0.000689, n=490
new WRR factor
1.010
1.005
1.000
0.995
28-Sep 29-Sep 30-Sep 01-Oct 02-Oct 03-Oct 04-Oct 05-Oct 06-Oct 07-Oct 08-Oct 09-Oct 10-Oct 11-Oct 12-Oct 13-Oct 14-Oct
0 50 100 150
data points

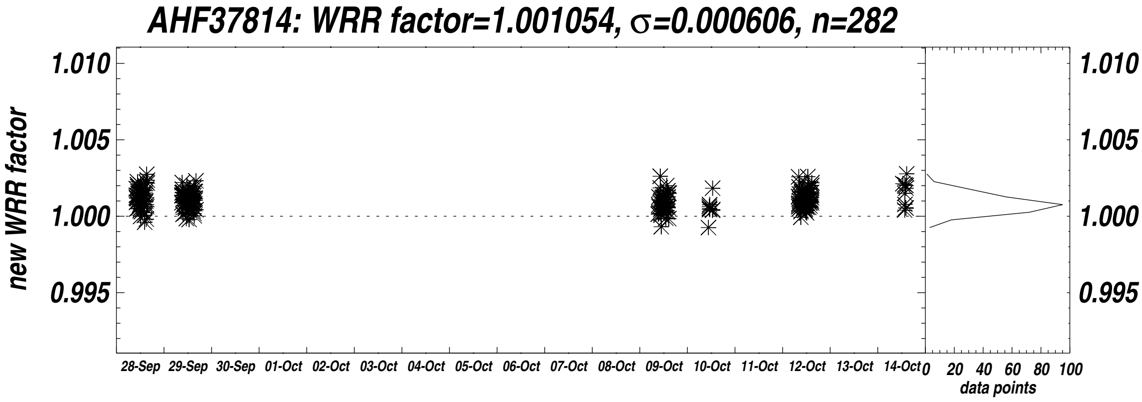
AHF37814: WRR factor=1.001054, σ=0.000606, n=282
new WRR factor
1.010
1.005
1.000
0.995
28-Sep 29-Sep 30-Sep 01-Oct 02-Oct 03-Oct 04-Oct 05-Oct 06-Oct 07-Oct 08-Oct 09-Oct 10-Oct 11-Oct 12-Oct 13-Oct 14-Oct
0 20 40 60 80 100
data points

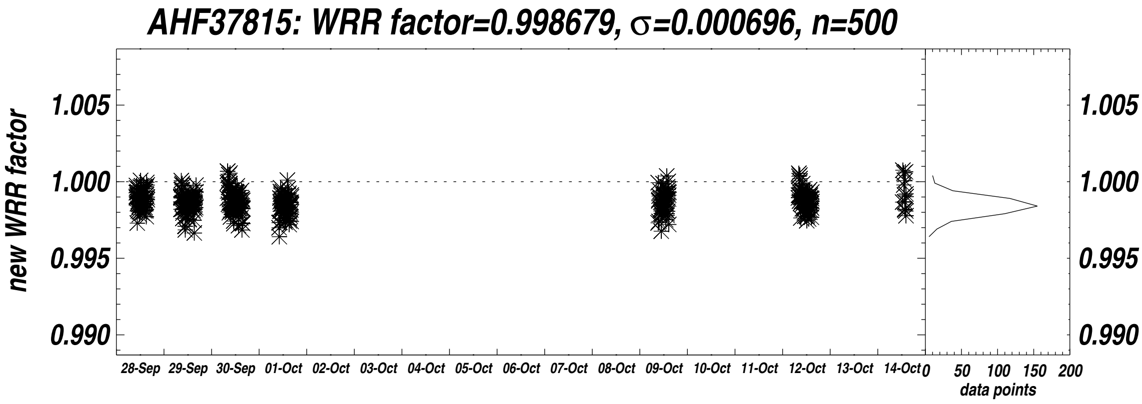
AHF37815: WRR factor=0.998679, σ=0.000696, n=500
new WRR factor
1.005
1.000
0.995
0.990
28-Sep 29-Sep 30-Sep 01-Oct 02-Oct 03-Oct 04-Oct 05-Oct 06-Oct 07-Oct 08-Oct 09-Oct 10-Oct 11-Oct 12-Oct 13-Oct 14-Oct
0 50 100 150 200
data points

AHF37816: WRR factor=0.999458, σ=0.000721, n=248

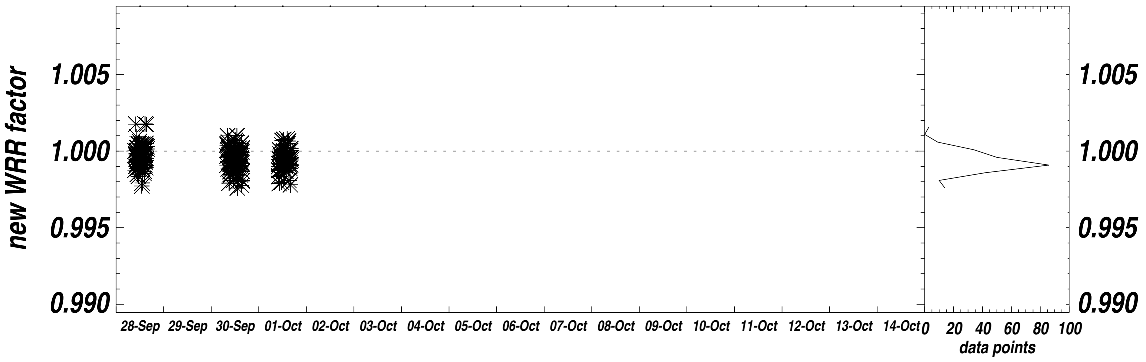

AWX31114: WRR factor=1.001209, σ=0.000693, n=488

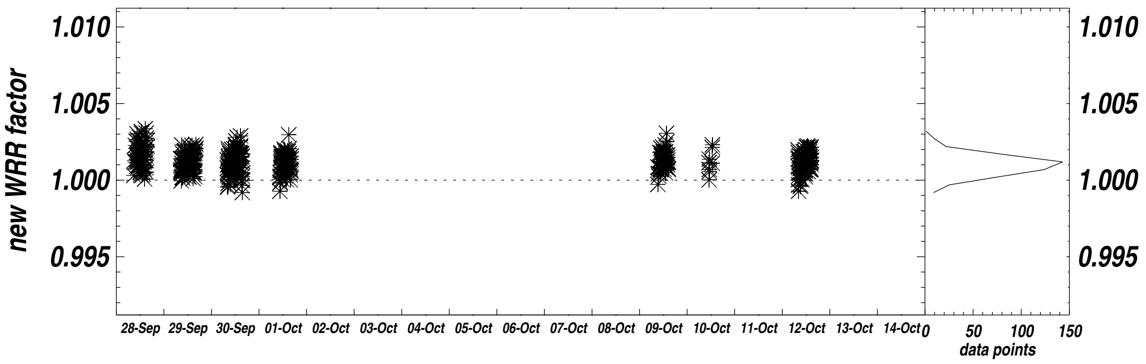

AWX32448: WRR factor=0.999986, σ=0.000737, n=395

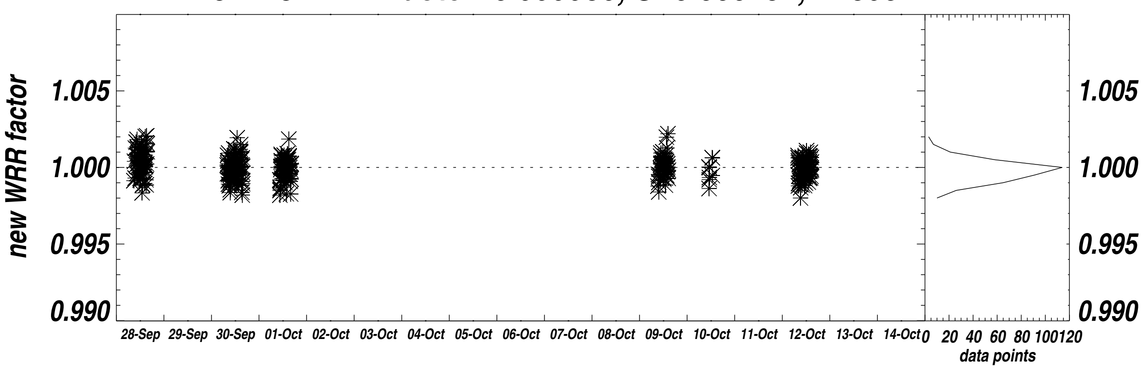

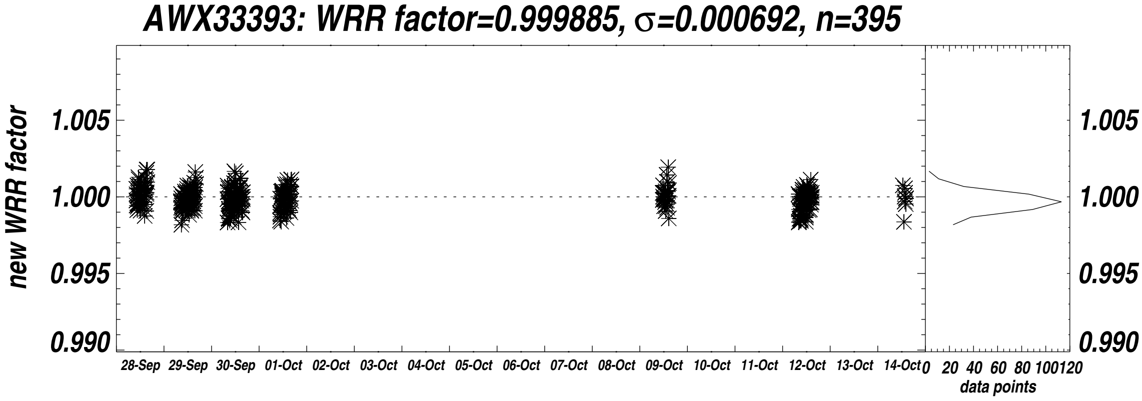
AWX33393: WRR factor=0.999885, σ=0.000692, n=395
new WRR factor
data points

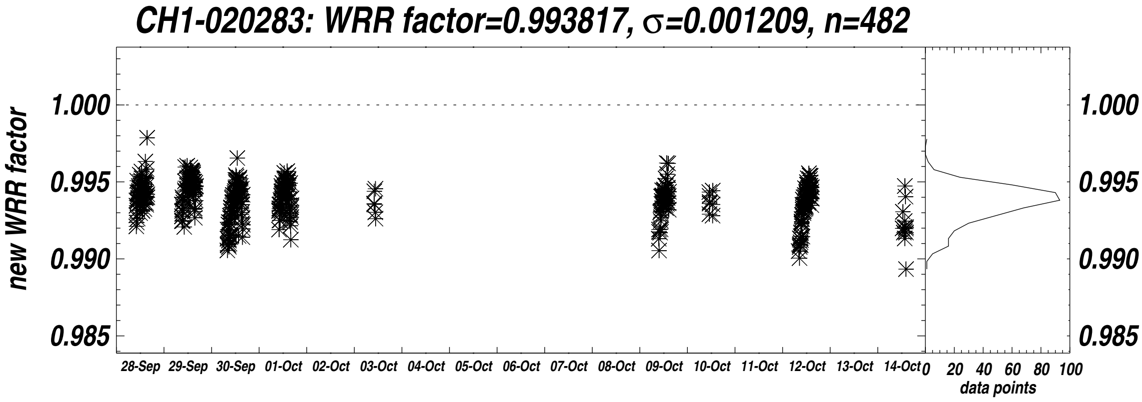
CH1-020283: WRR factor=0.993817, σ=0.001209, n=482
new WRR factor
data points

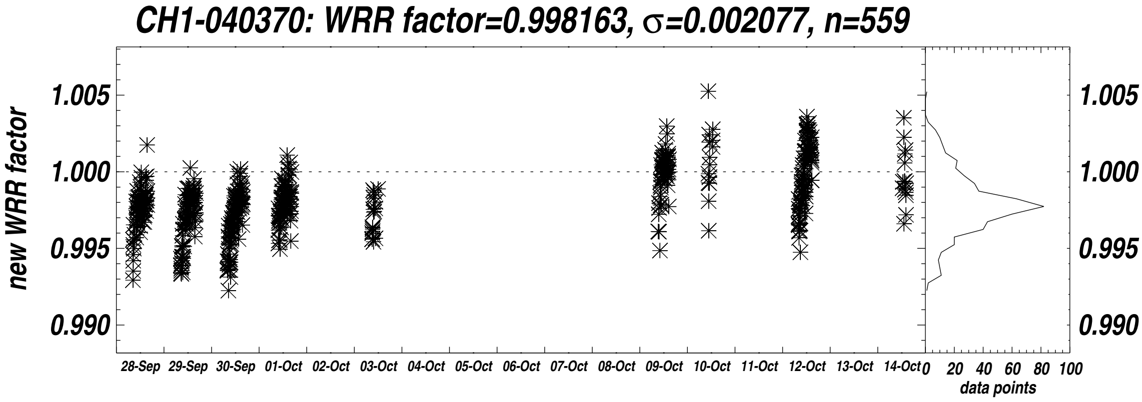
CH1-040370: WRR factor=0.998163, σ=0.002077, n=559
new WRR factor
data points

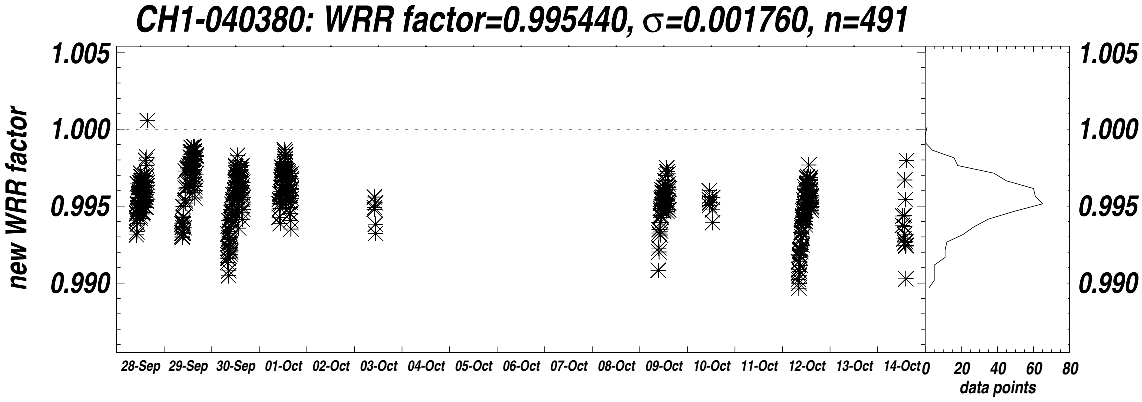
CH1-040380: WRR factor=0.995440, σ=0.001760, n=491
new WRR factor
1.005
1.000
0.995
0.990
28-Sep 29-Sep 30-Sep 01-Oct 02-Oct 03-Oct 04-Oct 05-Oct 06-Oct 07-Oct 08-Oct 09-Oct 10-Oct 11-Oct 12-Oct 13-Oct 14-Oct
0 20 40 60 80
data points

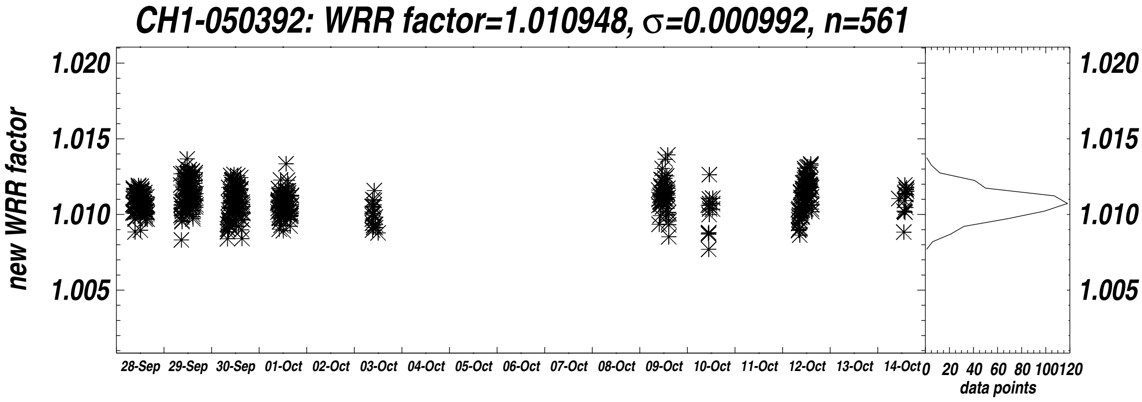
CH1-050392: WRR factor=1.010948, σ=0.000992, n=561
new WRR factor
1.020
1.015
1.010
1.005
28-Sep 29-Sep 30-Sep 01-Oct 02-Oct 03-Oct 04-Oct 05-Oct 06-Oct 07-Oct 08-Oct 09-Oct 10-Oct 11-Oct 12-Oct 13-Oct 14-Oct
0 20 40 60 80 100120
data points

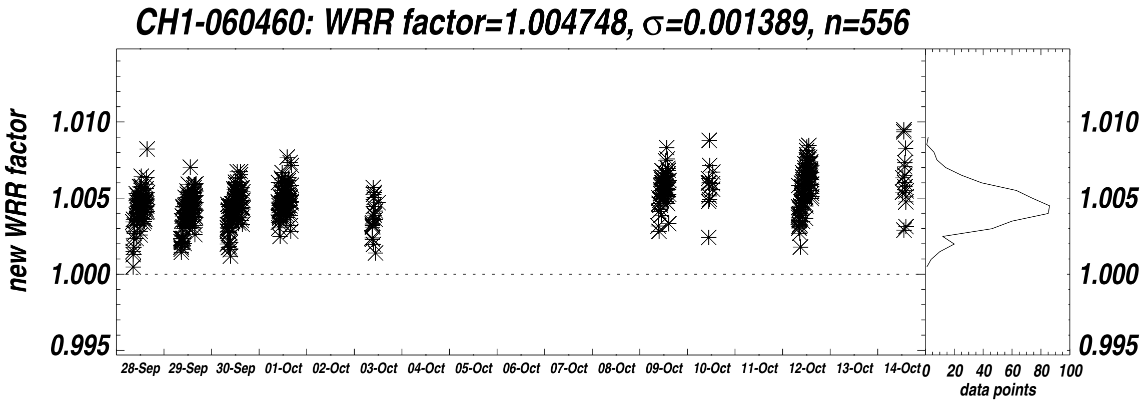
CH1-060460: WRR factor=1.004748, σ=0.001389, n=556
new WRR factor
1.010
1.005
1.000
0.995
28-Sep 29-Sep 30-Sep 01-Oct 02-Oct 03-Oct 04-Oct 05-Oct 06-Oct 07-Oct 08-Oct 09-Oct 10-Oct 11-Oct 12-Oct 13-Oct 14-Oct
0 20 40 60 80 100
data points

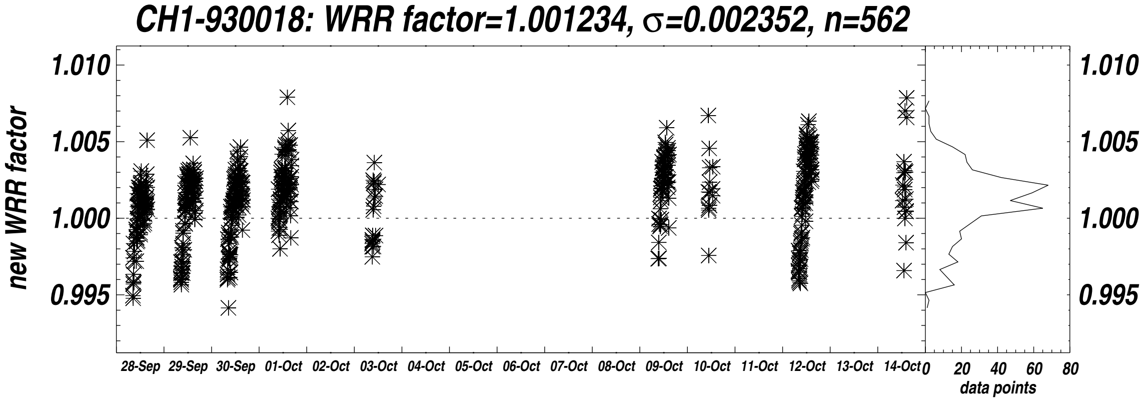
CH1-930018: WRR factor=1.001234, σ=0.002352, n=562
new WRR factor
1.010
1.005
1.000
0.995
28-Sep 29-Sep 30-Sep 01-Oct 02-Oct 03-Oct 04-Oct 05-Oct 06-Oct 07-Oct 08-Oct 09-Oct 10-Oct 11-Oct 12-Oct 13-Oct 14-Oct
0 20 40 60 80
data points

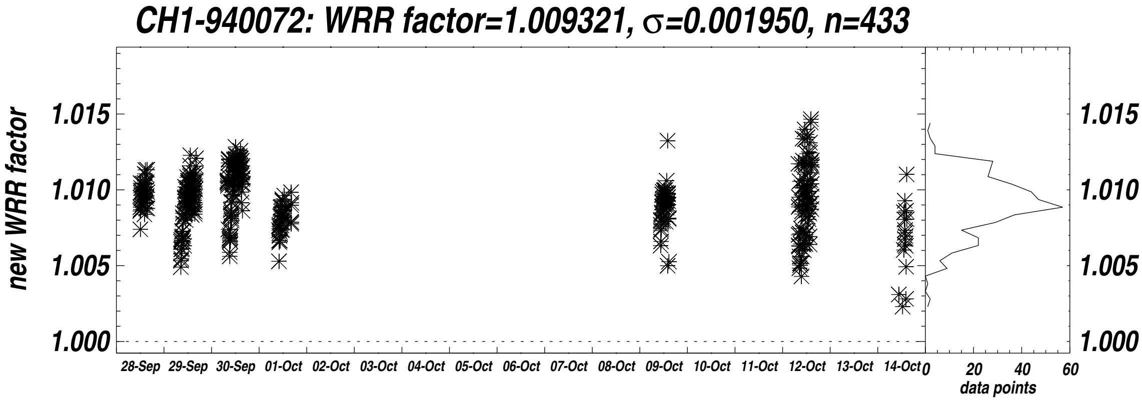
CH1-940072: WRR factor=1.009321, σ=0.001950, n=433
new WRR factor
1.015
1.010
1.005
1.000
28-Sep 29-Sep 30-Sep 01-Oct 02-Oct 03-Oct 04-Oct 05-Oct 06-Oct 07-Oct 08-Oct 09-Oct 10-Oct 11-Oct 12-Oct 13-Oct 14-Oct
0 20 40 60
data points

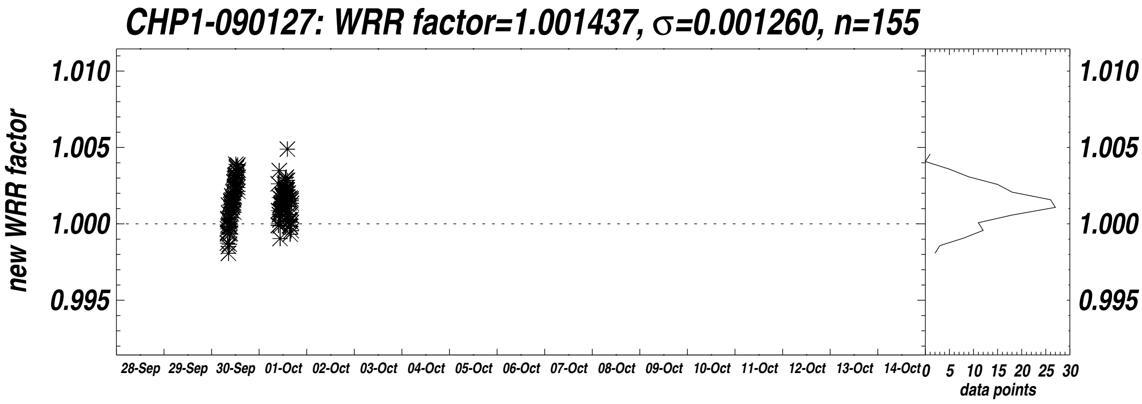
CHP1-090127: WRR factor=1.001437, σ=0.001260, n=155
new WRR factor
1.010
1.005
1.000
0.995
28-Sep 29-Sep 30-Sep 01-Oct 02-Oct 03-Oct 04-Oct 05-Oct 06-Oct 07-Oct 08-Oct 09-Oct 10-Oct 11-Oct 12-Oct 13-Oct 14-Oct
0 5 10 15 20 25 30
data points

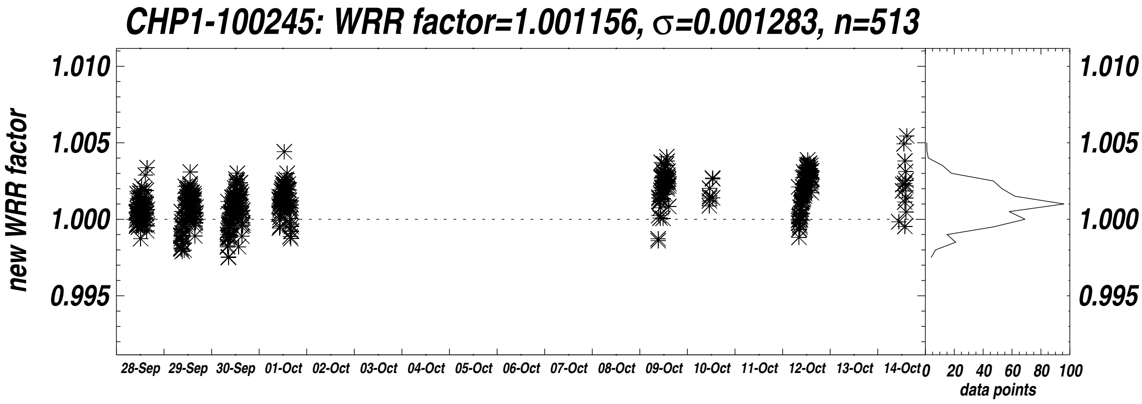
CHP1-100245: WRR factor=1.001156, σ=0.001283, n=513
new WRR factor
1.010
1.005
1.000
0.995
28-Sep 29-Sep 30-Sep 01-Oct 02-Oct 03-Oct 04-Oct 05-Oct 06-Oct 07-Oct 08-Oct 09-Oct 10-Oct 11-Oct 12-Oct 13-Oct 14-Oct
0 20 40 60 80 100
data points

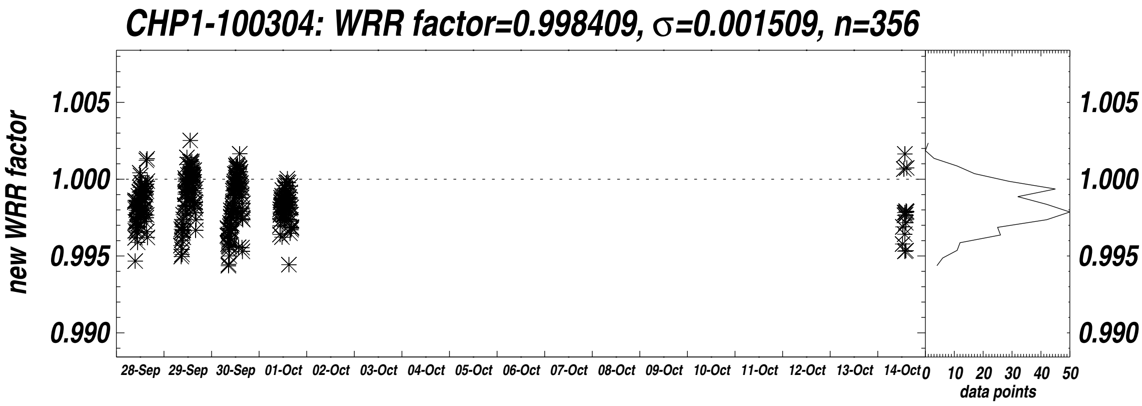
CHP1-100304: WRR factor=0.998409, σ=0.001509, n=356
new WRR factor
1.005
1.000
0.995
0.990
28-Sep 29-Sep 30-Sep 01-Oct 02-Oct 03-Oct 04-Oct 05-Oct 06-Oct 07-Oct 08-Oct 09-Oct 10-Oct 11-Oct 12-Oct 13-Oct 14-Oct
0 10 20 30 40 50
data points

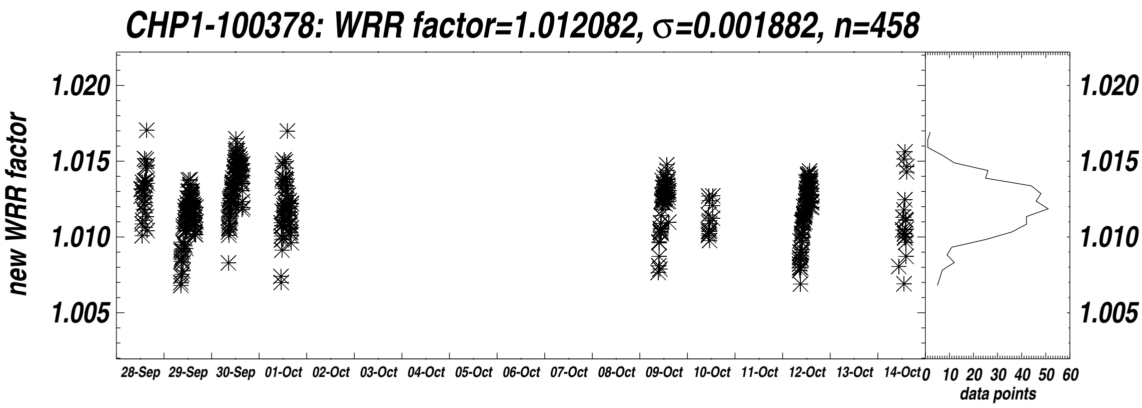
CHP1-100378: WRR factor=1.012082, σ=0.001882, n=458
new WRR factor
1.020
1.015
1.010
1.005
28-Sep 29-Sep 30-Sep 01-Oct 02-Oct 03-Oct 04-Oct 05-Oct 06-Oct 07-Oct 08-Oct 09-Oct 10-Oct 11-Oct 12-Oct 13-Oct 14-Oct
0 10 20 30 40 50 60
data points

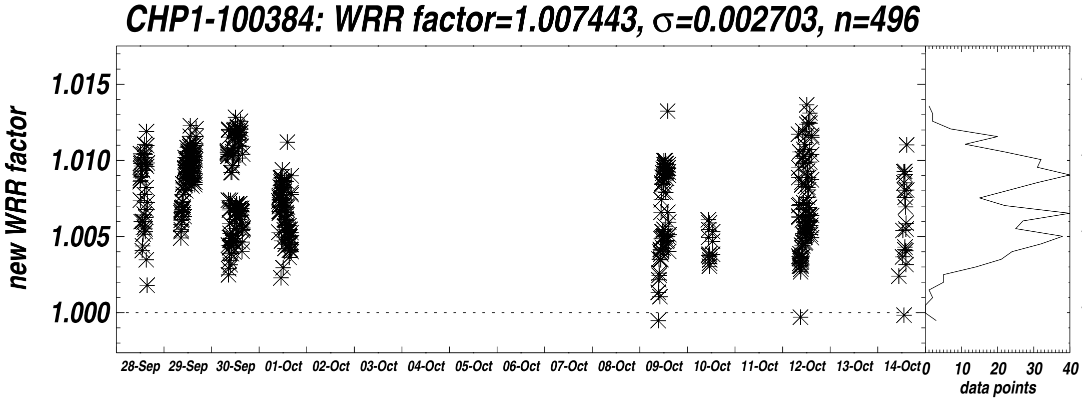
CHP1-100384: WRR factor=1.007443, σ=0.002703, n=496
new WRR factor
1.015
1.010
1.005
1.000
28-Sep 29-Sep 30-Sep 01-Oct 02-Oct 03-Oct 04-Oct 05-Oct 06-Oct 07-Oct 08-Oct 09-Oct 10-Oct 11-Oct 12-Oct 13-Oct 14-Oct
0 10 20 30 40
data points

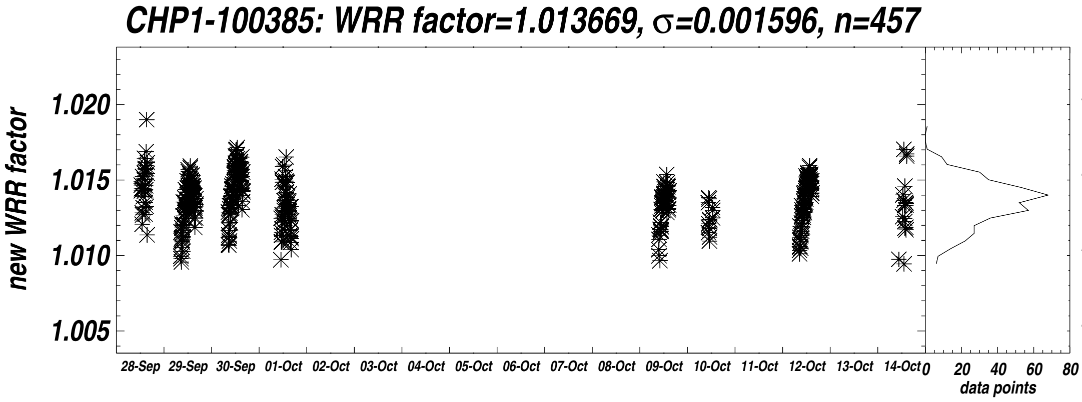
CHP1-100385: WRR factor=1.013669, σ=0.001596, n=457
new WRR factor
1.020
1.015
1.010
1.005
28-Sep 29-Sep 30-Sep 01-Oct 02-Oct 03-Oct 04-Oct 05-Oct 06-Oct 07-Oct 08-Oct 09-Oct 10-Oct 11-Oct 12-Oct 13-Oct 14-Oct
0 20 40 60 80
data points

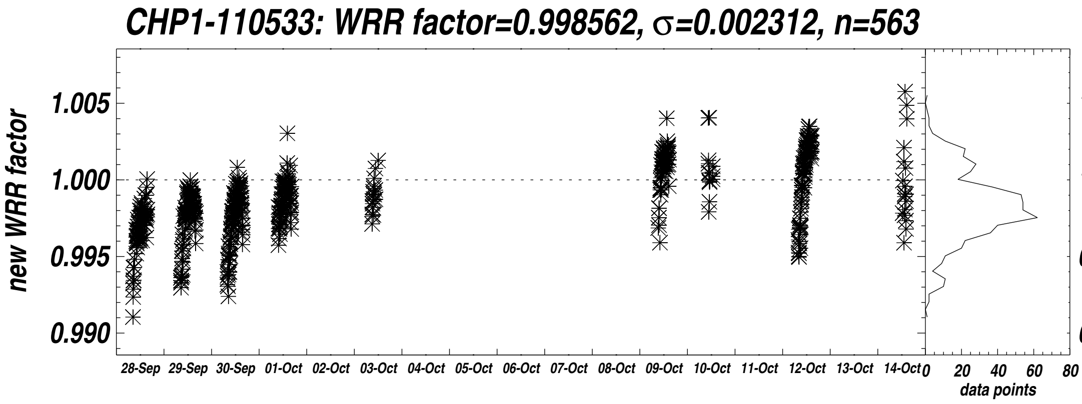
CHP1-110533: WRR factor=0.998562, σ=0.002312, n=563
new WRR factor
1.005
1.000
0.995
0.990
28-Sep 29-Sep 30-Sep 01-Oct 02-Oct 03-Oct 04-Oct 05-Oct 06-Oct 07-Oct 08-Oct 09-Oct 10-Oct 11-Oct 12-Oct 13-Oct 14-Oct
0 20 40 60 80
data points

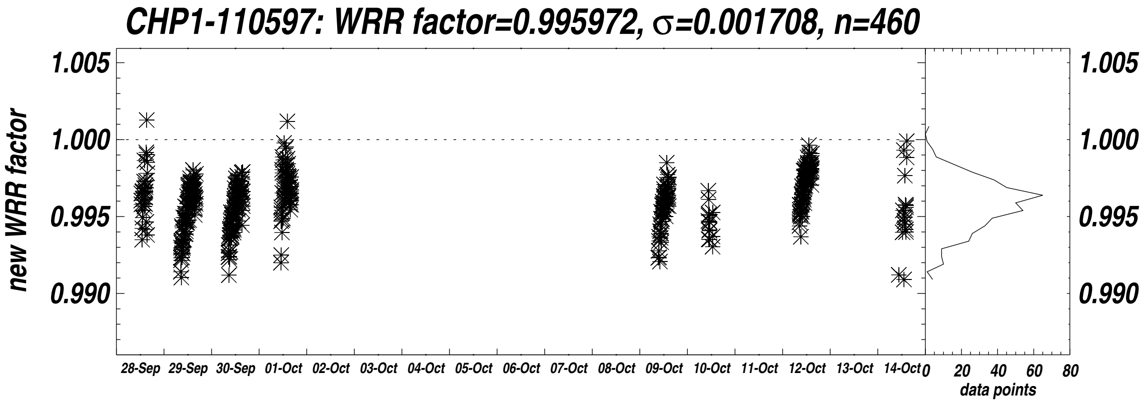
CHP1-110597: WRR factor=0.995972, σ=0.001708, n=460
new WRR factor
data points

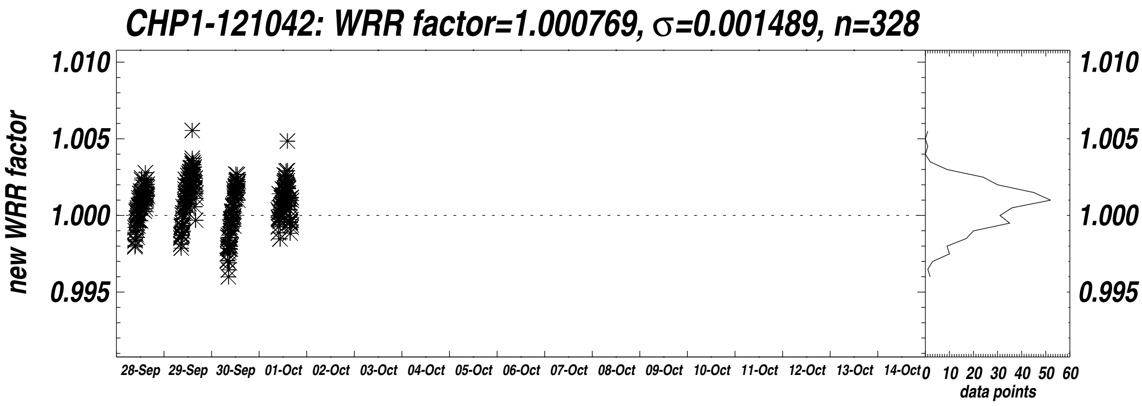
CHP1-121042: WRR factor=1.000769, σ=0.001489, n=328
new WRR factor
data points

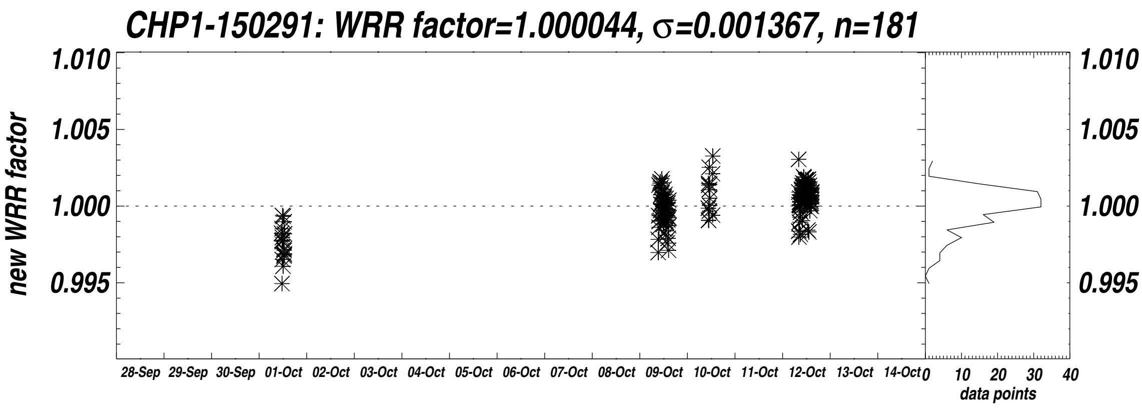
CHP1-150291: WRR factor=1.000044, σ=0.001367, n=181
new WRR factor
data points

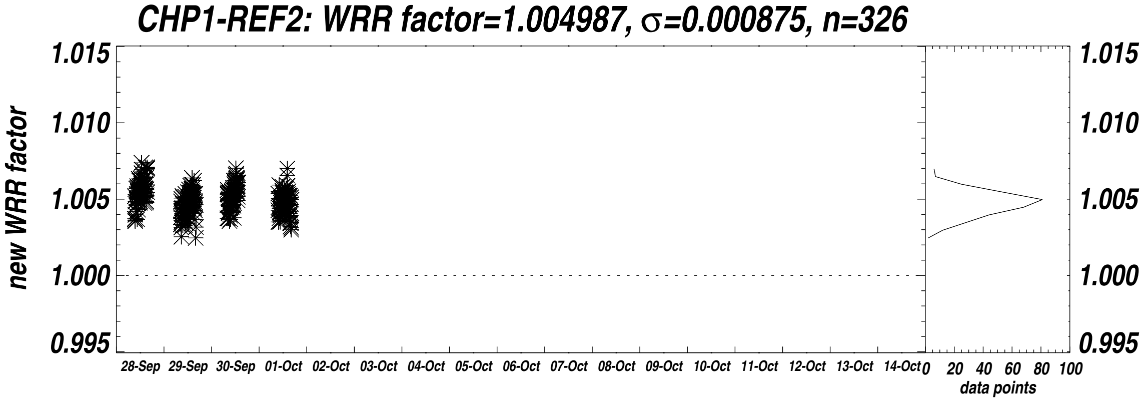
CHP1-REF2: WRR factor=1.004987, σ=0.000875, n=326
new WRR factor
data points

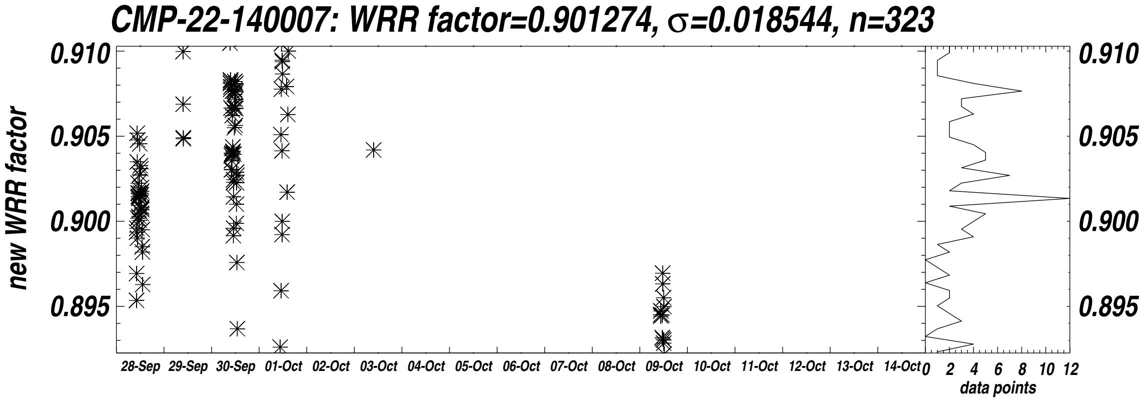
CMP-22-140007: WRR factor=0.901274, σ=0.018544, n=323
new WRR factor
data points

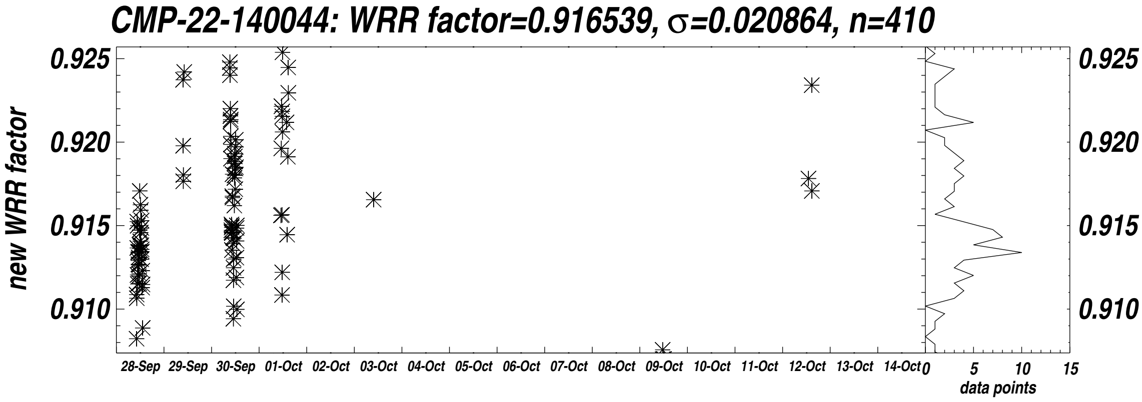
CMP-22-140044: WRR factor=0.916539, σ=0.020864, n=410
new WRR factor
data points

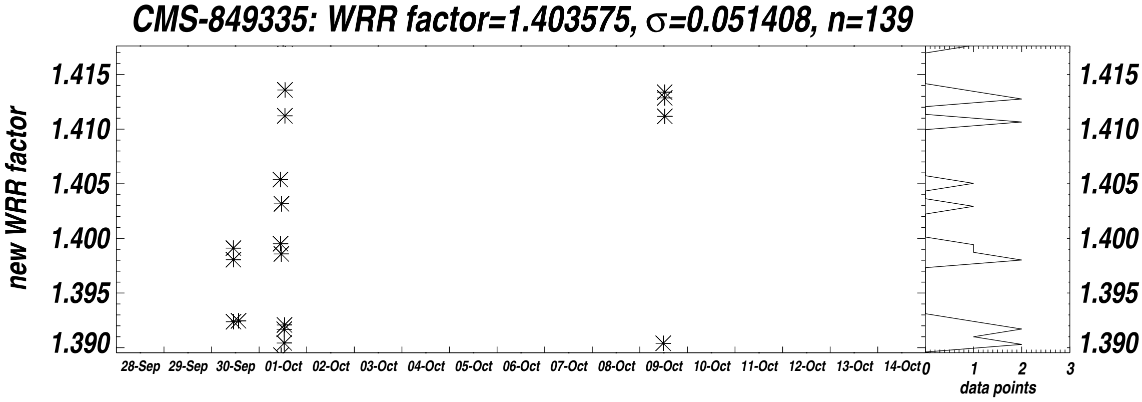
CMS-849335: WRR factor=1.403575, σ=0.051408, n=139
new WRR factor
1.415
1.410
1.405
1.400
1.395
1.390
28-Sep 29-Sep 30-Sep 01-Oct 02-Oct 03-Oct 04-Oct 05-Oct 06-Oct 07-Oct 08-Oct 09-Oct 10-Oct 11-Oct 12-Oct 13-Oct 14-Oct
0 1 2 3
data points

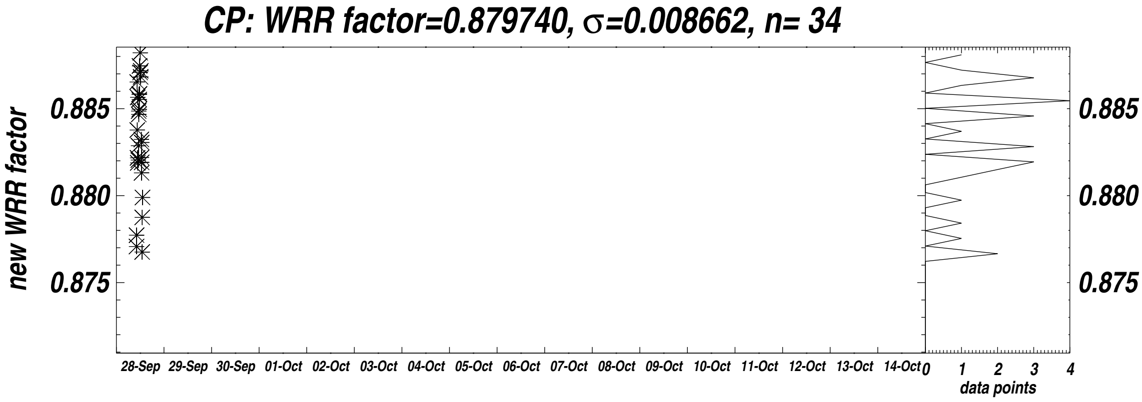
CP: WRR factor=0.879740, σ=0.008662, n= 34
new WRR factor
0.885
0.880
0.875
28-Sep 29-Sep 30-Sep 01-Oct 02-Oct 03-Oct 04-Oct 05-Oct 06-Oct 07-Oct 08-Oct 09-Oct 10-Oct 11-Oct 12-Oct 13-Oct 14-Oct
0 1 2 3 4
data points

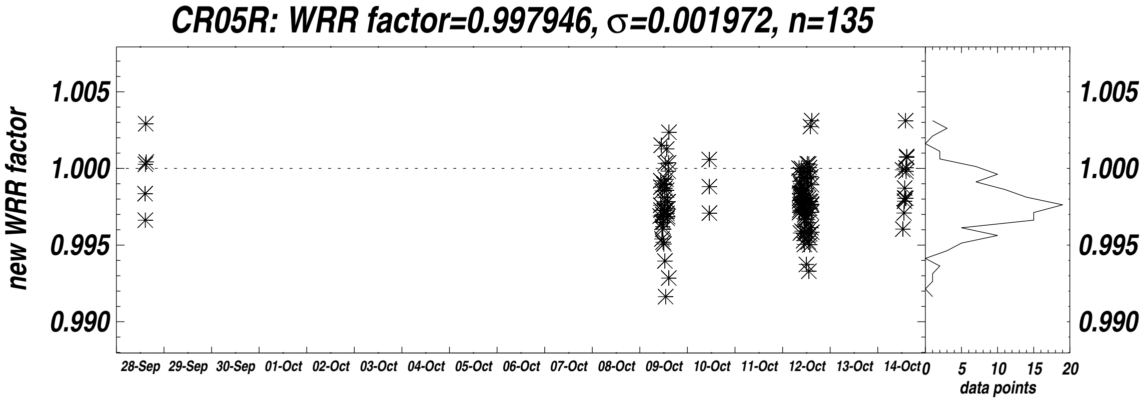
CR05R: WRR factor=0.997946, σ=0.001972, n=135
new WRR factor
1.005
1.000
0.995
0.990
28-Sep 29-Sep 30-Sep 01-Oct 02-Oct 03-Oct 04-Oct 05-Oct 06-Oct 07-Oct 08-Oct 09-Oct 10-Oct 11-Oct 12-Oct 13-Oct 14-Oct
0 5 10 15 20
data points

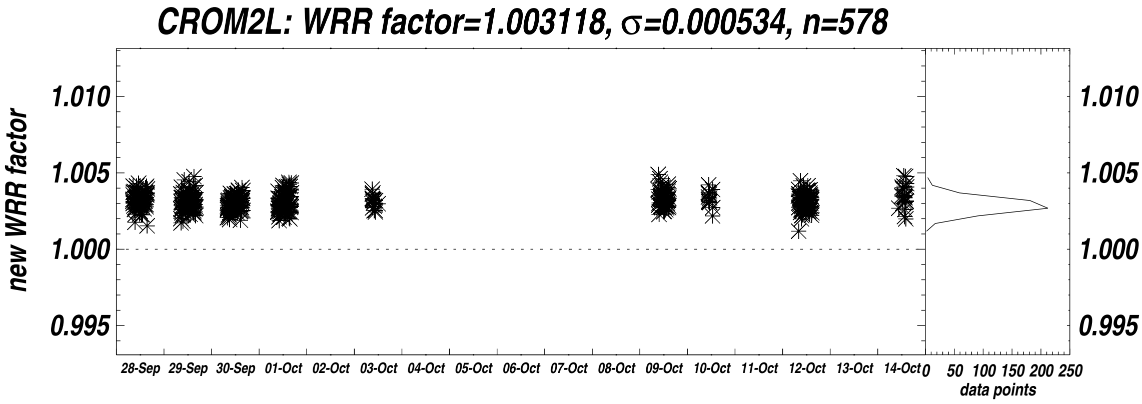
CROM2L: WRR factor=1.003118, σ=0.000534, n=578
new WRR factor
1.010
1.005
1.000
0.995
28-Sep 29-Sep 30-Sep 01-Oct 02-Oct 03-Oct 04-Oct 05-Oct 06-Oct 07-Oct 08-Oct 09-Oct 10-Oct 11-Oct 12-Oct 13-Oct 14-Oct
0 50 100 150 200 250
data points

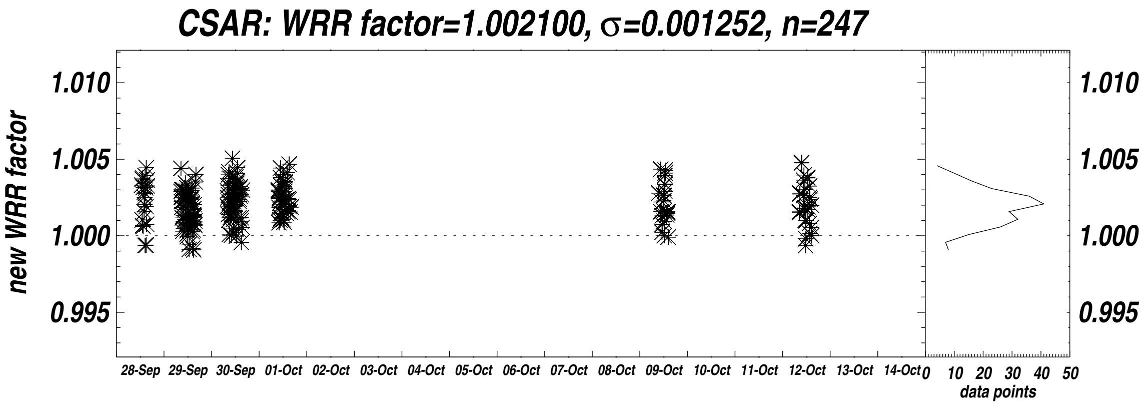
CSAR: WRR factor=1.002100, σ=0.001252, n=247
new WRR factor
1.010
1.005
1.000
0.995
28-Sep 29-Sep 30-Sep 01-Oct 02-Oct 03-Oct 04-Oct 05-Oct 06-Oct 07-Oct 08-Oct 09-Oct 10-Oct 11-Oct 12-Oct 13-Oct 14-Oct
0 10 20 30 40 50
data points

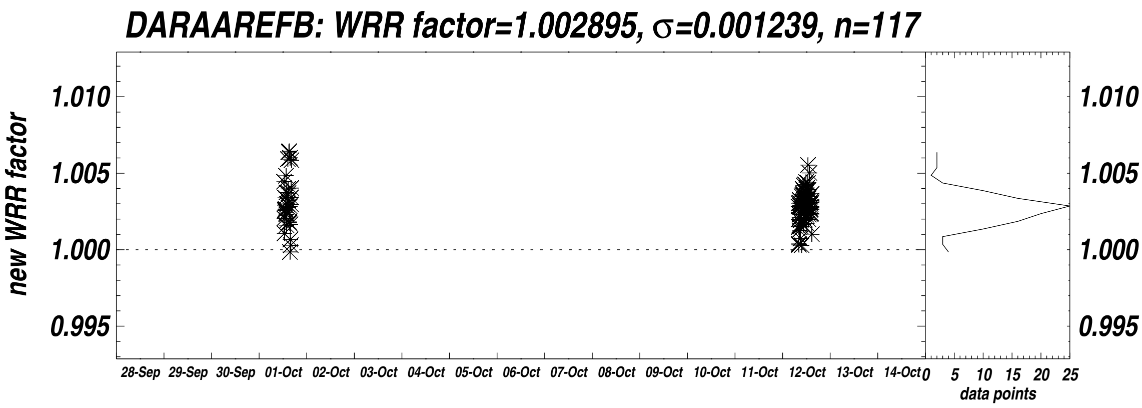
DARAAREFB: WRR factor=1.002895, σ=0.001239, n=117
new WRR factor
1.010
1.005
1.000
0.995
28-Sep 29-Sep 30-Sep 01-Oct 02-Oct 03-Oct 04-Oct 05-Oct 06-Oct 07-Oct 08-Oct 09-Oct 10-Oct 11-Oct 12-Oct 13-Oct 14-Oct
0 5 10 15 20 25
data points

DR01-8348: WRR factor=0.106812, σ=0.000181, n=357

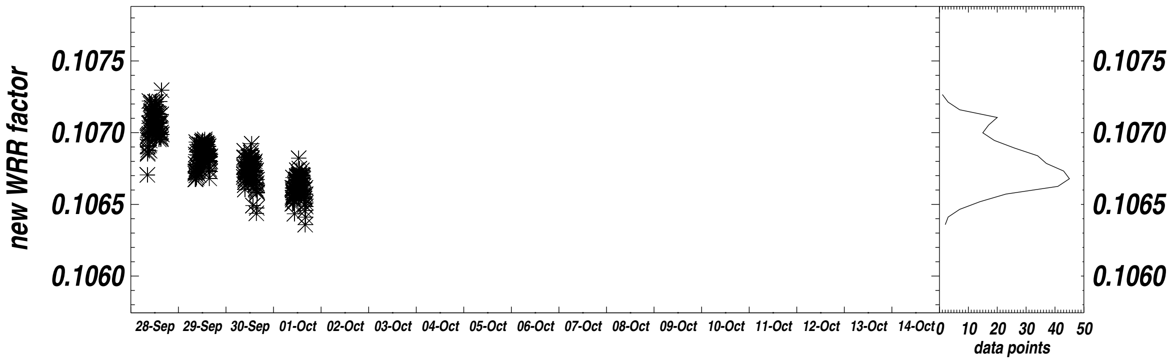

DR01-8377: WRR factor=0.081904, σ=0.000107, n=356

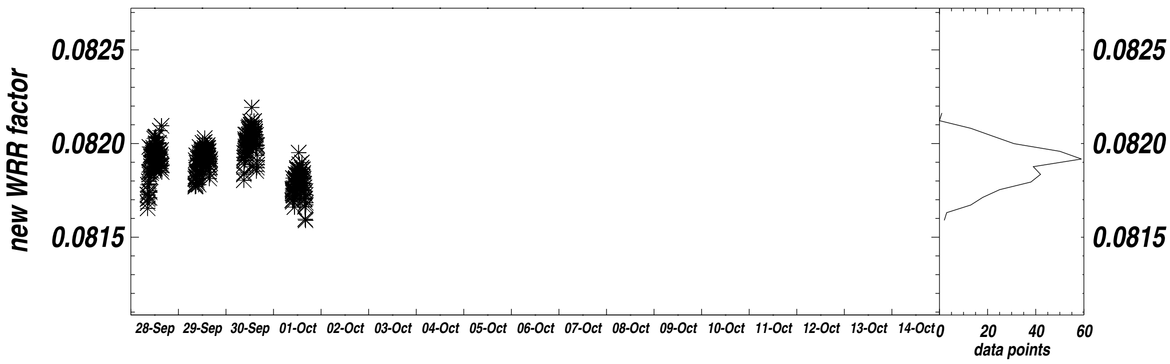

DR02-9191: WRR factor=0.084729, σ=0.000096, n=354

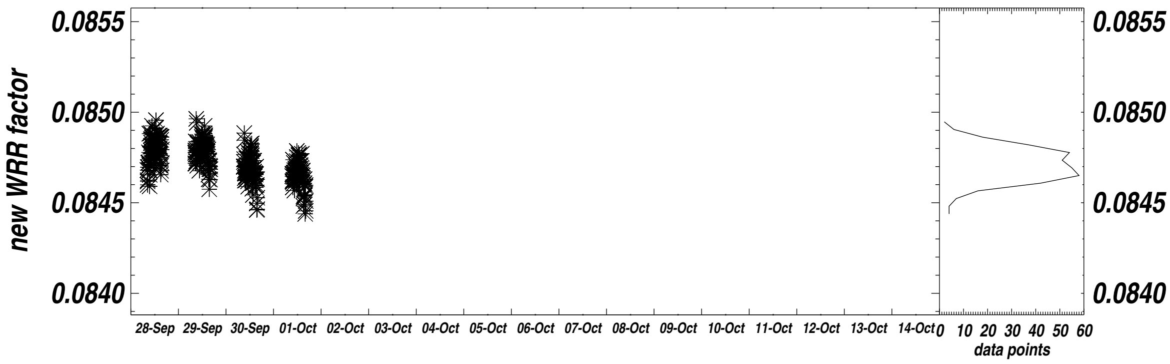

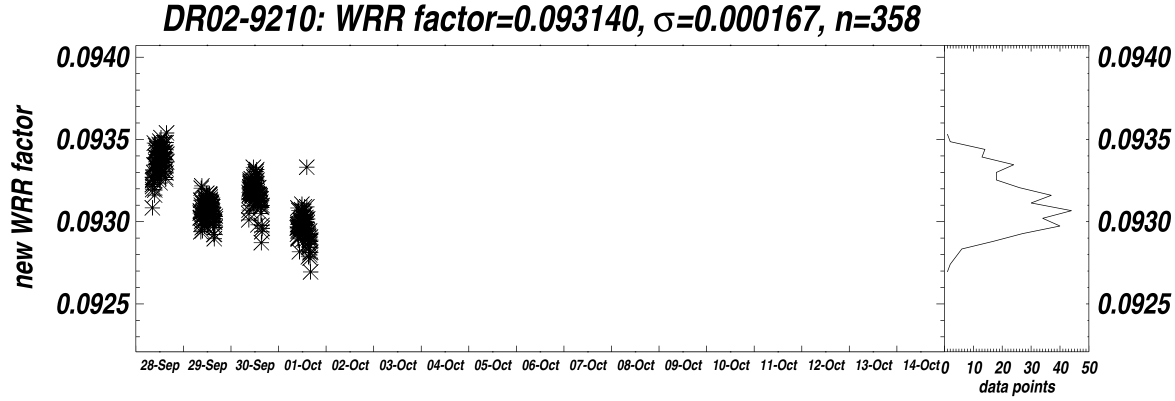
DR02-9210: WRR factor=0.093140, σ=0.000167, n=358
new WRR factor
0.0940
0.0935
0.0930
0.0925
28-Sep 29-Sep 30-Sep 01-Oct 02-Oct 03-Oct 04-Oct 05-Oct 06-Oct 07-Oct 08-Oct 09-Oct 10-Oct 11-Oct 12-Oct 13-Oct 14-Oct
0 10 20 30 40 50
data points

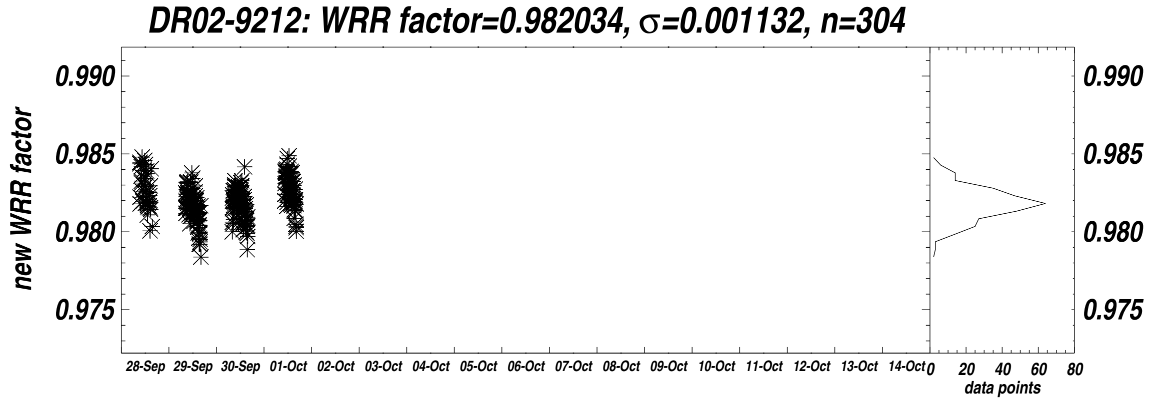
DR02-9212: WRR factor=0.982034, σ=0.001132, n=304
new WRR factor
0.990
0.985
0.980
0.975
28-Sep 29-Sep 30-Sep 01-Oct 02-Oct 03-Oct 04-Oct 05-Oct 06-Oct 07-Oct 08-Oct 09-Oct 10-Oct 11-Oct 12-Oct 13-Oct 14-Oct
0 20 40 60 80
data points

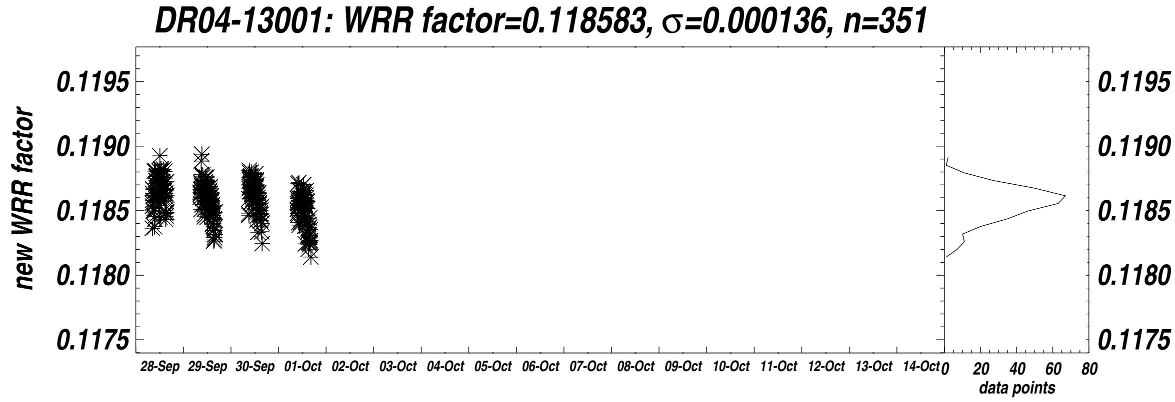
DR04-13001: WRR factor=0.118583, σ=0.000136, n=351
new WRR factor
0.1195
0.1190
0.1185
0.1180
0.1175
28-Sep 29-Sep 30-Sep 01-Oct 02-Oct 03-Oct 04-Oct 05-Oct 06-Oct 07-Oct 08-Oct 09-Oct 10-Oct 11-Oct 12-Oct 13-Oct 14-Oct
0 20 40 60 80
data points

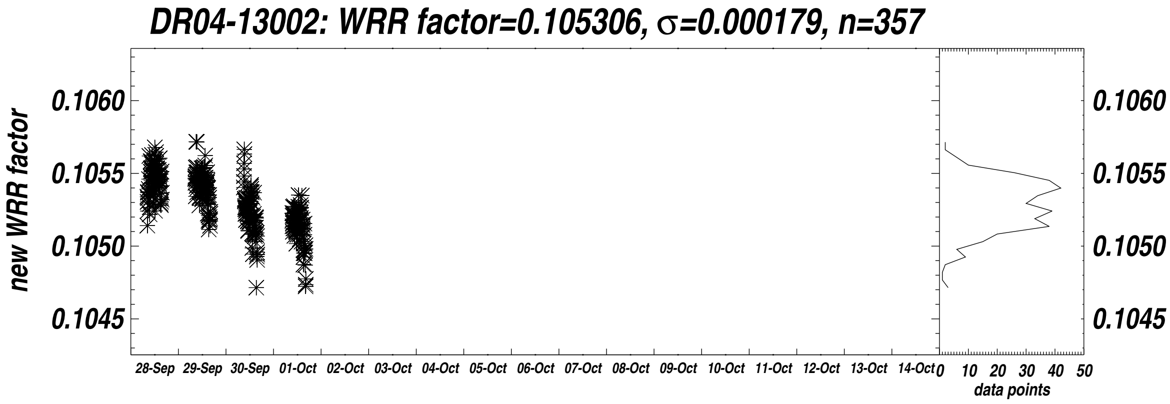
DR04-13002: WRR factor=0.105306, σ=0.000179, n=357
new WRR factor
0.1060
0.1055
0.1050
0.1045
28-Sep 29-Sep 30-Sep 01-Oct 02-Oct 03-Oct 04-Oct 05-Oct 06-Oct 07-Oct 08-Oct 09-Oct 10-Oct 11-Oct 12-Oct 13-Oct 14-Oct
0 10 20 30 40 50
data points

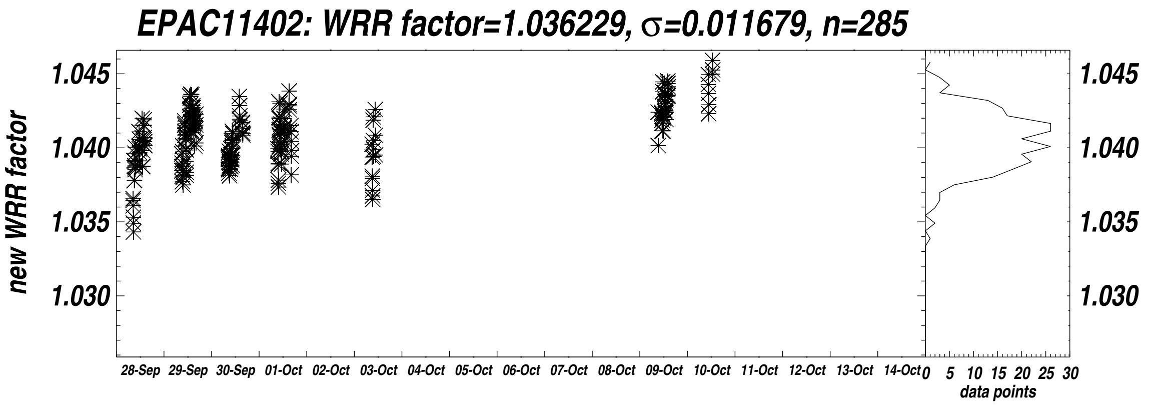
EPAC11402: WRR factor=1.036229, σ=0.011679, n=285
new WRR factor
1.045
1.040
1.035
1.030
28-Sep 29-Sep 30-Sep 01-Oct 02-Oct 03-Oct 04-Oct 05-Oct 06-Oct 07-Oct 08-Oct 09-Oct 10-Oct 11-Oct 12-Oct 13-Oct 14-Oct
0 5 10 15 20 25 30
data points

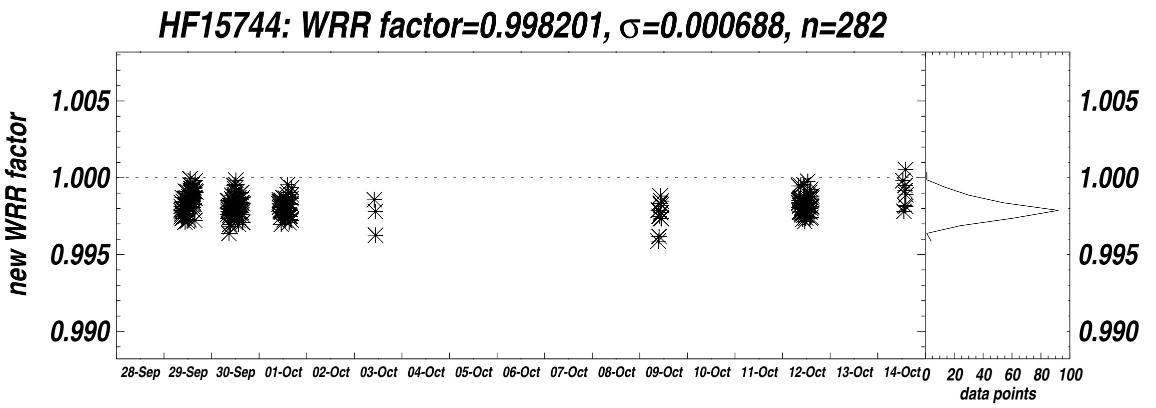
HF15744: WRR factor=0.998201, σ=0.000688, n=282
new WRR factor
1.005
1.000
0.995
0.990
28-Sep 29-Sep 30-Sep 01-Oct 02-Oct 03-Oct 04-Oct 05-Oct 06-Oct 07-Oct 08-Oct 09-Oct 10-Oct 11-Oct 12-Oct 13-Oct 14-Oct
0 20 40 60 80 100
data points

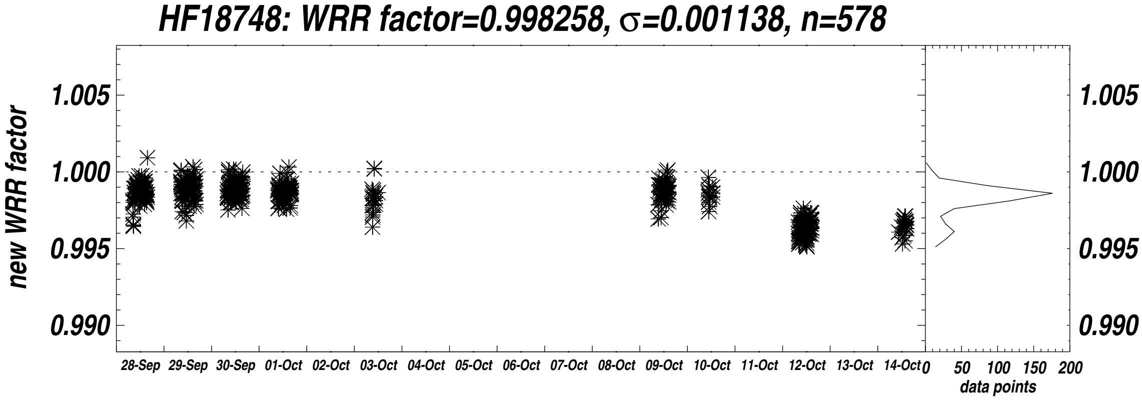
HF18748: WRR factor=0.998258, σ=0.001138, n=578
new WRR factor
1.005
1.000
0.995
0.990
28-Sep 29-Sep 30-Sep 01-Oct 02-Oct 03-Oct 04-Oct 05-Oct 06-Oct 07-Oct 08-Oct 09-Oct 10-Oct 11-Oct 12-Oct 13-Oct 14-Oct
0 50 100 150 200
data points

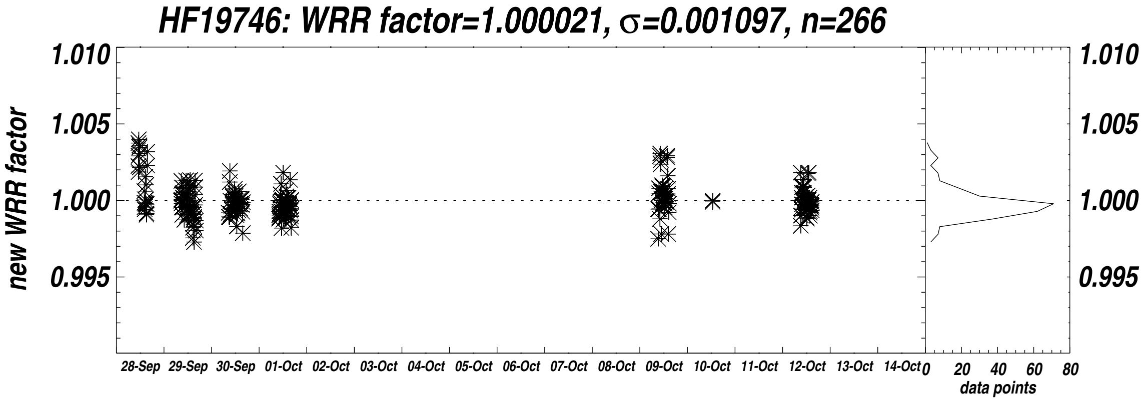
HF19746: WRR factor=1.000021, σ=0.001097, n=266
new WRR factor
1.010
1.005
1.000
0.995
28-Sep 29-Sep 30-Sep 01-Oct 02-Oct 03-Oct 04-Oct 05-Oct 06-Oct 07-Oct 08-Oct 09-Oct 10-Oct 11-Oct 12-Oct 13-Oct 14-Oct
0 20 40 60 80
data points

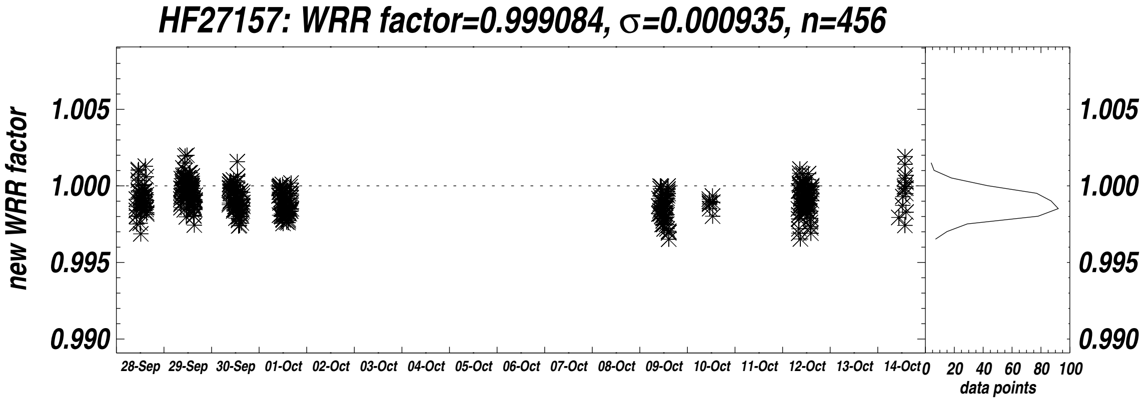
HF27157: WRR factor=0.999084, σ=0.000935, n=456
new WRR factor
1.005
1.000
0.995
0.990
28-Sep 29-Sep 30-Sep 01-Oct 02-Oct 03-Oct 04-Oct 05-Oct 06-Oct 07-Oct 08-Oct 09-Oct 10-Oct 11-Oct 12-Oct 13-Oct 14-Oct
0 20 40 60 80 100
data points

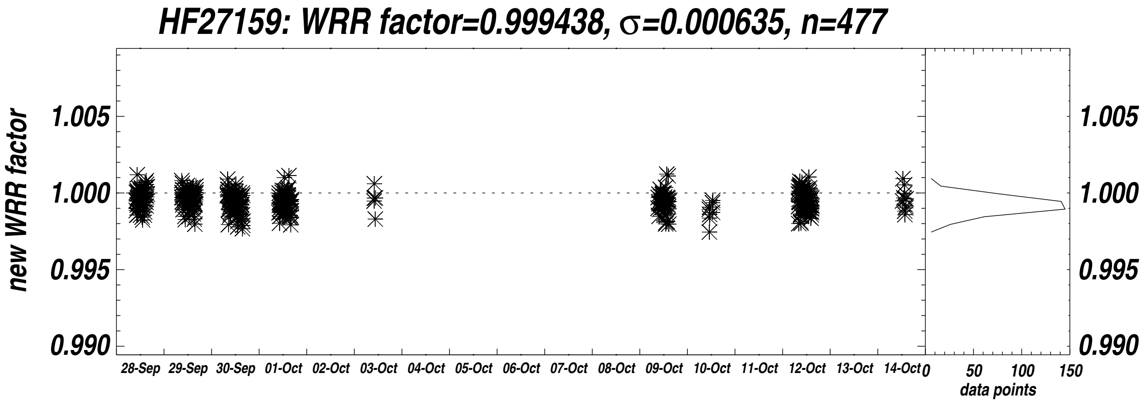
HF27159: WRR factor=0.999438, σ=0.000635, n=477
new WRR factor
1.005
1.000
0.995
0.990
28-Sep 29-Sep 30-Sep 01-Oct 02-Oct 03-Oct 04-Oct 05-Oct 06-Oct 07-Oct 08-Oct 09-Oct 10-Oct 11-Oct 12-Oct 13-Oct 14-Oct
0 50 100 150
data points

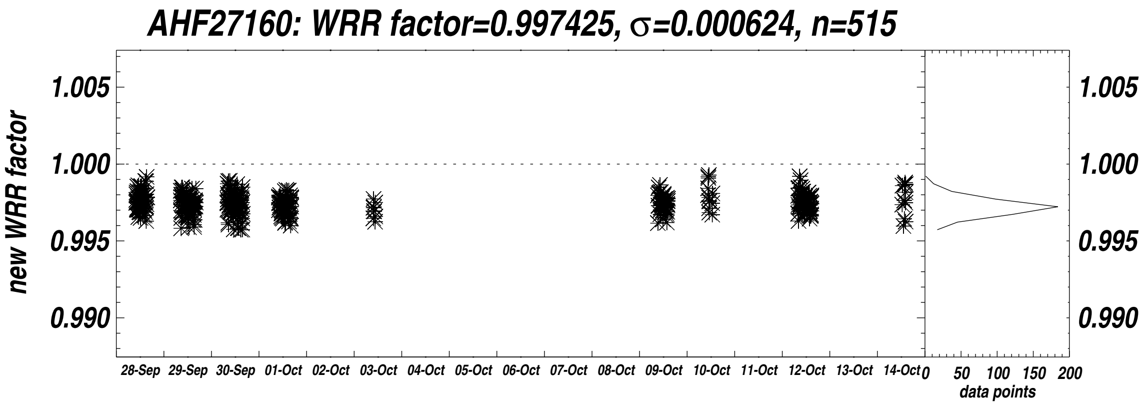
AHF27160: WRR factor=0.997425, σ=0.000624, n=515
new WRR factor
1.005
1.000
0.995
0.990
28-Sep 29-Sep 30-Sep 01-Oct 02-Oct 03-Oct 04-Oct 05-Oct 06-Oct 07-Oct 08-Oct 09-Oct 10-Oct 11-Oct 12-Oct 13-Oct 14-Oct
0 50 100 150 200
data points

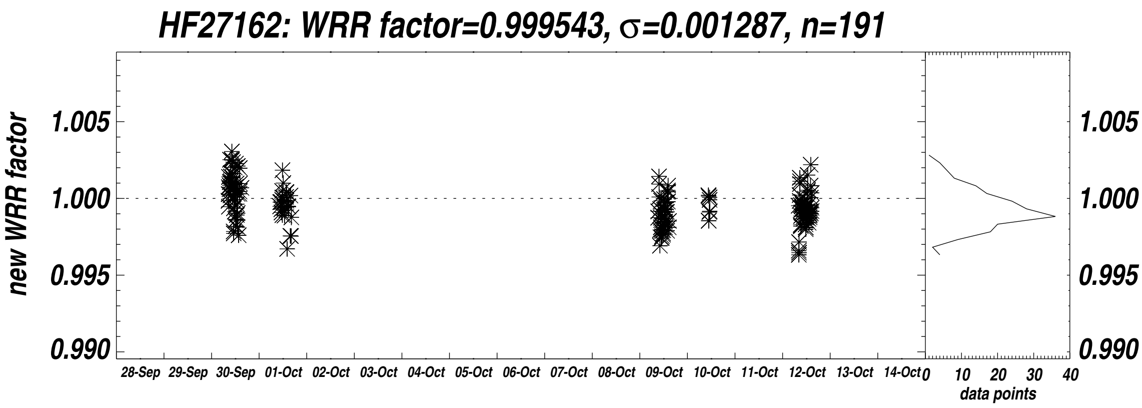
HF27162: WRR factor=0.999543, σ=0.001287, n=191
new WRR factor
1.005
1.000
0.995
0.990
28-Sep 29-Sep 30-Sep 01-Oct 02-Oct 03-Oct 04-Oct 05-Oct 06-Oct 07-Oct 08-Oct 09-Oct 10-Oct 11-Oct 12-Oct 13-Oct 14-Oct
0 10 20 30 40
data points

HF27796: WRR factor=0.996033, σ=0.001454, n=271

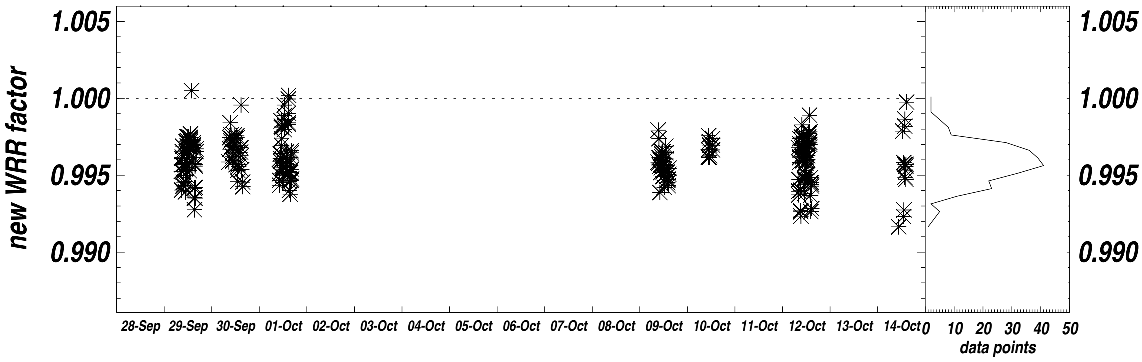

AHF30497: WRR factor=0.999590, σ=0.000600, n=483

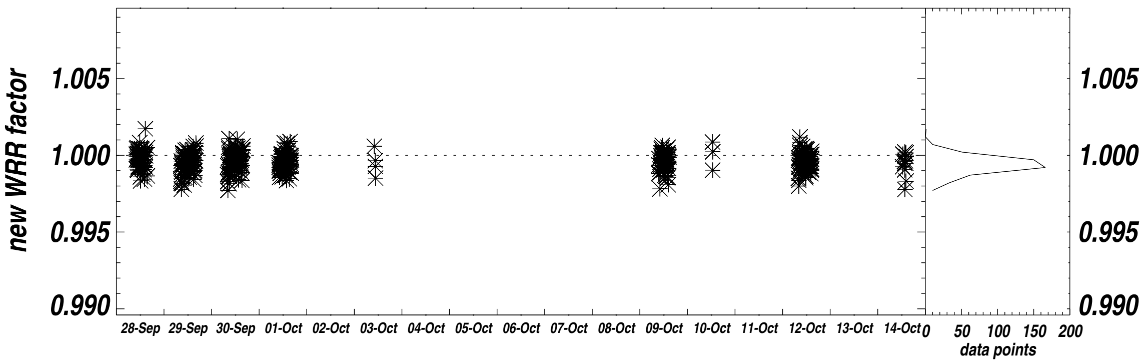

IRS02-1504: WRR factor=0.991175, σ=0.005399, n=297

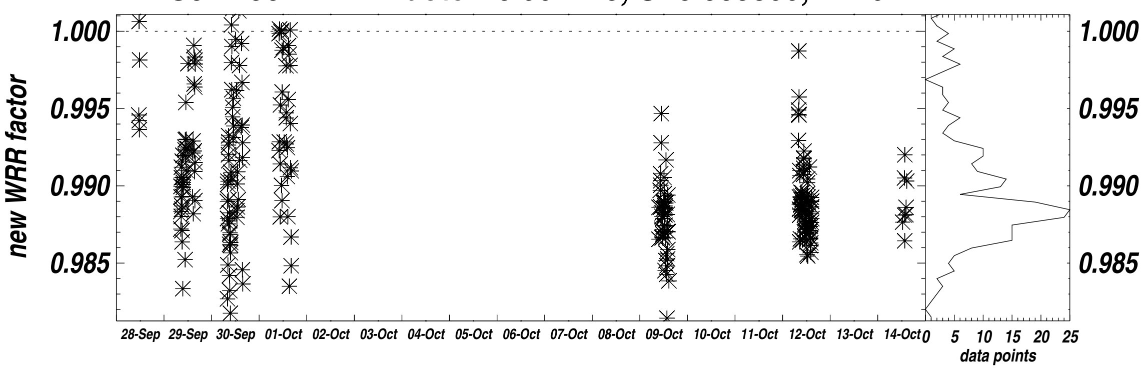

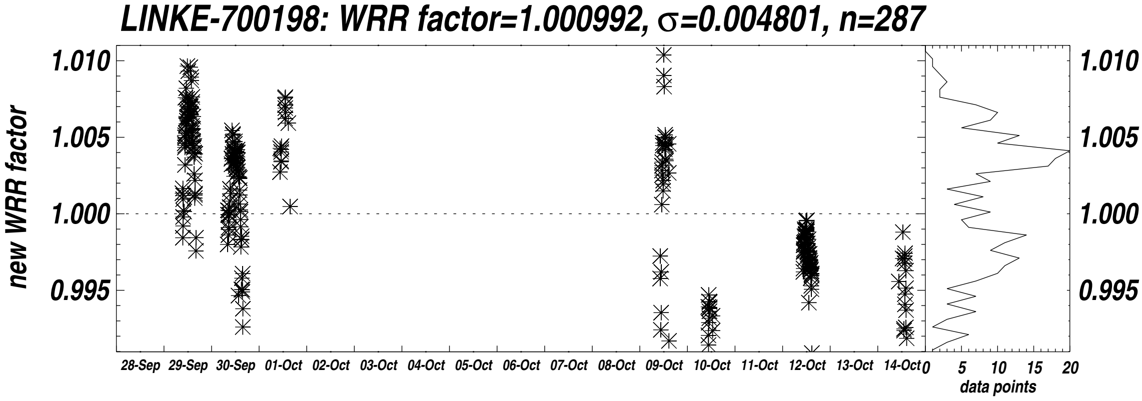
LINKE-700198: WRR factor=1.000992, σ=0.004801, n=287
new WRR factor
1.010
1.005
1.000
0.995
28-Sep 29-Sep 30-Sep 01-Oct 02-Oct 03-Oct 04-Oct 05-Oct 06-Oct 07-Oct 08-Oct 09-Oct 10-Oct 11-Oct 12-Oct 13-Oct 14-Oct
0 5 10 15 20
data points

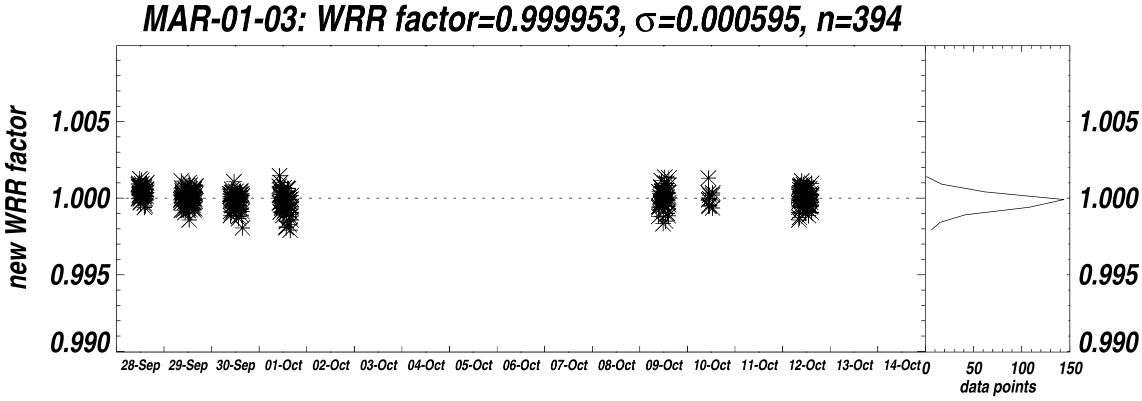
MAR-01-03: WRR factor=0.999953, σ=0.000595, n=394
new WRR factor
1.005
1.000
0.995
0.990
28-Sep 29-Sep 30-Sep 01-Oct 02-Oct 03-Oct 04-Oct 05-Oct 06-Oct 07-Oct 08-Oct 09-Oct 10-Oct 11-Oct 12-Oct 13-Oct 14-Oct
0 50 100 150
data points

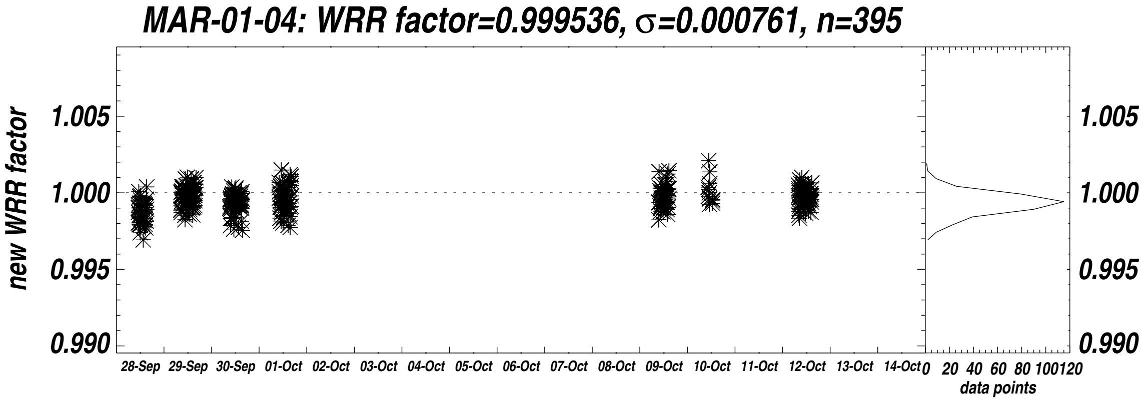
MAR-01-04: WRR factor=0.999536, σ=0.000761, n=395
new WRR factor
1.005
1.000
0.995
0.990
28-Sep 29-Sep 30-Sep 01-Oct 02-Oct 03-Oct 04-Oct 05-Oct 06-Oct 07-Oct 08-Oct 09-Oct 10-Oct 11-Oct 12-Oct 13-Oct 14-Oct
0 20 40 60 80 100 120
data points

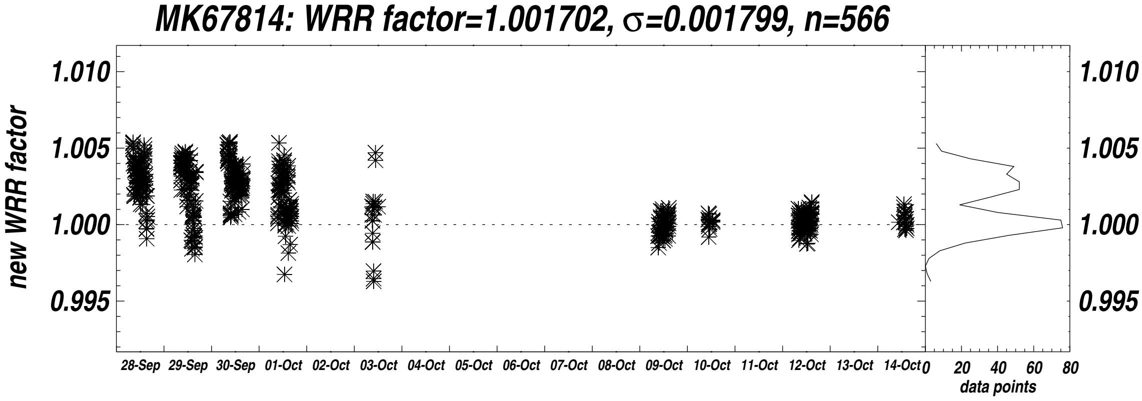
MK67814: WRR factor=1.001702, σ=0.001799, n=566
new WRR factor
1.010
1.005
1.000
0.995
28-Sep 29-Sep 30-Sep 01-Oct 02-Oct 03-Oct 04-Oct 05-Oct 06-Oct 07-Oct 08-Oct 09-Oct 10-Oct 11-Oct 12-Oct 13-Oct 14-Oct
0 20 40 60 80
data points

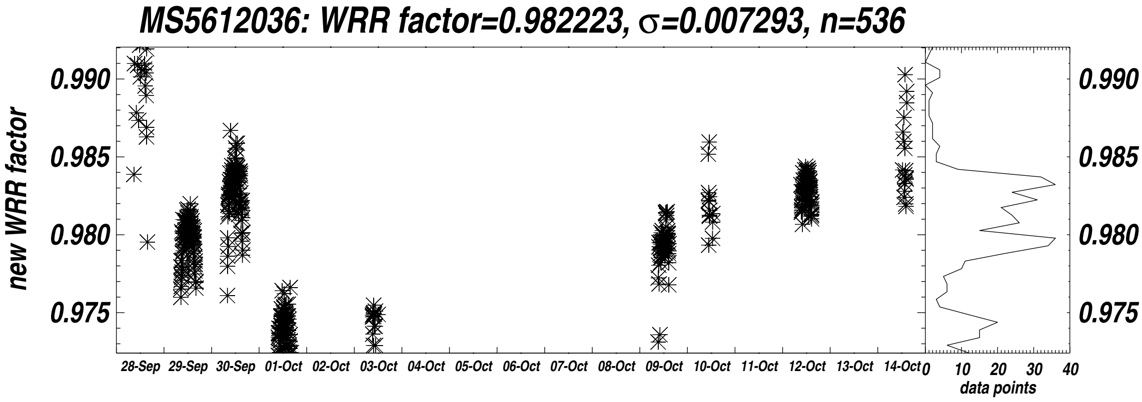
MS5612036: WRR factor=0.982223, σ=0.007293, n=536
new WRR factor
0.990
0.985
0.980
0.975
28-Sep 29-Sep 30-Sep 01-Oct 02-Oct 03-Oct 04-Oct 05-Oct 06-Oct 07-Oct 08-Oct 09-Oct 10-Oct 11-Oct 12-Oct 13-Oct 14-Oct
0 10 20 30 40
data points

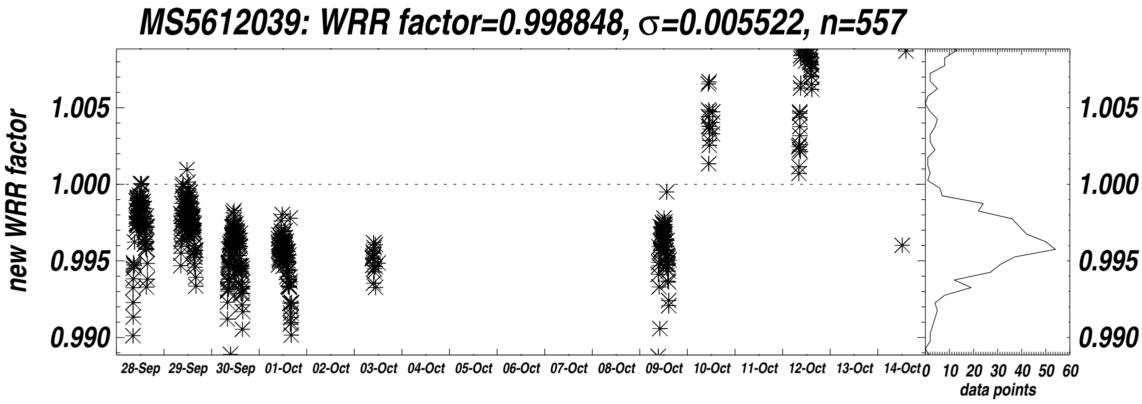
MS5612039: WRR factor=0.998848, σ=0.005522, n=557
new WRR factor
1.005
1.000
0.995
0.990
28-Sep 29-Sep 30-Sep 01-Oct 02-Oct 03-Oct 04-Oct 05-Oct 06-Oct 07-Oct 08-Oct 09-Oct 10-Oct 11-Oct 12-Oct 13-Oct 14-Oct
0 10 20 30 40 50 60
data points

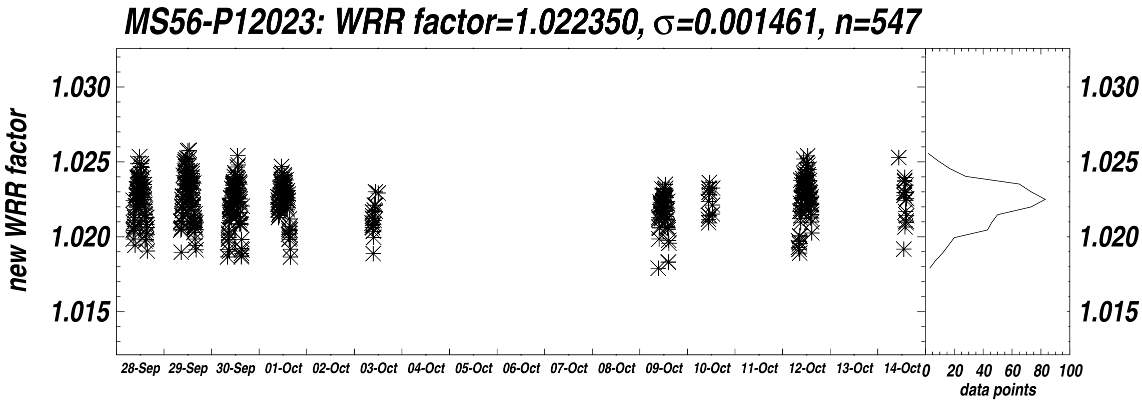
MS56-P12023: WRR factor=1.022350, σ=0.001461, n=547
new WRR factor
1.030
1.025
1.020
1.015
28-Sep 29-Sep 30-Sep 01-Oct 02-Oct 03-Oct 04-Oct 05-Oct 06-Oct 07-Oct 08-Oct 09-Oct 10-Oct 11-Oct 12-Oct 13-Oct 14-Oct
0 20 40 60 80 100
data points

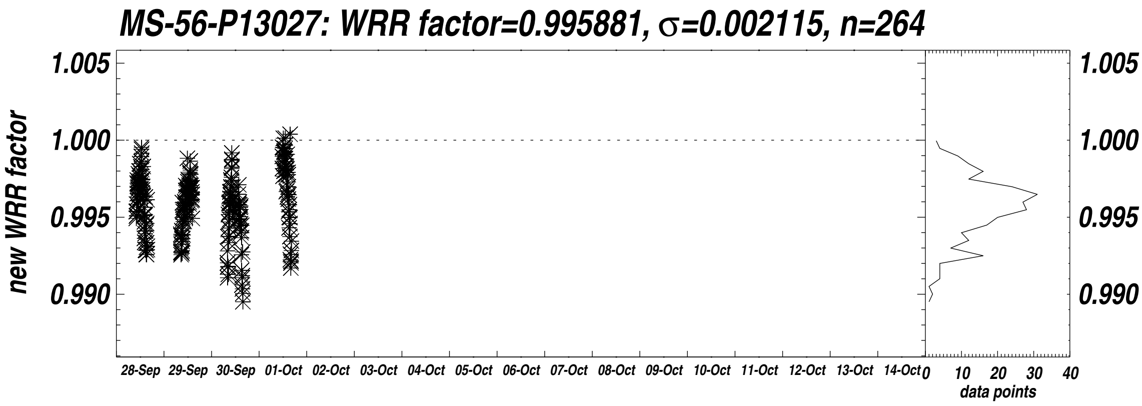
MS-56-P13027: WRR factor=0.995881, σ=0.002115, n=264
new WRR factor
1.005
1.000
0.995
0.990
28-Sep 29-Sep 30-Sep 01-Oct 02-Oct 03-Oct 04-Oct 05-Oct 06-Oct 07-Oct 08-Oct 09-Oct 10-Oct 11-Oct 12-Oct 13-Oct 14-Oct
0 10 20 30 40
data points

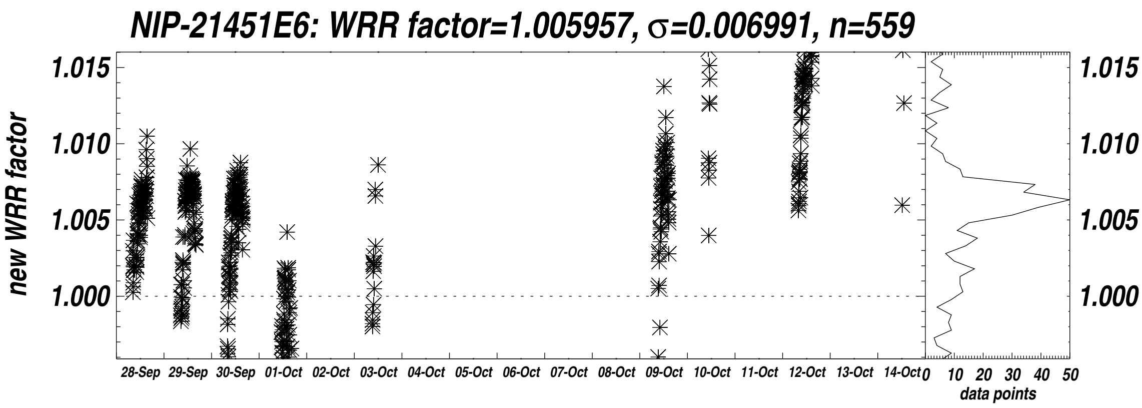
NIP-21451E6: WRR factor=1.005957, σ=0.006991, n=559
new WRR factor
1.015
1.010
1.005
1.000
28-Sep 29-Sep 30-Sep 01-Oct 02-Oct 03-Oct 04-Oct 05-Oct 06-Oct 07-Oct 08-Oct 09-Oct 10-Oct 11-Oct 12-Oct 13-Oct 14-Oct
0 10 20 30 40 50
data points

NIP-23927E6: WRR factor=1.000885, σ=0.007214, n=554

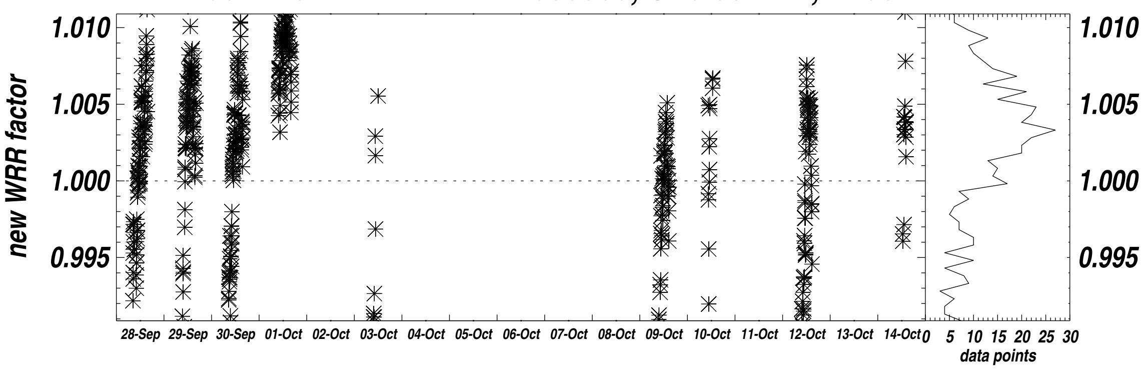

NIP-25738E6: WRR factor=0.991889, σ=0.006224, n=540

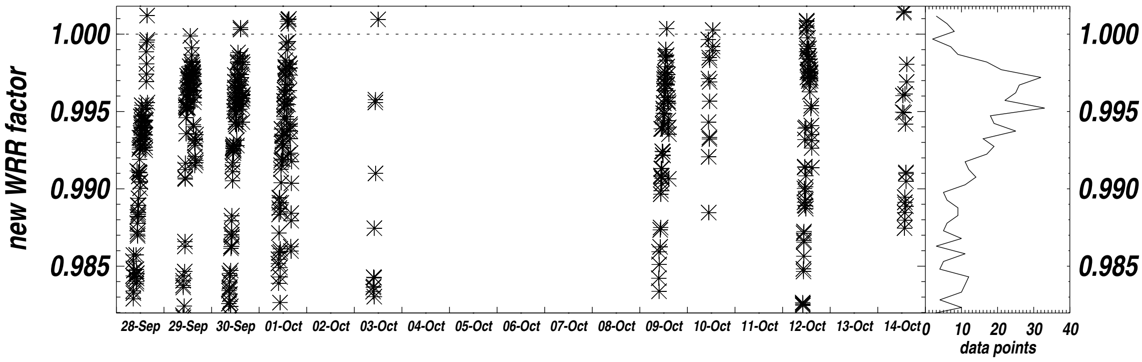

NIP-26626E6: WRR factor=1.000334, σ=0.004506, n=550

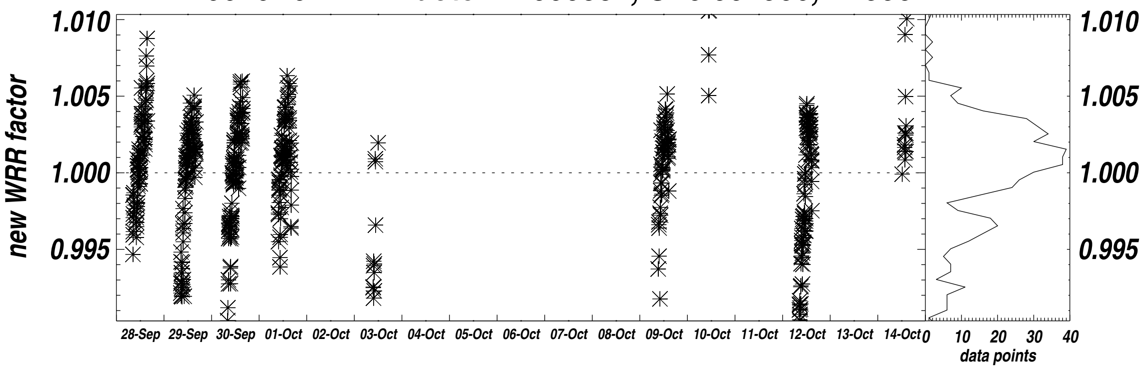

NIP-31144E6: WRR factor=0.996836, σ=0.004738, n=561

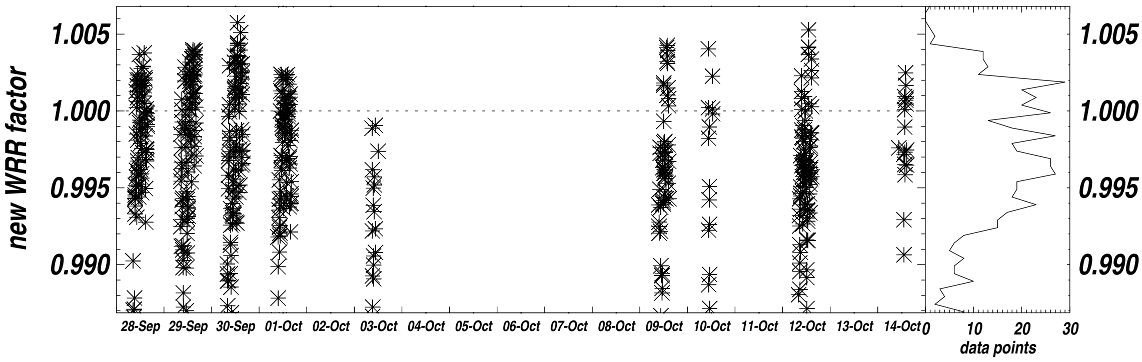

NIP-35356E6: WRR factor=1.011018, σ=0.002721, n=234

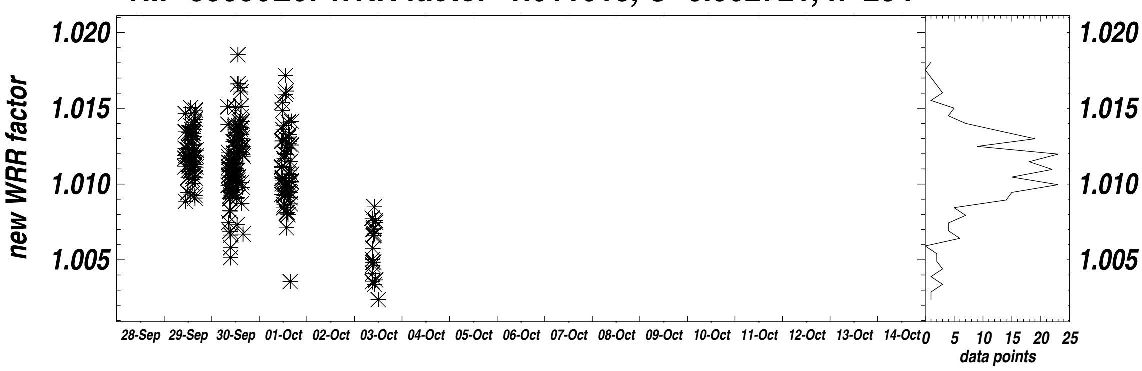

PAC3: WRR factor=1.002190, σ=0.000553, n=576

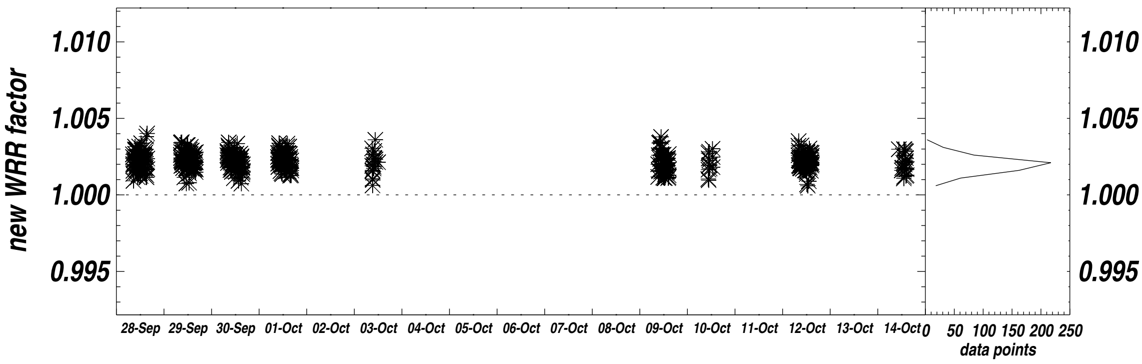

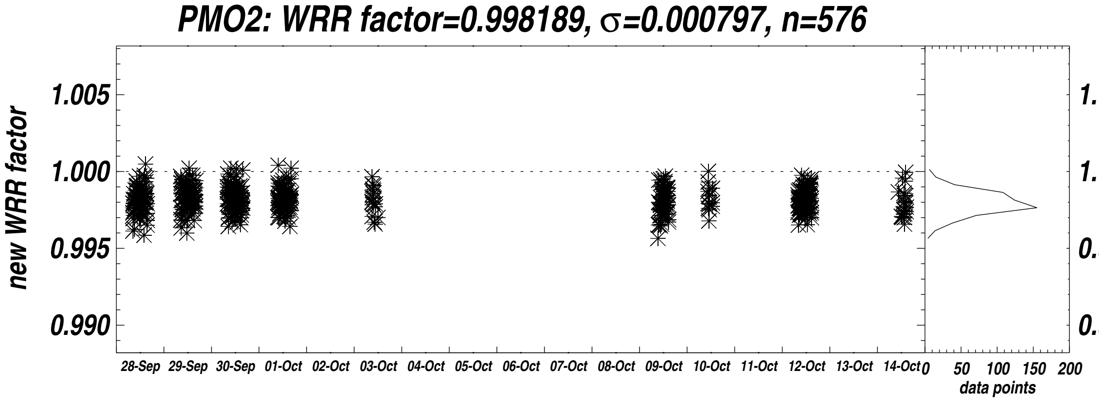
PMO2: WRR factor=0.998189, σ=0.000797, n=576
new WRR factor
1.005
1.000
0.995
0.990
28-Sep 29-Sep 30-Sep 01-Oct 02-Oct 03-Oct 04-Oct 05-Oct 06-Oct 07-Oct 08-Oct 09-Oct 10-Oct 11-Oct 12-Oct 13-Oct 14-Oct
0 50 100 150 200
data points

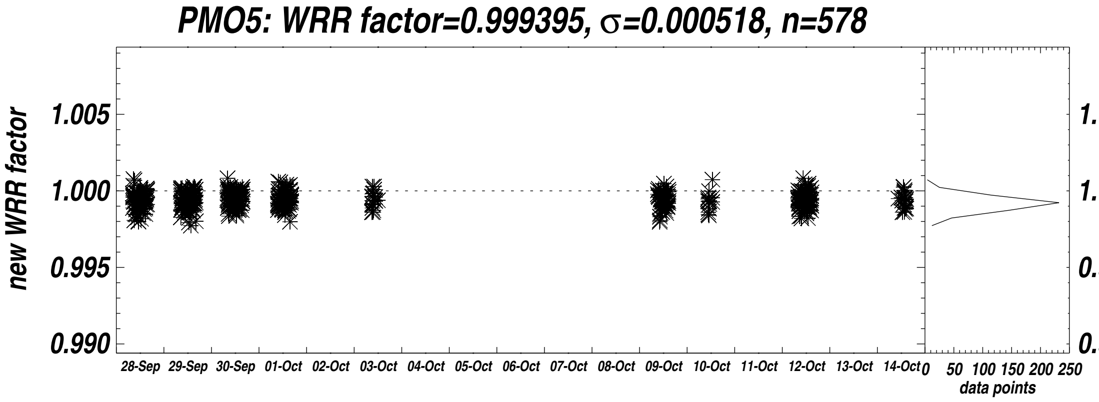
PMO5: WRR factor=0.999395, σ=0.000518, n=578
new WRR factor
1.005
1.000
0.995
0.990
28-Sep 29-Sep 30-Sep 01-Oct 02-Oct 03-Oct 04-Oct 05-Oct 06-Oct 07-Oct 08-Oct 09-Oct 10-Oct 11-Oct 12-Oct 13-Oct 14-Oct
0 50 100 150 200 250
data points

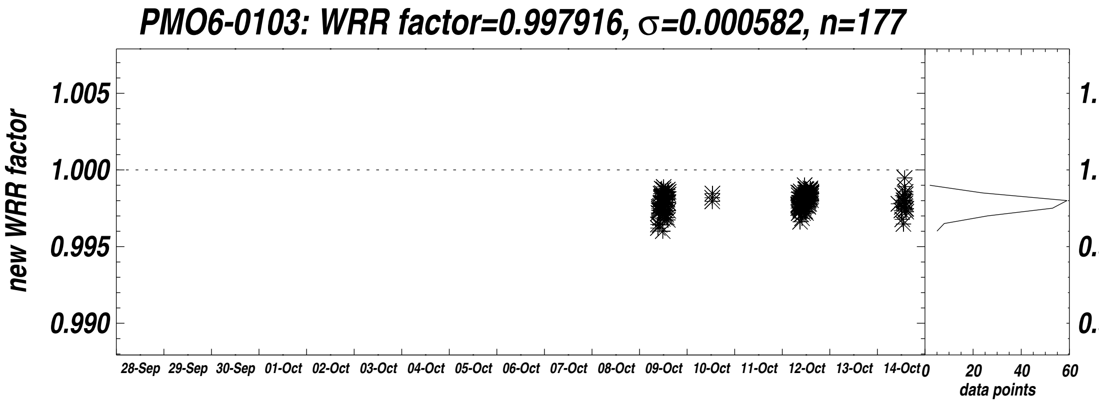
PMO6-0103: WRR factor=0.997916, σ=0.000582, n=177
new WRR factor
1.005
1.000
0.995
0.990
28-Sep 29-Sep 30-Sep 01-Oct 02-Oct 03-Oct 04-Oct 05-Oct 06-Oct 07-Oct 08-Oct 09-Oct 10-Oct 11-Oct 12-Oct 13-Oct 14-Oct
0 20 40 60
data points

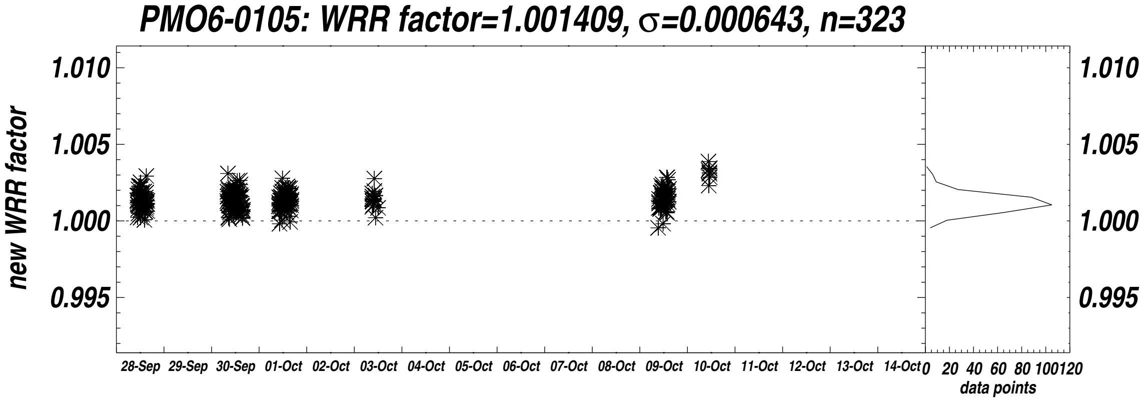
PMO6-0105: WRR factor=1.001409, σ=0.000643, n=323
new WRR factor
1.010
1.005
1.000
0.995
28-Sep 29-Sep 30-Sep 01-Oct 02-Oct 03-Oct 04-Oct 05-Oct 06-Oct 07-Oct 08-Oct 09-Oct 10-Oct 11-Oct 12-Oct 13-Oct 14-Oct
0 20 40 60 80 100 120
data points

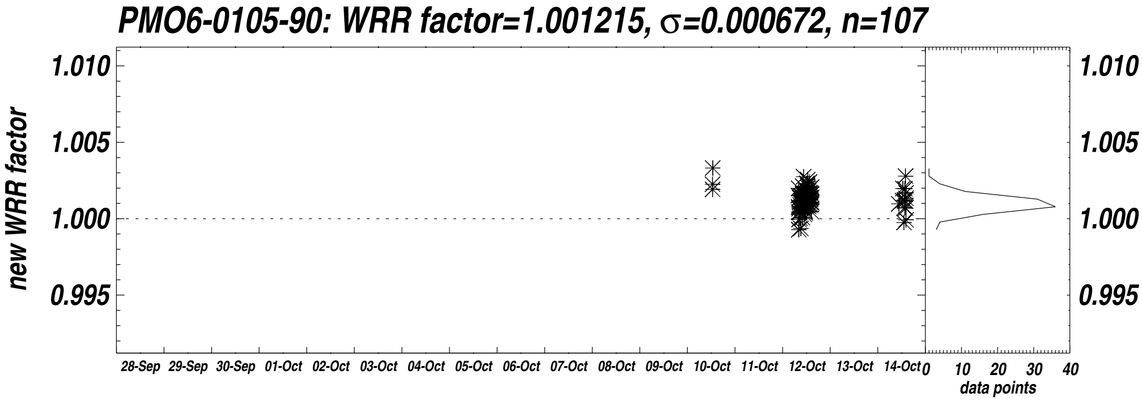
PMO6-0105-90: WRR factor=1.001215, σ=0.000672, n=107
new WRR factor
1.010
1.005
1.000
0.995
28-Sep 29-Sep 30-Sep 01-Oct 02-Oct 03-Oct 04-Oct 05-Oct 06-Oct 07-Oct 08-Oct 09-Oct 10-Oct 11-Oct 12-Oct 13-Oct 14-Oct
0 10 20 30 40
data points

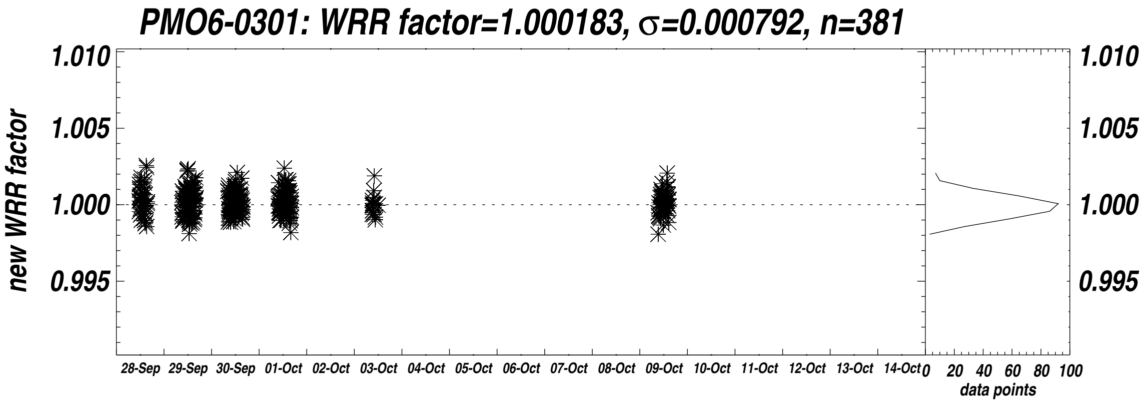
PMO6-0301: WRR factor=1.000183, σ=0.000792, n=381
new WRR factor
1.010
1.005
1.000
0.995
28-Sep 29-Sep 30-Sep 01-Oct 02-Oct 03-Oct 04-Oct 05-Oct 06-Oct 07-Oct 08-Oct 09-Oct 10-Oct 11-Oct 12-Oct 13-Oct 14-Oct
0 20 40 60 80 100
data points

PMO6-0401D: WRR factor=1.020799, σ=0.000475, n=563

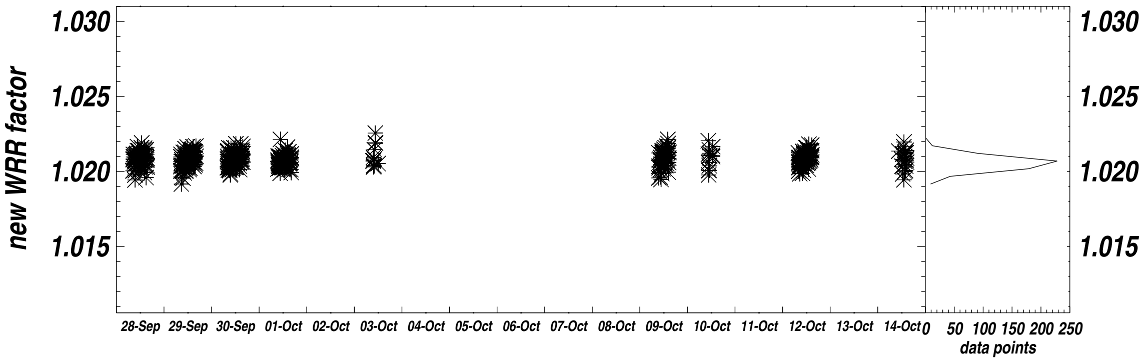

PMO6-0403: WRR factor=0.999753, σ=0.000597, n=414

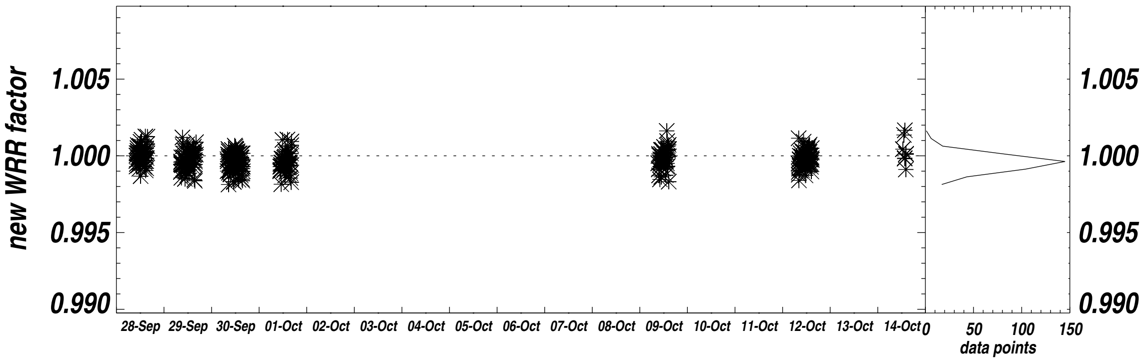

PMO6-0404: WRR factor=0.998208, σ=0.000649, n=307

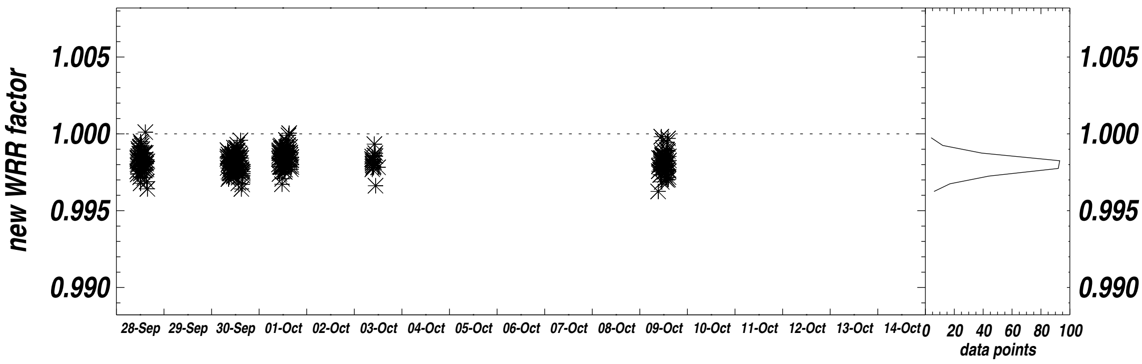

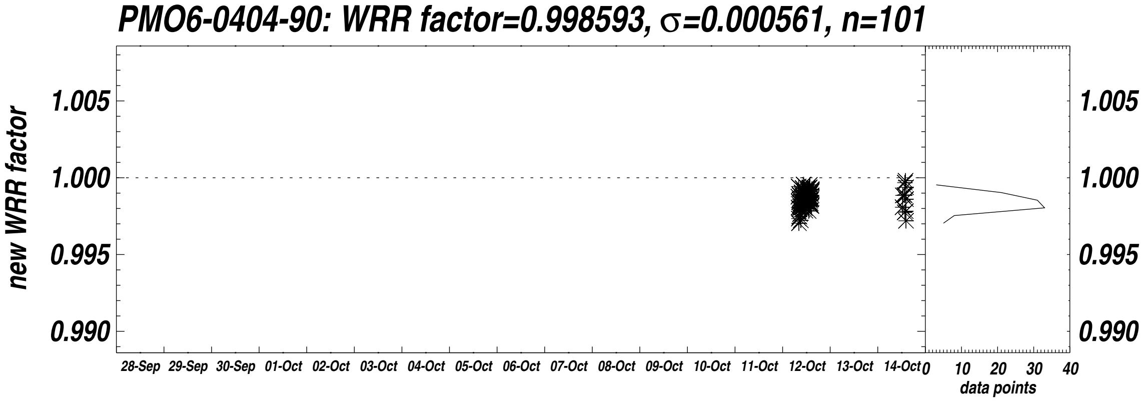
PMO6-0404-90: WRR factor=0.998593, σ=0.000561, n=101
new WRR factor
1.005
1.000
0.995
0.990
28-Sep 29-Sep 30-Sep 01-Oct 02-Oct 03-Oct 04-Oct 05-Oct 06-Oct 07-Oct 08-Oct 09-Oct 10-Oct 11-Oct 12-Oct 13-Oct 14-Oct
0 10 20 30 40
data points

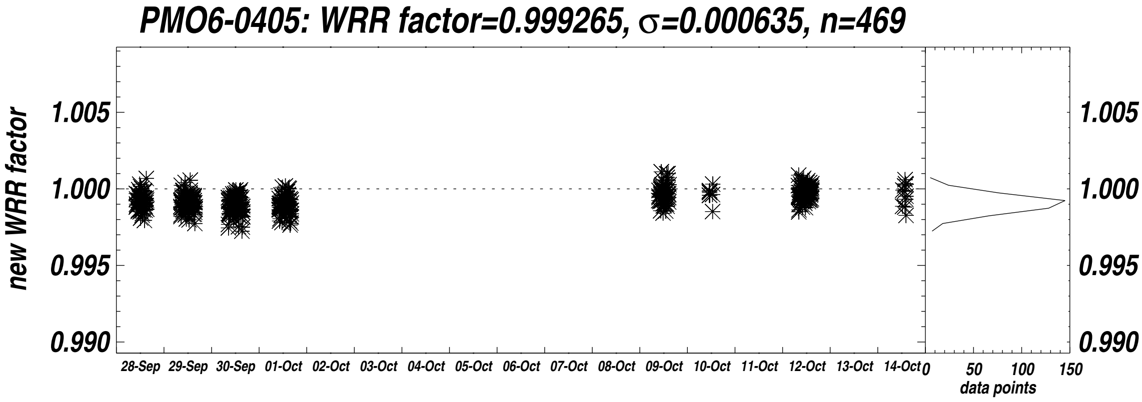
PMO6-0405: WRR factor=0.999265, σ=0.000635, n=469
new WRR factor
1.005
1.000
0.995
0.990
28-Sep 29-Sep 30-Sep 01-Oct 02-Oct 03-Oct 04-Oct 05-Oct 06-Oct 07-Oct 08-Oct 09-Oct 10-Oct 11-Oct 12-Oct 13-Oct 14-Oct
0 50 100 150
data points

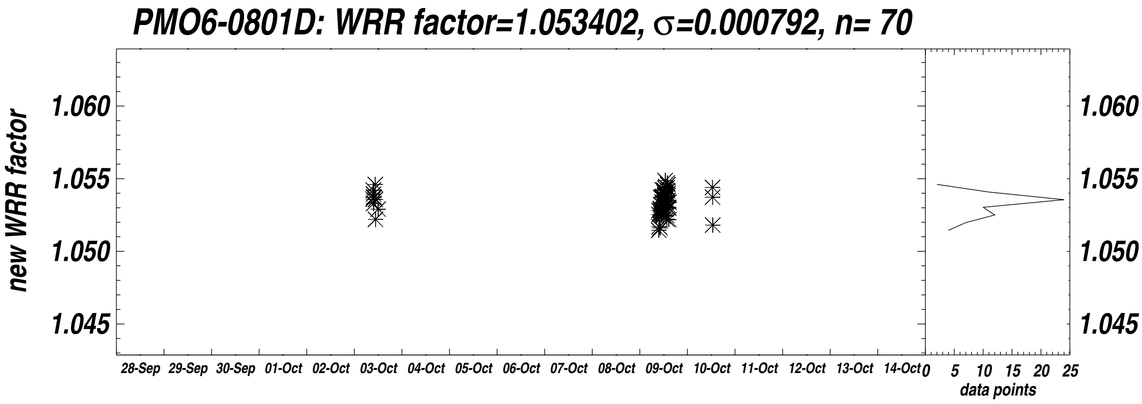
PMO6-0801D: WRR factor=1.053402, σ=0.000792, n= 70
new WRR factor
1.060
1.055
1.050
1.045
28-Sep 29-Sep 30-Sep 01-Oct 02-Oct 03-Oct 04-Oct 05-Oct 06-Oct 07-Oct 08-Oct 09-Oct 10-Oct 11-Oct 12-Oct 13-Oct 14-Oct
0 5 10 15 20 25
data points

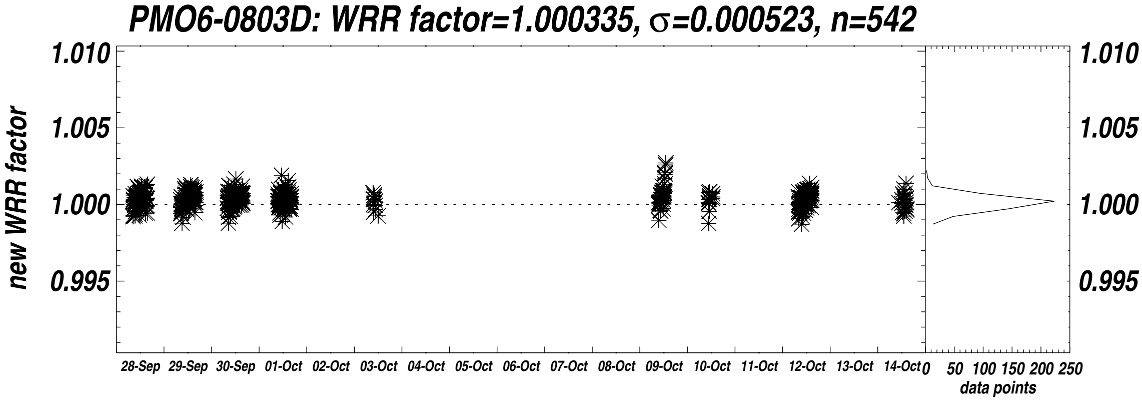
PMO6-0803D: WRR factor=1.000335, σ=0.000523, n=542
new WRR factor
1.010
1.005
1.000
0.995
28-Sep 29-Sep 30-Sep 01-Oct 02-Oct 03-Oct 04-Oct 05-Oct 06-Oct 07-Oct 08-Oct 09-Oct 10-Oct 11-Oct 12-Oct 13-Oct 14-Oct
0 50 100 150 200 250
data points

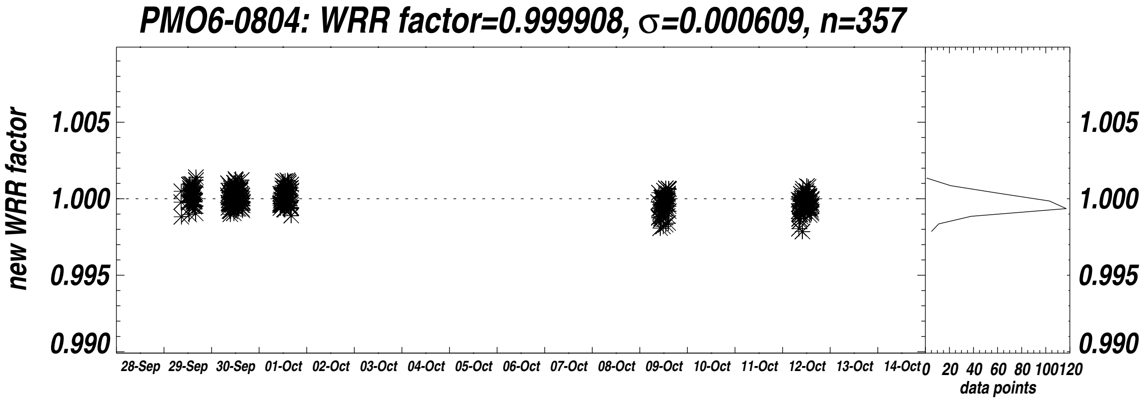
PMO6-0804: WRR factor=0.999908, σ=0.000609, n=357
new WRR factor
1.005
1.000
0.995
0.990
28-Sep 29-Sep 30-Sep 01-Oct 02-Oct 03-Oct 04-Oct 05-Oct 06-Oct 07-Oct 08-Oct 09-Oct 10-Oct 11-Oct 12-Oct 13-Oct 14-Oct
0 20 40 60 80 100120
data points

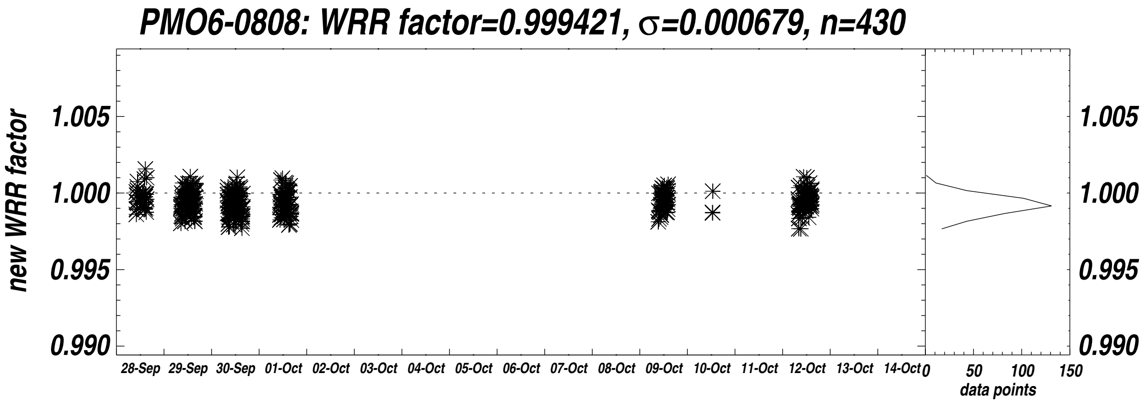
PMO6-0808: WRR factor=0.999421, σ=0.000679, n=430
new WRR factor
1.005
1.000
0.995
0.990
28-Sep 29-Sep 30-Sep 01-Oct 02-Oct 03-Oct 04-Oct 05-Oct 06-Oct 07-Oct 08-Oct 09-Oct 10-Oct 11-Oct 12-Oct 13-Oct 14-Oct
0 50 100 150
data points

PMO6-0810D: WRR factor=0.999918, σ=0.000548, n=418

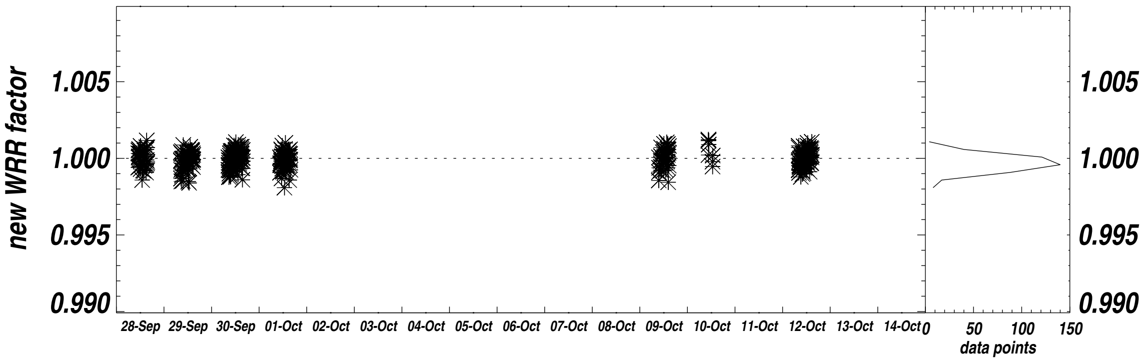

PMO6-0816D: WRR factor=0.999947, σ=0.001689, n=338

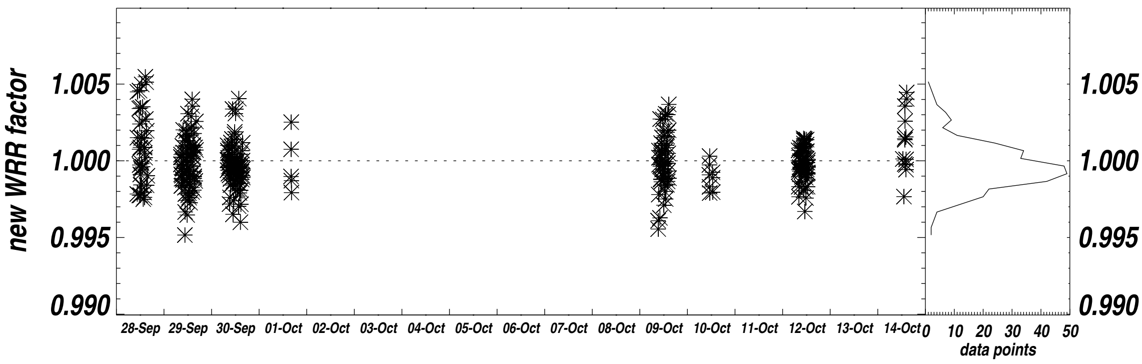

PMO6-0817: WRR factor=0.999516, σ=0.000624, n=312

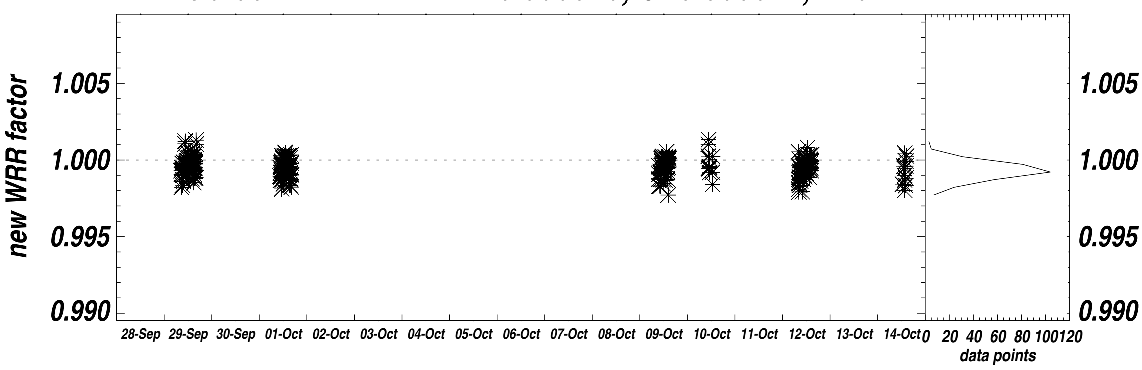

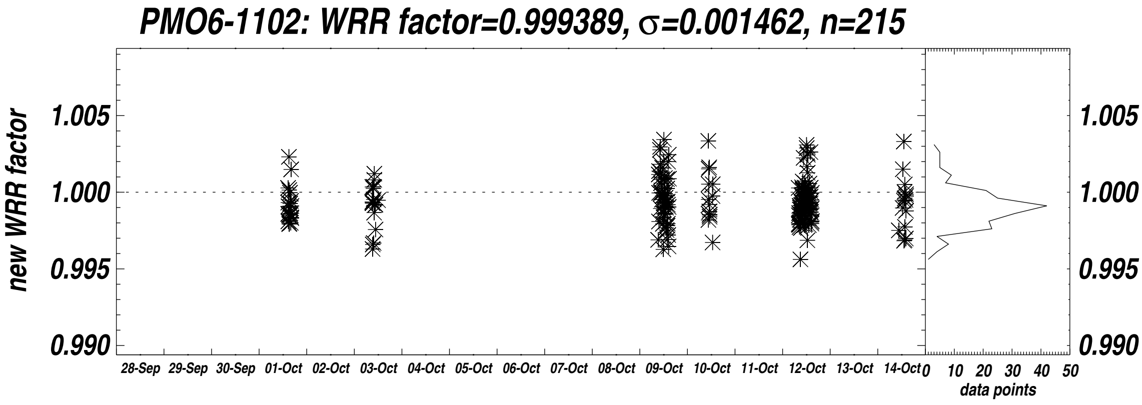
PMO6-1102: WRR factor=0.999389, σ=0.001462, n=215
new WRR factor
1.005
1.000
0.995
0.990
28-Sep 29-Sep 30-Sep 01-Oct 02-Oct 03-Oct 04-Oct 05-Oct 06-Oct 07-Oct 08-Oct 09-Oct 10-Oct 11-Oct 12-Oct 13-Oct 14-Oct
0 10 20 30 40 50
data points

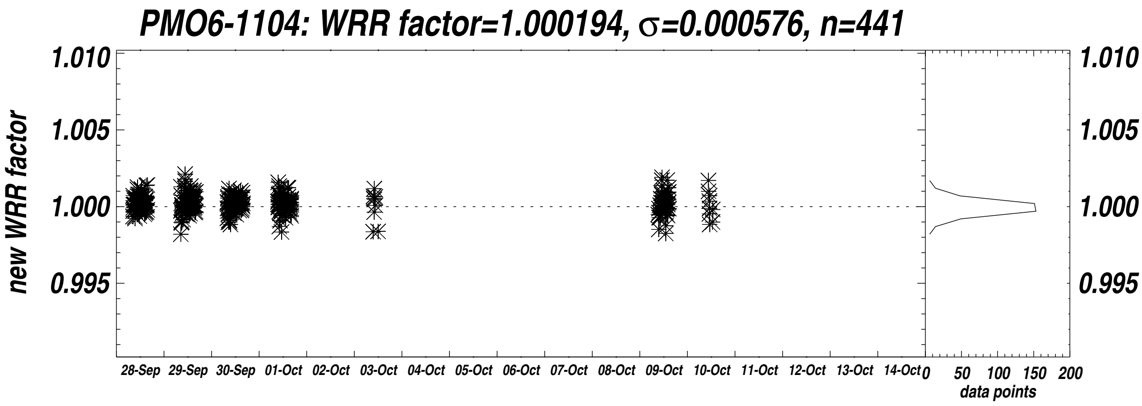
PMO6-1104: WRR factor=1.000194, σ=0.000576, n=441
new WRR factor
1.010
1.005
1.000
0.995
28-Sep 29-Sep 30-Sep 01-Oct 02-Oct 03-Oct 04-Oct 05-Oct 06-Oct 07-Oct 08-Oct 09-Oct 10-Oct 11-Oct 12-Oct 13-Oct 14-Oct
0 50 100 150 200
data points

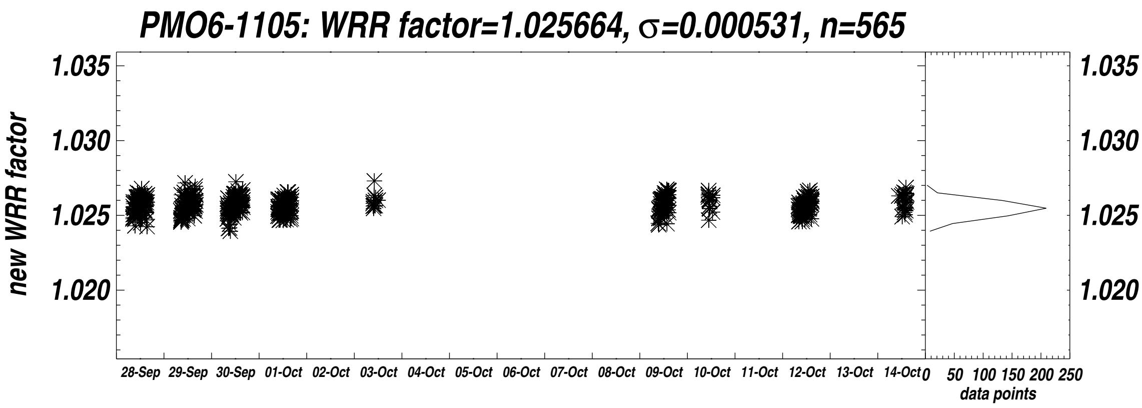
PMO6-1105: WRR factor=1.025664, σ=0.000531, n=565
new WRR factor
1.035
1.030
1.025
1.020
28-Sep 29-Sep 30-Sep 01-Oct 02-Oct 03-Oct 04-Oct 05-Oct 06-Oct 07-Oct 08-Oct 09-Oct 10-Oct 11-Oct 12-Oct 13-Oct 14-Oct
0 50 100 150 200 250
data points

PMO6-1106: WRR factor=1.027588, σ=0.000622, n=542

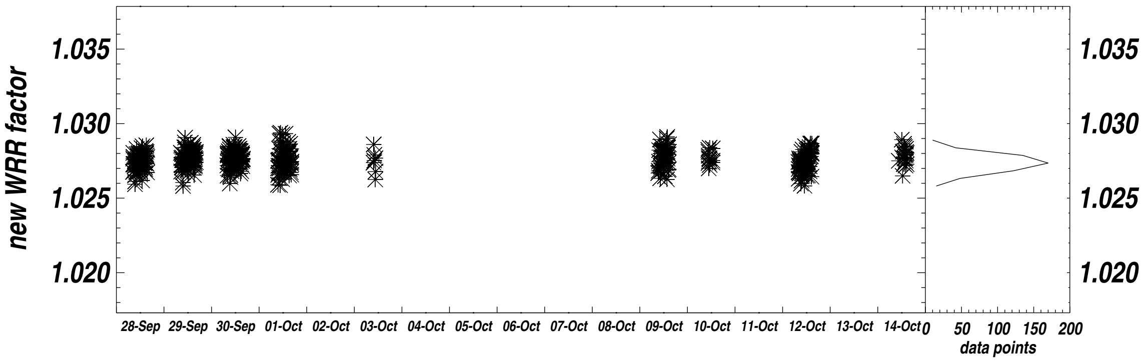

PMO6-1107: WRR factor=1.024318, σ=0.000611, n=549

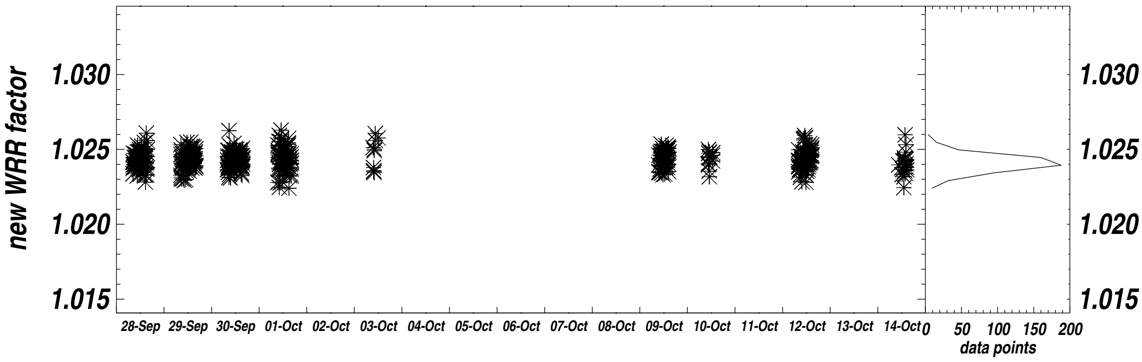

PMO6-1109: WRR factor=0.998732, σ=0.000990, n=277

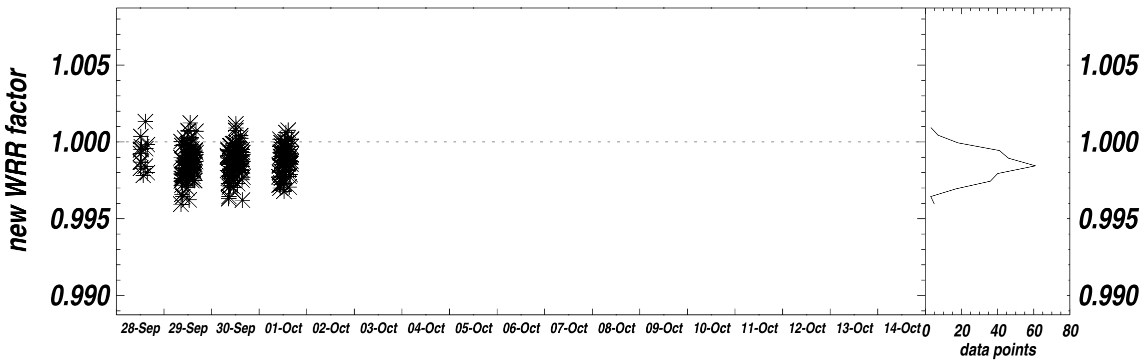

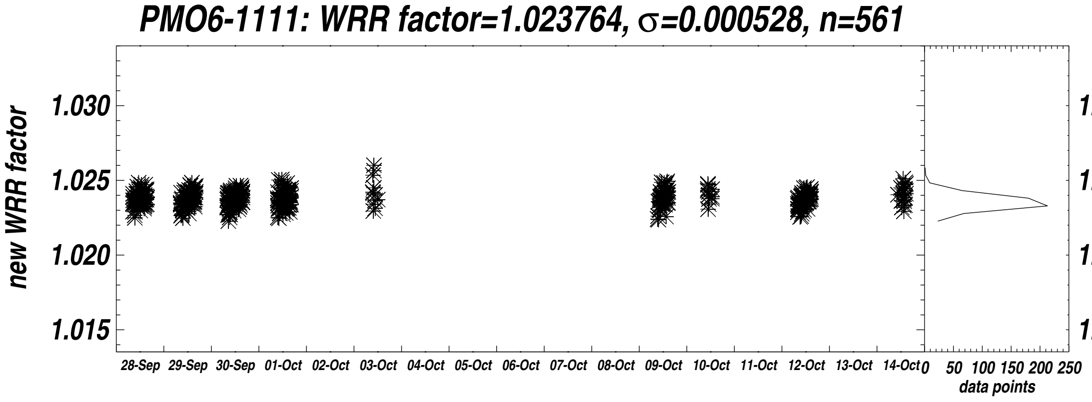
PMO6-1111: WRR factor=1.023764, σ=0.000528, n=561
new WRR factor
1.030
1.025
1.020
1.015
28-Sep 29-Sep 30-Sep 01-Oct 02-Oct 03-Oct 04-Oct 05-Oct 06-Oct 07-Oct 08-Oct 09-Oct 10-Oct 11-Oct 12-Oct 13-Oct 14-Oct
0 50 100 150 200 250
data points

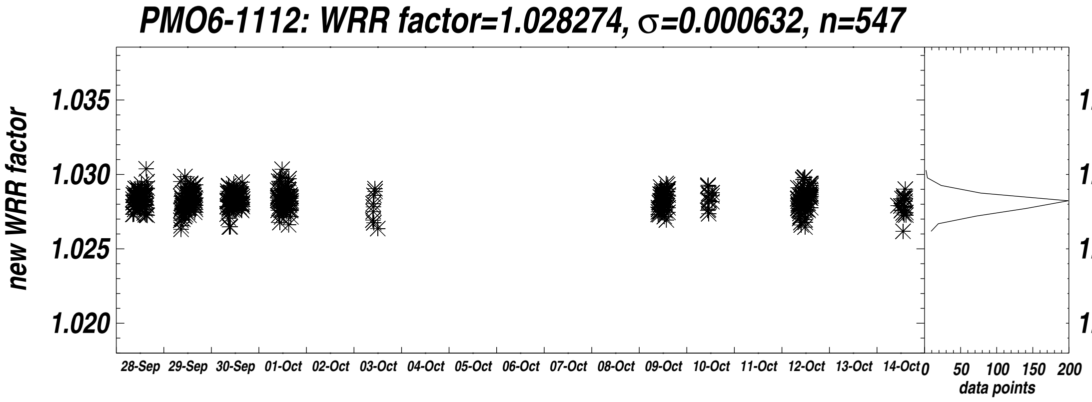
PMO6-1112: WRR factor=1.028274, σ=0.000632, n=547
new WRR factor
1.035
1.030
1.025
1.020
28-Sep 29-Sep 30-Sep 01-Oct 02-Oct 03-Oct 04-Oct 05-Oct 06-Oct 07-Oct 08-Oct 09-Oct 10-Oct 11-Oct 12-Oct 13-Oct 14-Oct
0 50 100 150 200
data points

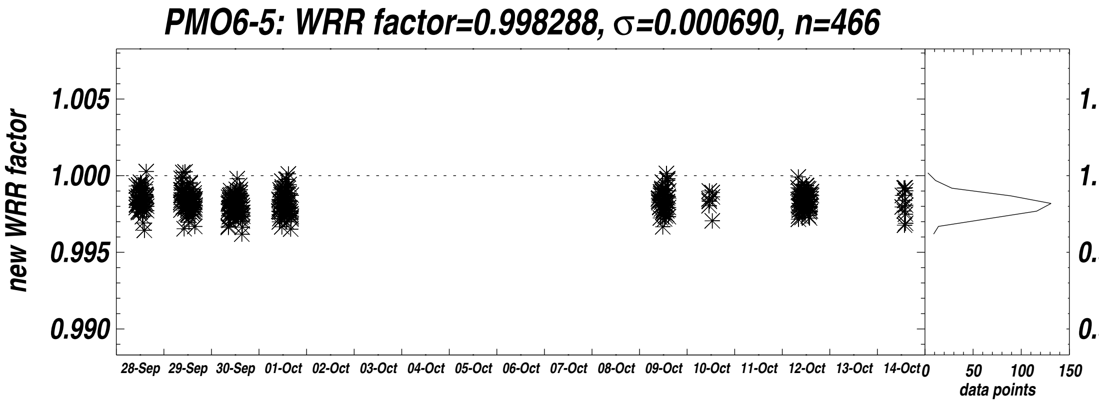
PMO6-5: WRR factor=0.998288, σ=0.000690, n=466
new WRR factor
1.005
1.000
0.995
0.990
28-Sep 29-Sep 30-Sep 01-Oct 02-Oct 03-Oct 04-Oct 05-Oct 06-Oct 07-Oct 08-Oct 09-Oct 10-Oct 11-Oct 12-Oct 13-Oct 14-Oct
0 50 100 150
data points

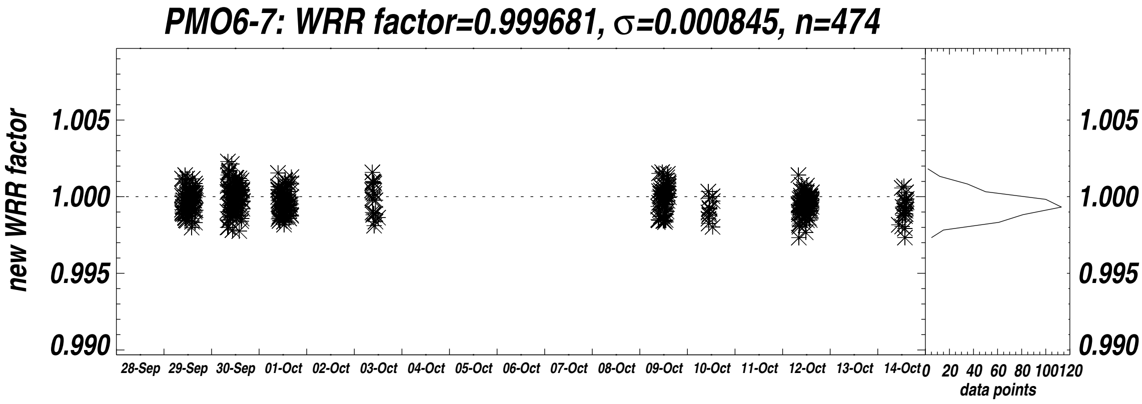
PMO6-7: WRR factor=0.999681, σ=0.000845, n=474
new WRR factor
1.005
1.000
0.995
0.990
28-Sep 29-Sep 30-Sep 01-Oct 02-Oct 03-Oct 04-Oct 05-Oct 06-Oct 07-Oct 08-Oct 09-Oct 10-Oct 11-Oct 12-Oct 13-Oct 14-Oct
0 20 40 60 80 100120
data points

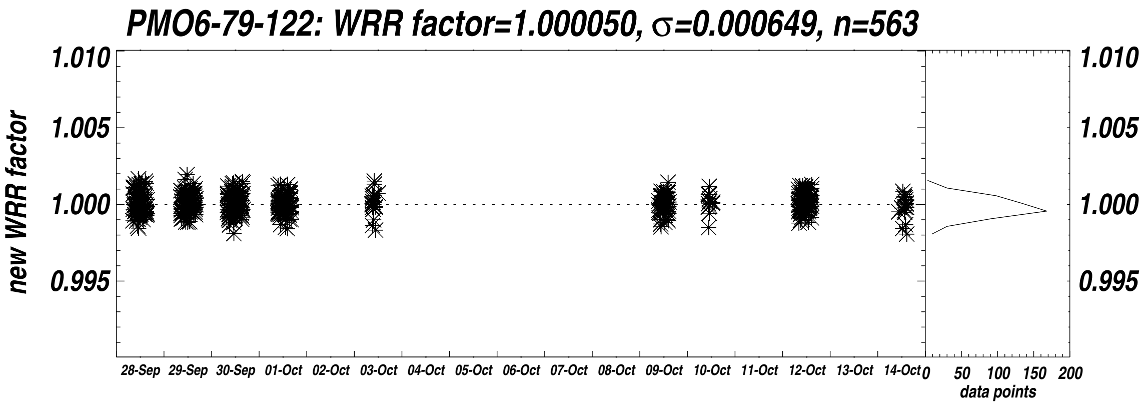
PMO6-79-122: WRR factor=1.000050, σ=0.000649, n=563
new WRR factor
1.010
1.005
1.000
0.995
28-Sep 29-Sep 30-Sep 01-Oct 02-Oct 03-Oct 04-Oct 05-Oct 06-Oct 07-Oct 08-Oct 09-Oct 10-Oct 11-Oct 12-Oct 13-Oct 14-Oct
0 50 100 150 200
data points

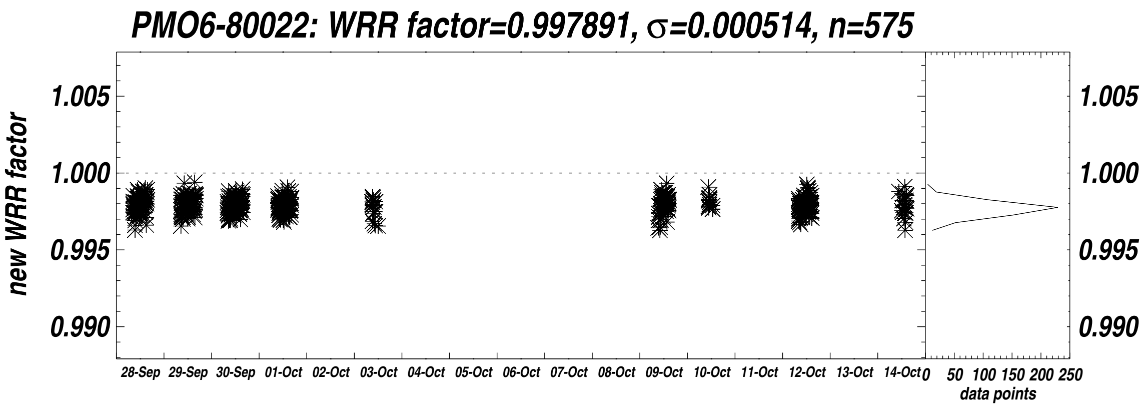
PMO6-80022: WRR factor=0.997891, σ=0.000514, n=575
new WRR factor
1.005
1.000
0.995
0.990
28-Sep 29-Sep 30-Sep 01-Oct 02-Oct 03-Oct 04-Oct 05-Oct 06-Oct 07-Oct 08-Oct 09-Oct 10-Oct 11-Oct 12-Oct 13-Oct 14-Oct
0 50 100 150 200 250
data points

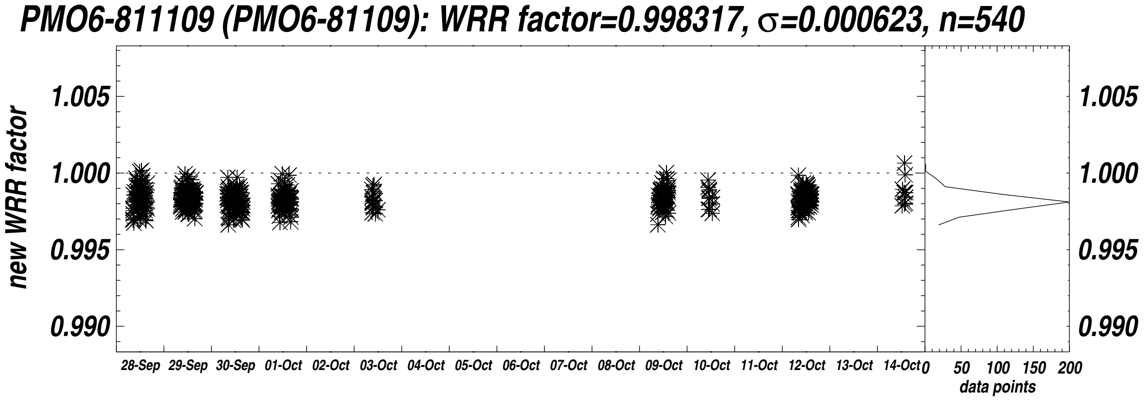
PMO6-811109 (PMO6-81109): WRR factor=0.998317, σ=0.000623, n=540
new WRR factor
1.005
1.000
0.995
0.990
28-Sep 29-Sep 30-Sep 01-Oct 02-Oct 03-Oct 04-Oct 05-Oct 06-Oct 07-Oct 08-Oct 09-Oct 10-Oct 11-Oct 12-Oct 13-Oct 14-Oct
0 50 100 150 200
data points

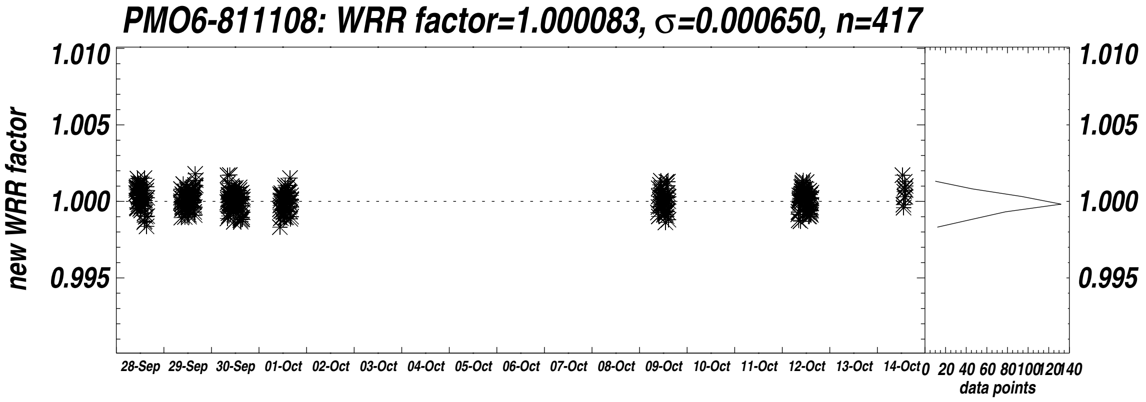
PMO6-811108: WRR factor=1.000083, σ=0.000650, n=417
new WRR factor
1.010
1.005
1.000
0.995
28-Sep 29-Sep 30-Sep 01-Oct 02-Oct 03-Oct 04-Oct 05-Oct 06-Oct 07-Oct 08-Oct 09-Oct 10-Oct 11-Oct 12-Oct 13-Oct 14-Oct
0 20 40 60 80 100 120 140
data points

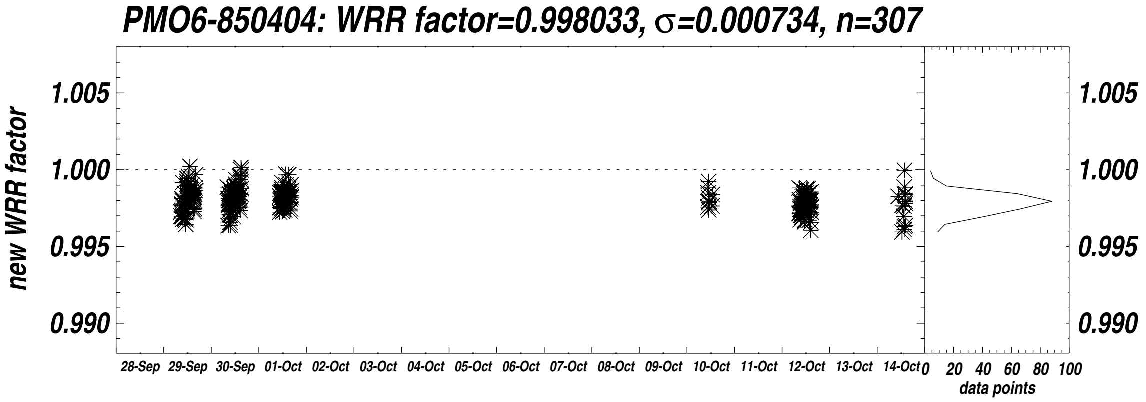
PMO6-850404: WRR factor=0.998033, σ=0.000734, n=307
new WRR factor
1.005
1.000
0.995
0.990
28-Sep 29-Sep 30-Sep 01-Oct 02-Oct 03-Oct 04-Oct 05-Oct 06-Oct 07-Oct 08-Oct 09-Oct 10-Oct 11-Oct 12-Oct 13-Oct 14-Oct
0 20 40 60 80 100
data points

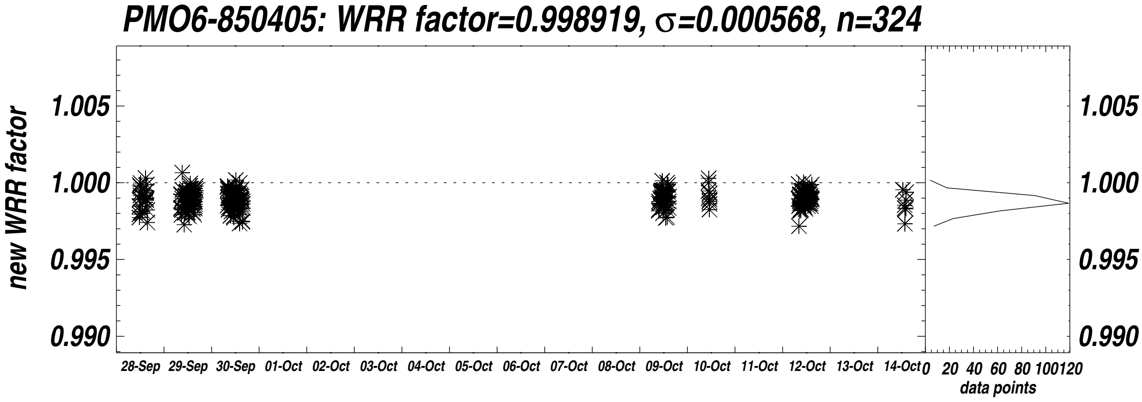
PMO6-850405: WRR factor=0.998919, σ=0.000568, n=324
new WRR factor
1.005
1.000
0.995
0.990
28-Sep 29-Sep 30-Sep 01-Oct 02-Oct 03-Oct 04-Oct 05-Oct 06-Oct 07-Oct 08-Oct 09-Oct 10-Oct 11-Oct 12-Oct 13-Oct 14-Oct
0 20 40 60 80 100120
data points

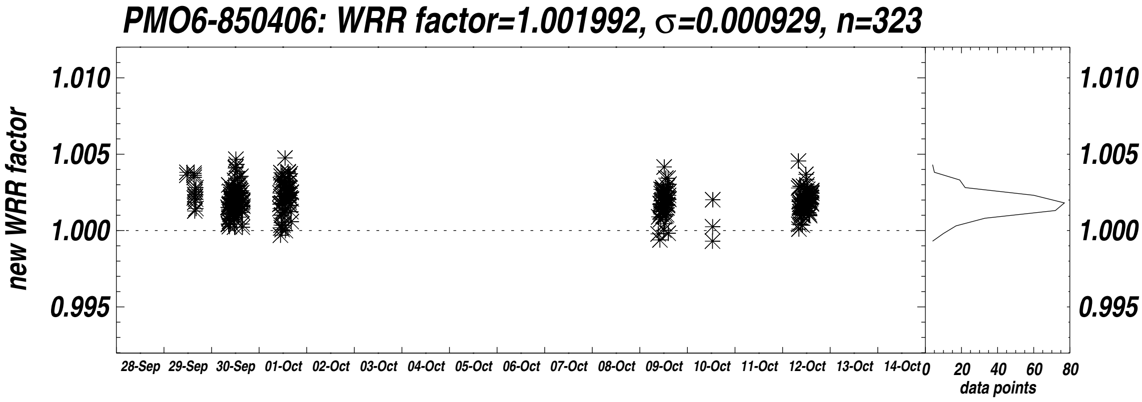
PMO6-850406: WRR factor=1.001992, σ=0.000929, n=323
new WRR factor
1.010
1.005
1.000
0.995
28-Sep 29-Sep 30-Sep 01-Oct 02-Oct 03-Oct 04-Oct 05-Oct 06-Oct 07-Oct 08-Oct 09-Oct 10-Oct 11-Oct 12-Oct 13-Oct 14-Oct
0 20 40 60 80
data points

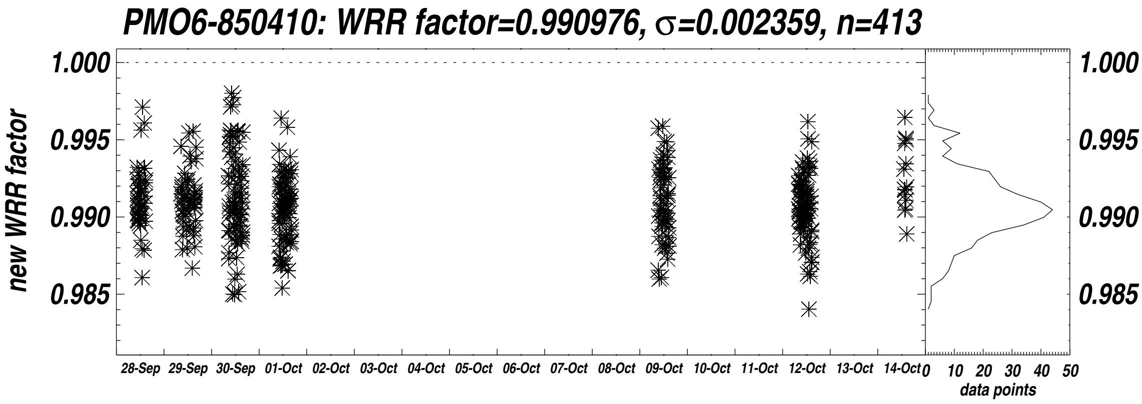
PMO6-850410: WRR factor=0.990976, σ=0.002359, n=413
new WRR factor
1.000
0.995
0.990
0.985
28-Sep 29-Sep 30-Sep 01-Oct 02-Oct 03-Oct 04-Oct 05-Oct 06-Oct 07-Oct 08-Oct 09-Oct 10-Oct 11-Oct 12-Oct 13-Oct 14-Oct
0 10 20 30 40 50
data points

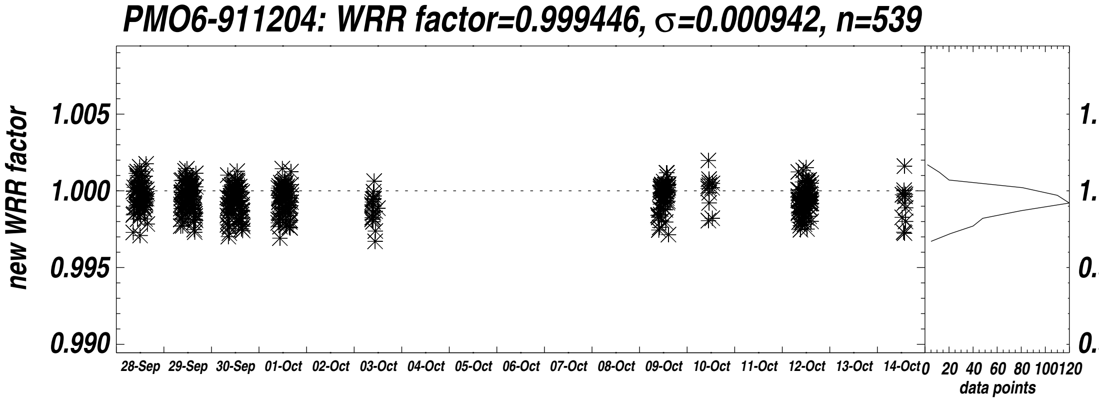
PMO6-911204: WRR factor=0.999446, σ=0.000942, n=539
new WRR factor
data points

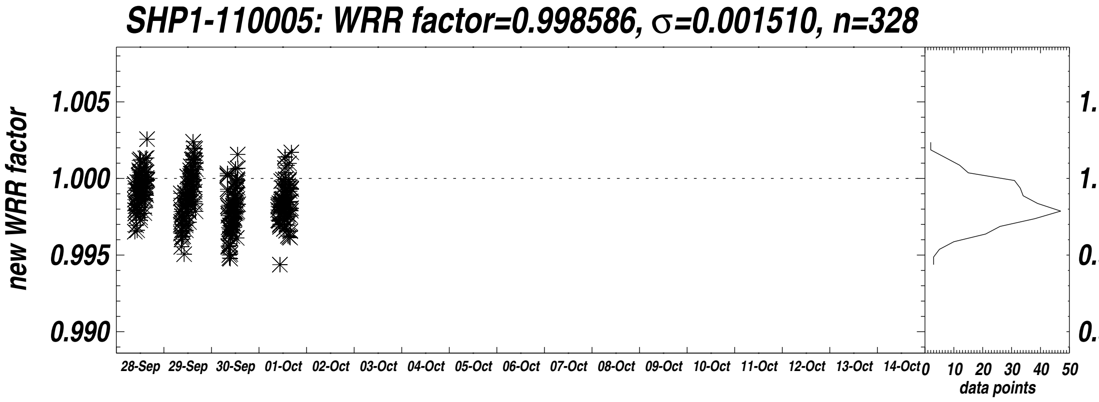
SHP1-110005: WRR factor=0.998586, σ=0.001510, n=328
new WRR factor
data points

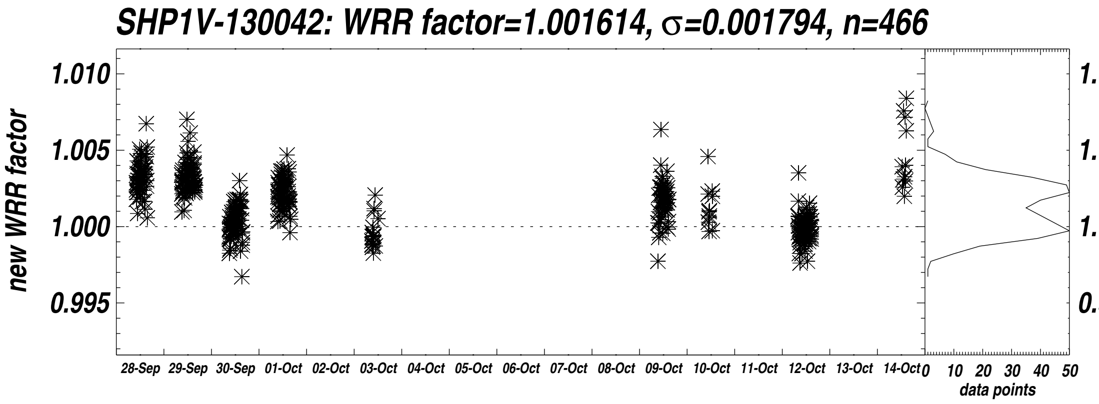
SHP1V-130042: WRR factor=1.001614, σ=0.001794, n=466
new WRR factor
data points

SIAR-2A: WRR factor=0.991432, σ=0.002513, n=221

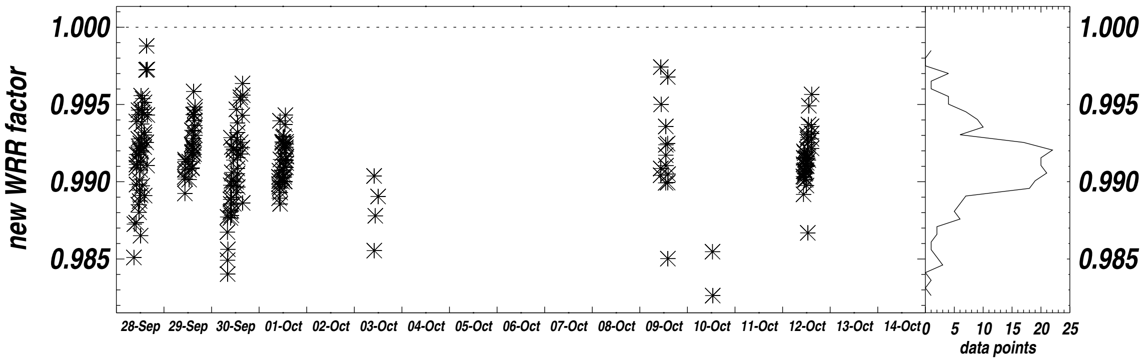

SIAR-2B: WRR factor=1.000941, σ=0.002229, n=210

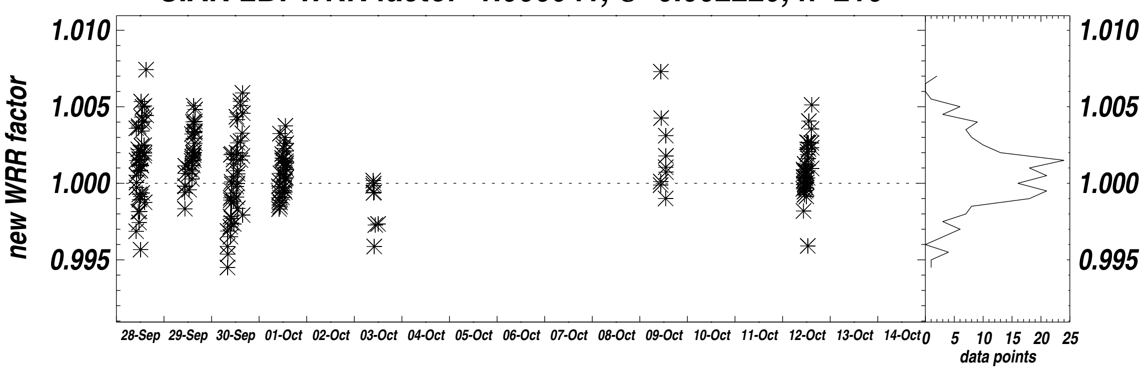

SIAR-2C: WRR factor=0.998949, σ=0.000753, n=392

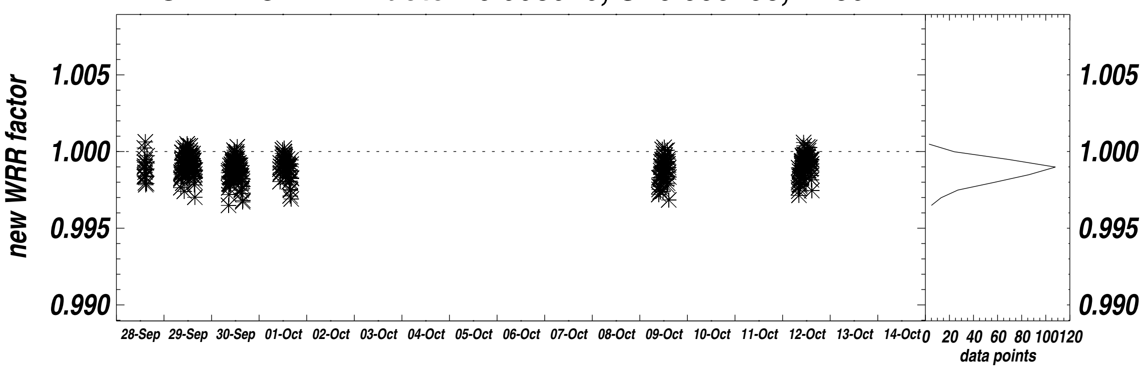

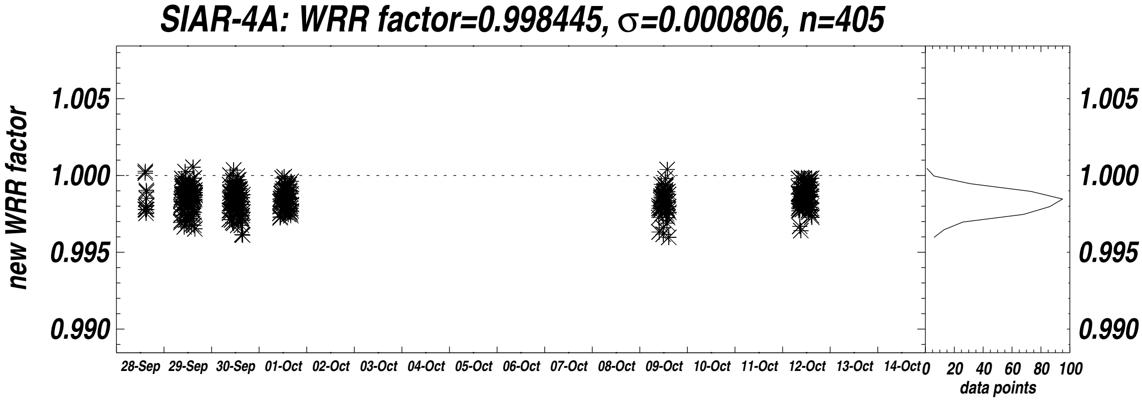
SIAR-4A: WRR factor=0.998445, σ=0.000806, n=405
new WRR factor
1.005
1.000
0.995
0.990
28-Sep 29-Sep 30-Sep 01-Oct 02-Oct 03-Oct 04-Oct 05-Oct 06-Oct 07-Oct 08-Oct 09-Oct 10-Oct 11-Oct 12-Oct 13-Oct 14-Oct
0 20 40 60 80 100
data points

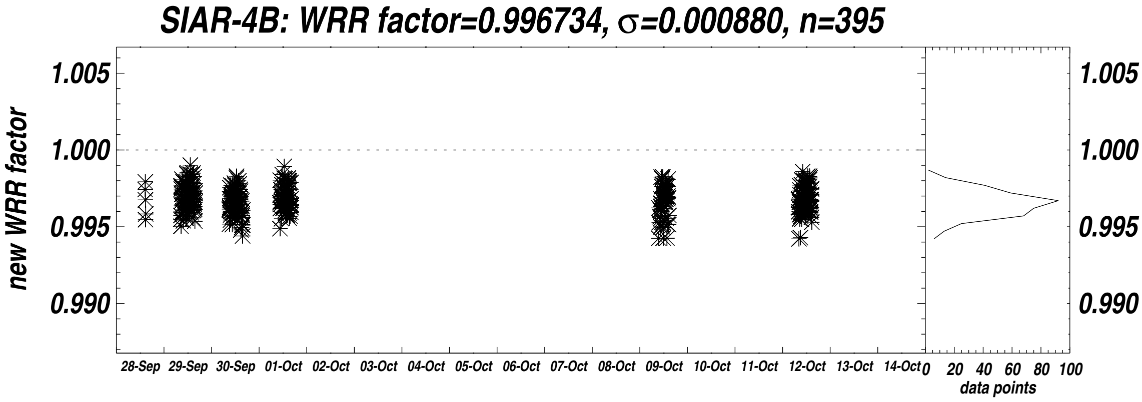
SIAR-4B: WRR factor=0.996734, σ=0.000880, n=395
new WRR factor
1.005
1.000
0.995
0.990
28-Sep 29-Sep 30-Sep 01-Oct 02-Oct 03-Oct 04-Oct 05-Oct 06-Oct 07-Oct 08-Oct 09-Oct 10-Oct 11-Oct 12-Oct 13-Oct 14-Oct
0 20 40 60 80 100
data points

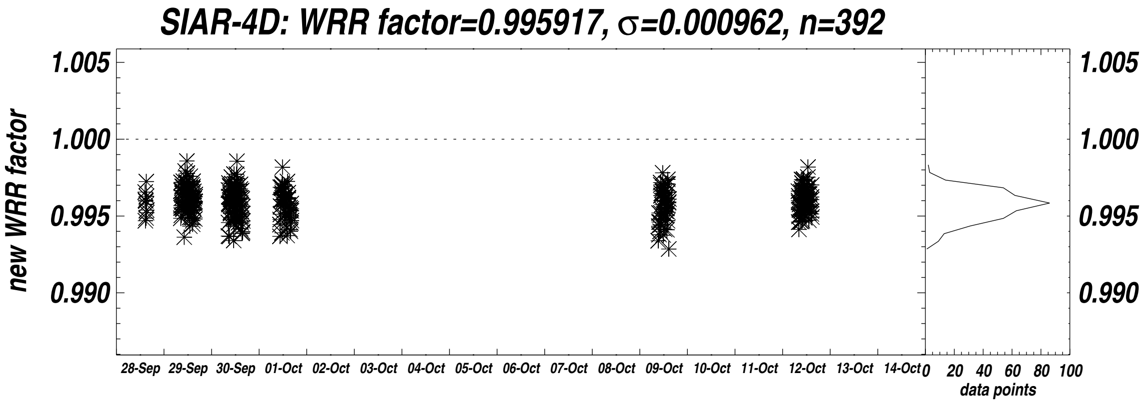
SIAR-4D: WRR factor=0.995917, σ=0.000962, n=392
new WRR factor
1.005
1.000
0.995
0.990
28-Sep 29-Sep 30-Sep 01-Oct 02-Oct 03-Oct 04-Oct 05-Oct 06-Oct 07-Oct 08-Oct 09-Oct 10-Oct 11-Oct 12-Oct 13-Oct 14-Oct
0 20 40 60 80 100
data points

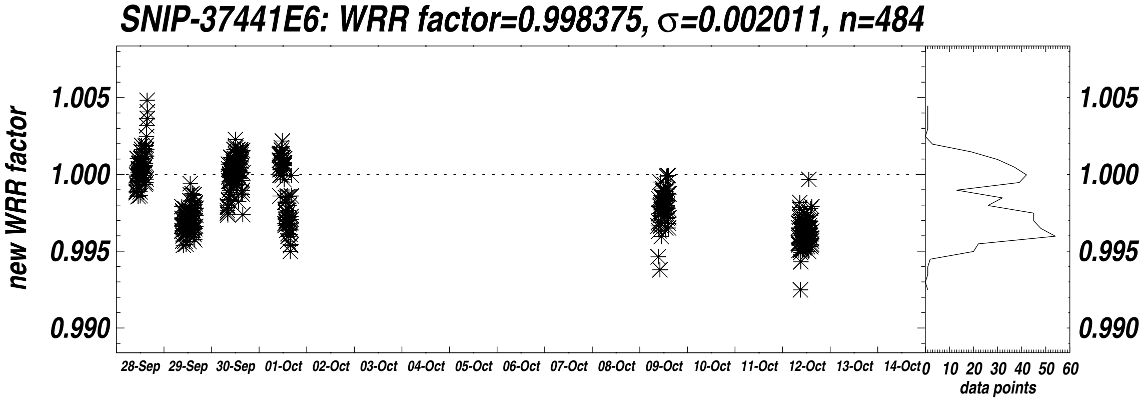
SNIP-37441E6: WRR factor=0.998375, σ=0.002011, n=484
new WRR factor
data points

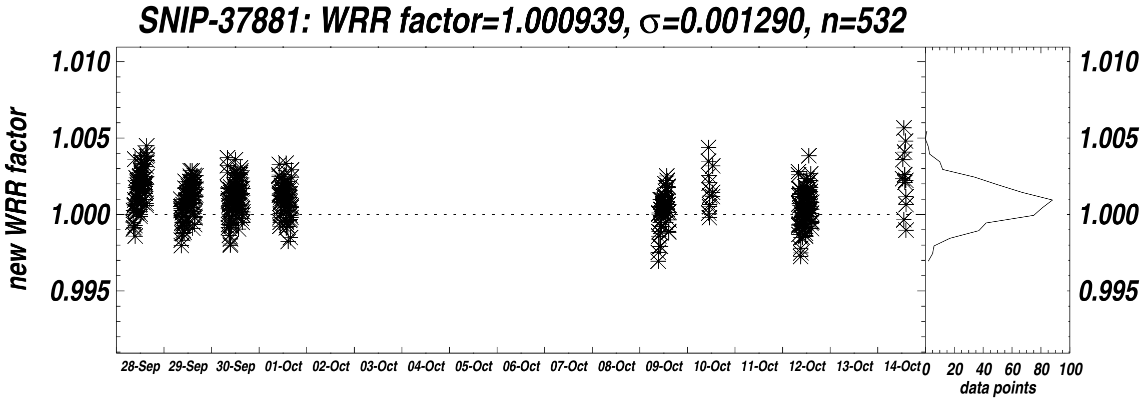
SNIP-37881: WRR factor=1.000939, σ=0.001290, n=532
new WRR factor
data points

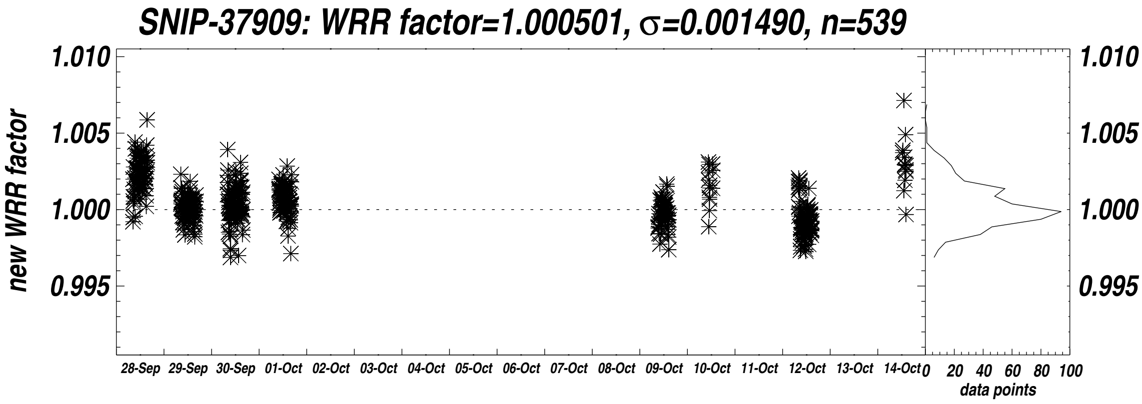
SNIP-37909: WRR factor=1.000501, σ=0.001490, n=539
new WRR factor
data points

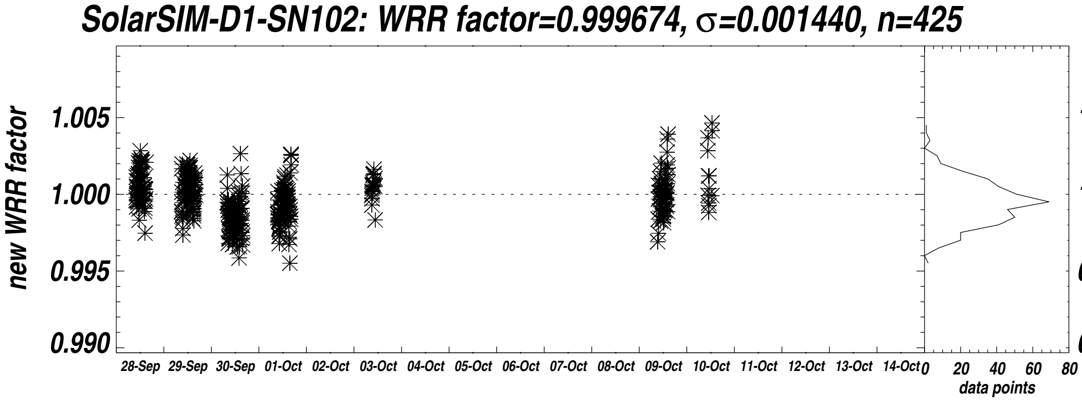
SolarSIM-D1-SN102: WRR factor=0.999674, σ=0.001440, n=425
new WRR factor
1.005
1.000
0.995
0.990
28-Sep 29-Sep 30-Sep 01-Oct 02-Oct 03-Oct 04-Oct 05-Oct 06-Oct 07-Oct 08-Oct 09-Oct 10-Oct 11-Oct 12-Oct 13-Oct 14-Oct
0 20 40 60 80
data points

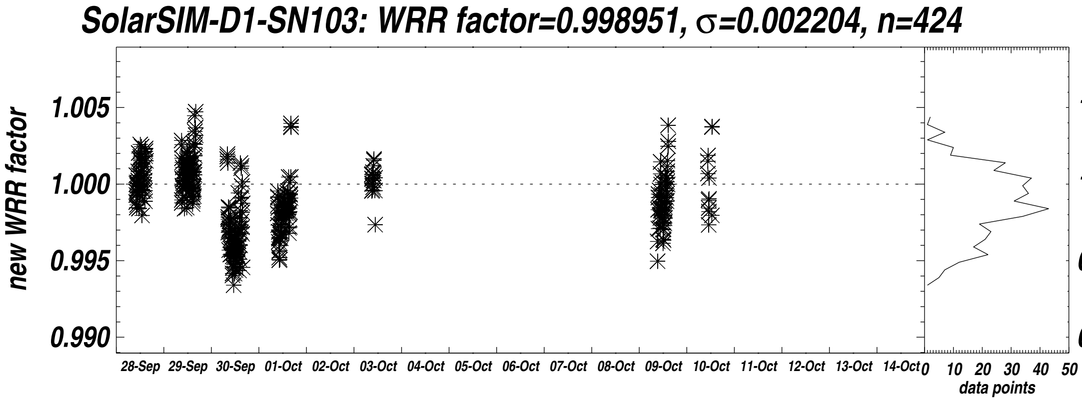
SolarSIM-D1-SN103: WRR factor=0.998951, σ=0.002204, n=424
new WRR factor
1.005
1.000
0.995
0.990
28-Sep 29-Sep 30-Sep 01-Oct 02-Oct 03-Oct 04-Oct 05-Oct 06-Oct 07-Oct 08-Oct 09-Oct 10-Oct 11-Oct 12-Oct 13-Oct 14-Oct
0 10 20 30 40 50
data points

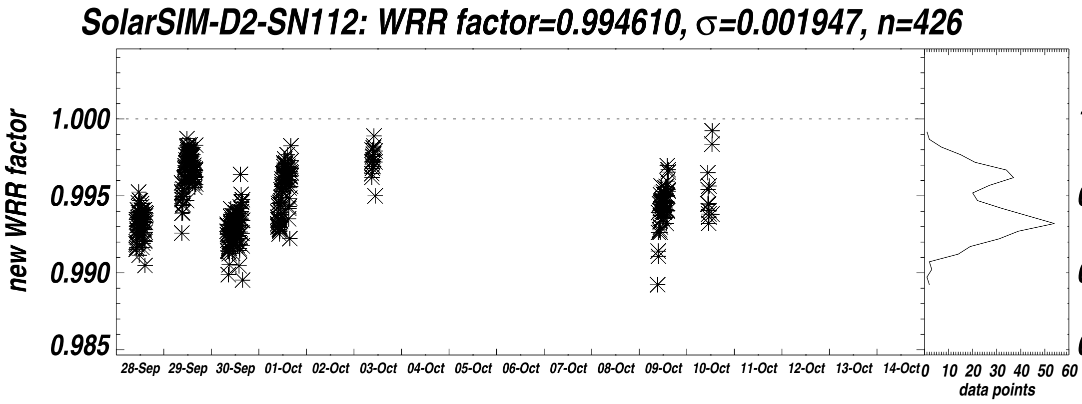
SolarSIM-D2-SN112: WRR factor=0.994610, σ=0.001947, n=426
new WRR factor
1.000
0.995
0.990
0.985
28-Sep 29-Sep 30-Sep 01-Oct 02-Oct 03-Oct 04-Oct 05-Oct 06-Oct 07-Oct 08-Oct 09-Oct 10-Oct 11-Oct 12-Oct 13-Oct 14-Oct
0 10 20 30 40 50 60
data points

SolarSIM-D2-SN113: WRR factor=0.999494, σ=0.002533, n=430

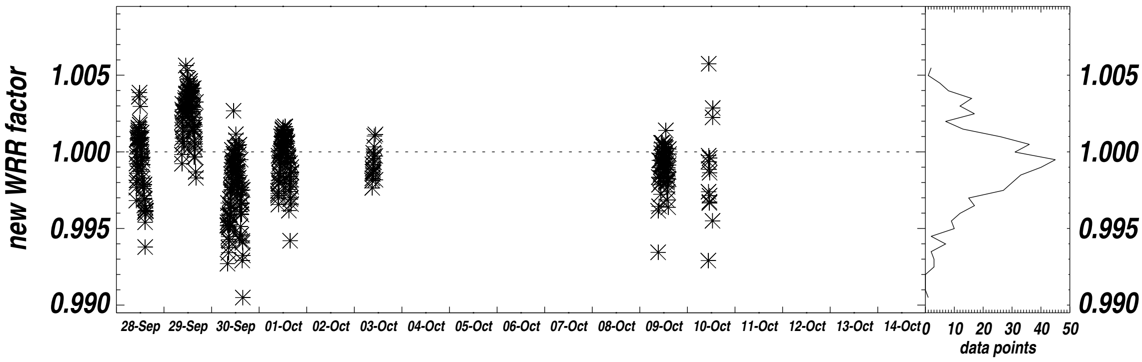

TMI67502: WRR factor=1.000999, σ=0.001104, n=487

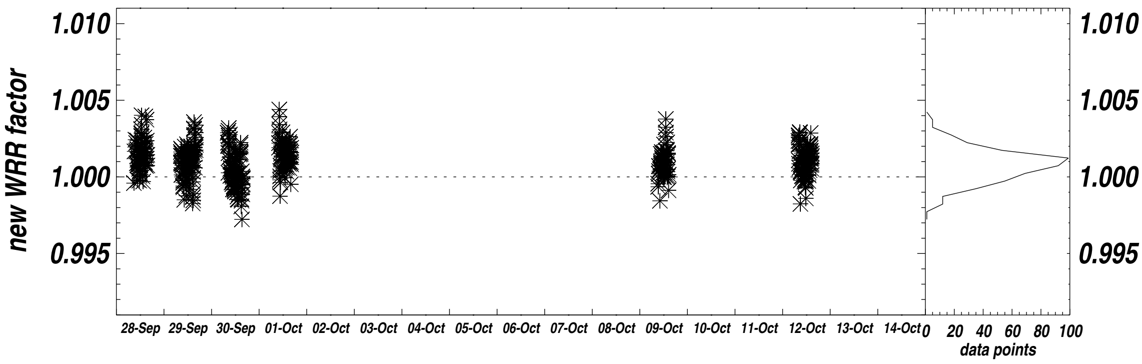

TMI67605: WRR factor=0.998546, σ=0.002138, n=116

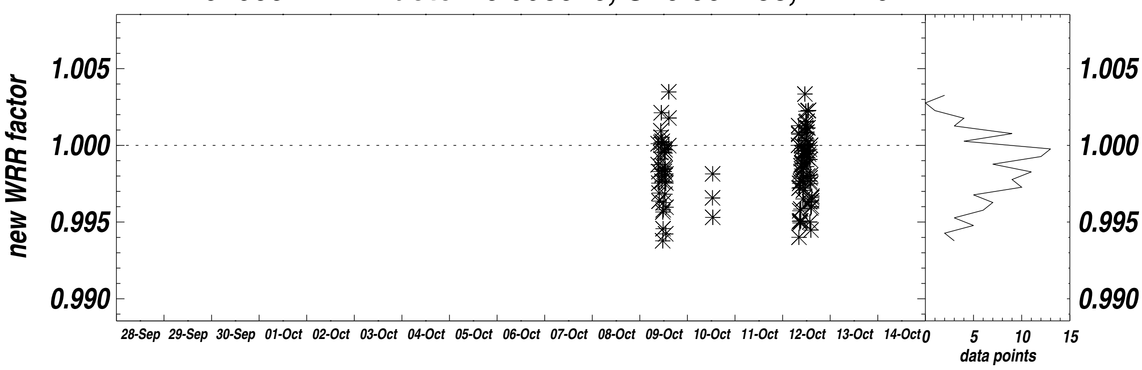

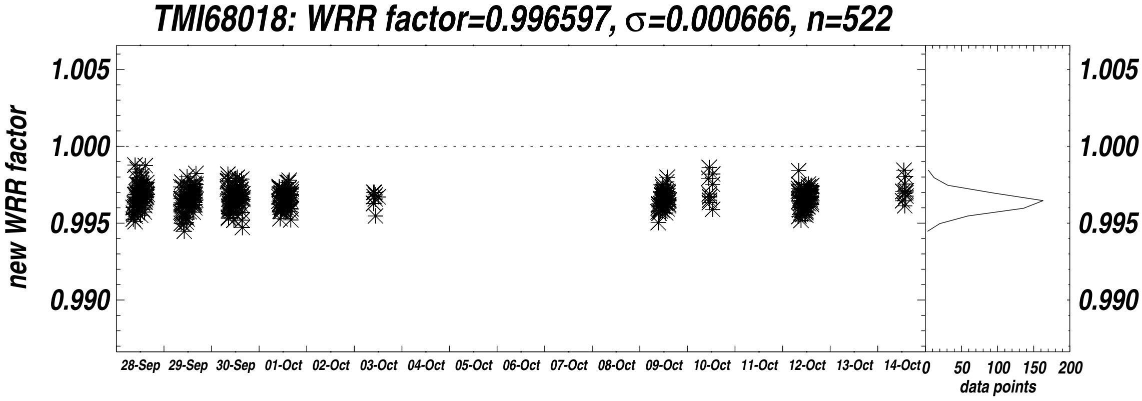
TMI68018: WRR factor=0.996597, σ=0.000666, n=522
new WRR factor
1.005
1.000
0.995
0.990
28-Sep 29-Sep 30-Sep 01-Oct 02-Oct 03-Oct 04-Oct 05-Oct 06-Oct 07-Oct 08-Oct 09-Oct 10-Oct 11-Oct 12-Oct 13-Oct 14-Oct
0 50 100 150 200
data points

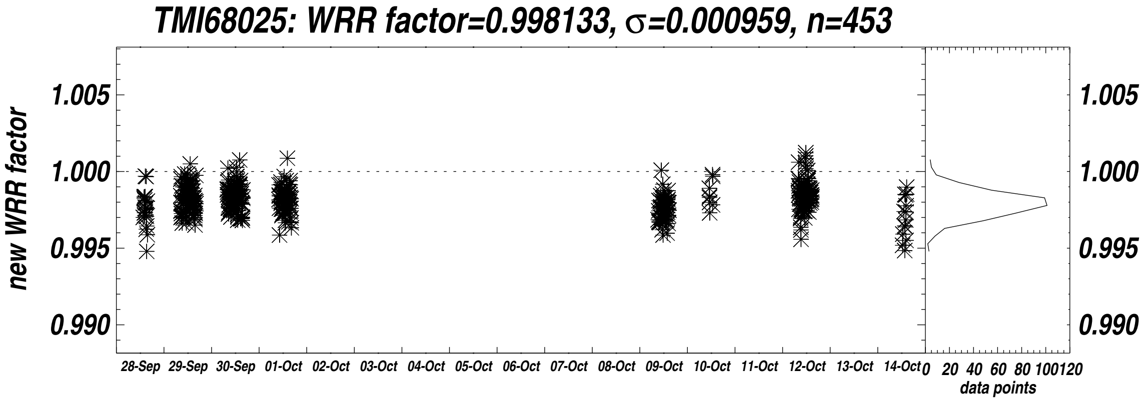
TMI68025: WRR factor=0.998133, σ=0.000959, n=453
new WRR factor
1.005
1.000
0.995
0.990
28-Sep 29-Sep 30-Sep 01-Oct 02-Oct 03-Oct 04-Oct 05-Oct 06-Oct 07-Oct 08-Oct 09-Oct 10-Oct 11-Oct 12-Oct 13-Oct 14-Oct
0 20 40 60 80 100120
data points

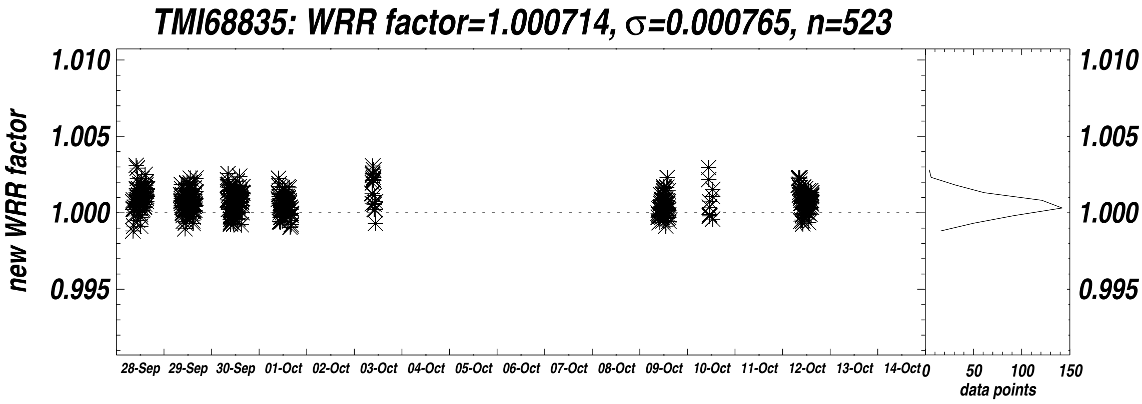
TMI68835: WRR factor=1.000714, σ=0.000765, n=523
new WRR factor
1.010
1.005
1.000
0.995
28-Sep 29-Sep 30-Sep 01-Oct 02-Oct 03-Oct 04-Oct 05-Oct 06-Oct 07-Oct 08-Oct 09-Oct 10-Oct 11-Oct 12-Oct 13-Oct 14-Oct
0 50 100 150
data points

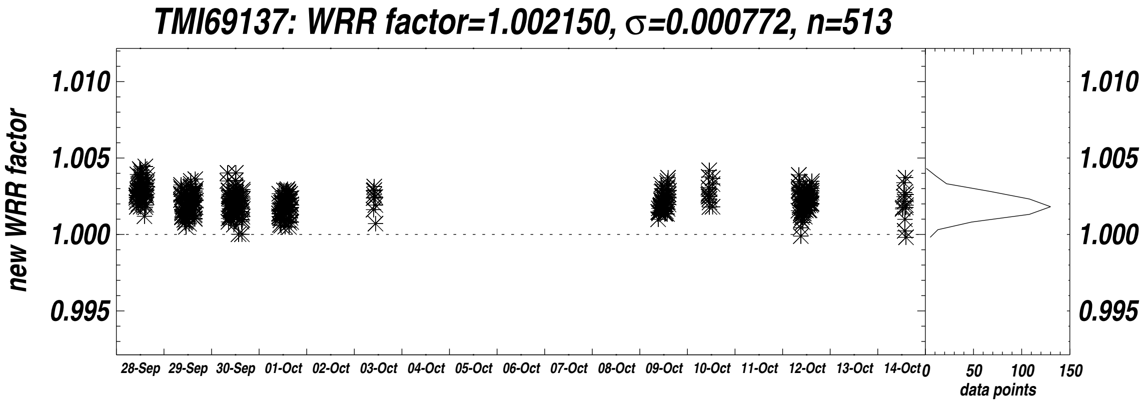
TMI69137: WRR factor=1.002150, σ=0.000772, n=513
new WRR factor
1.010
1.005
1.000
0.995
28-Sep 29-Sep 30-Sep 01-Oct 02-Oct 03-Oct 04-Oct 05-Oct 06-Oct 07-Oct 08-Oct 09-Oct 10-Oct 11-Oct 12-Oct 13-Oct 14-Oct
0 50 100 150
data points

Chapter 4 Auxiliary Data

4.1 Direct and Diffuse Irradiance

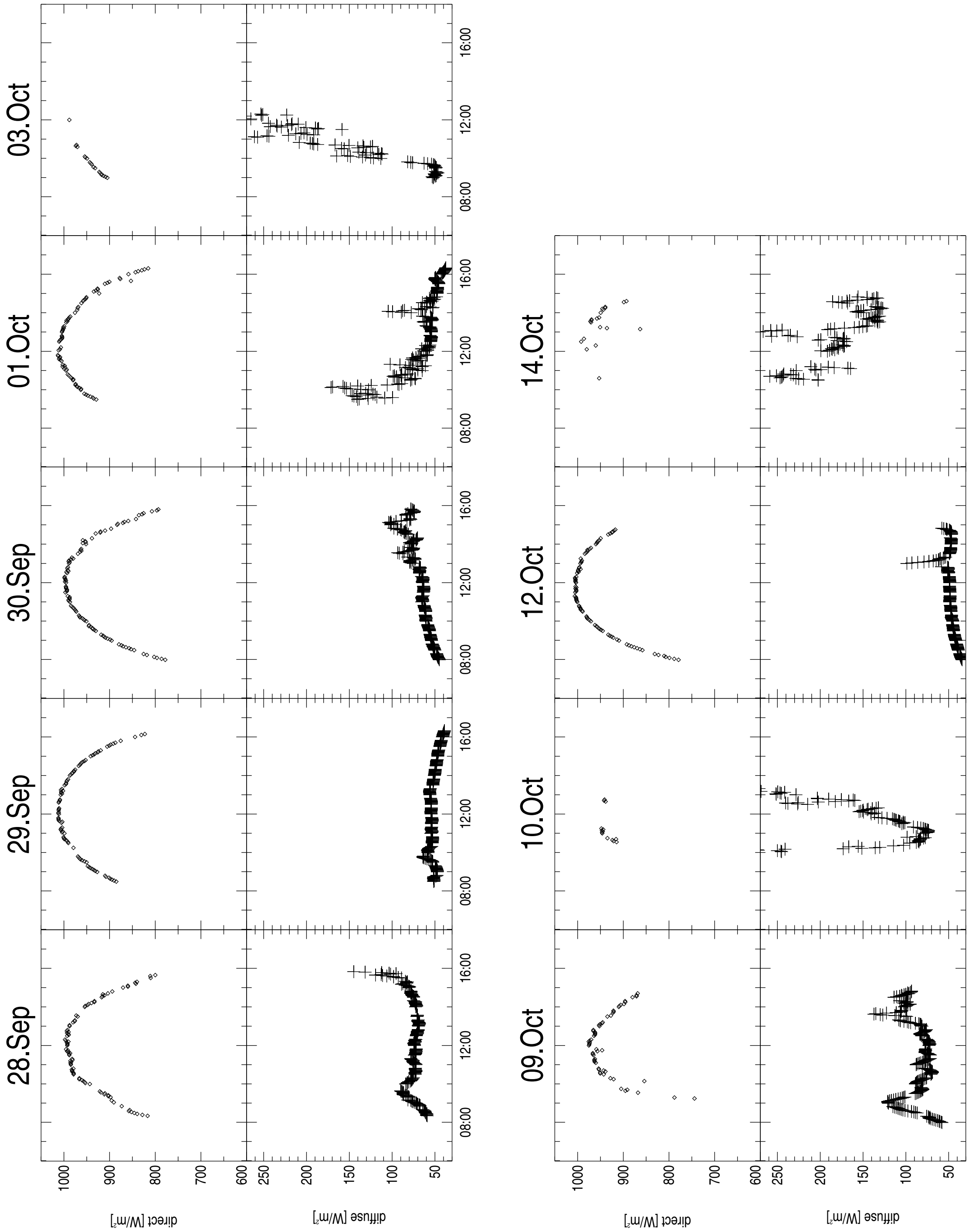

Direct (WRR) and diffuse irradiance (shaded K&Z CM22 S/N 020059).

4.2 Airmass and Aerosol Optical Depth (AOD)

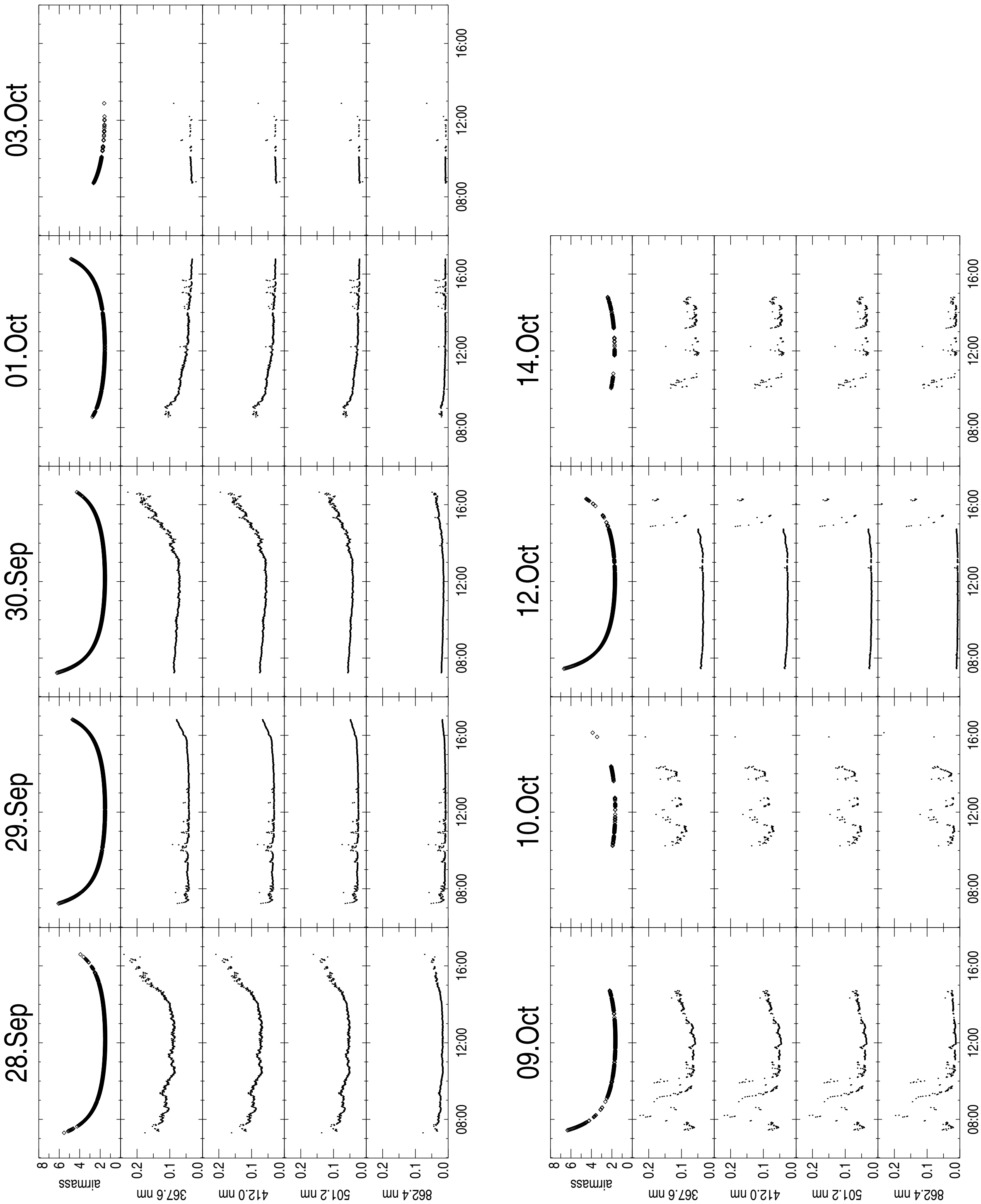

A four-channel Precision Filter Radiometer (PFR) was used to determine AOD.

4.3 Scattering Parameters

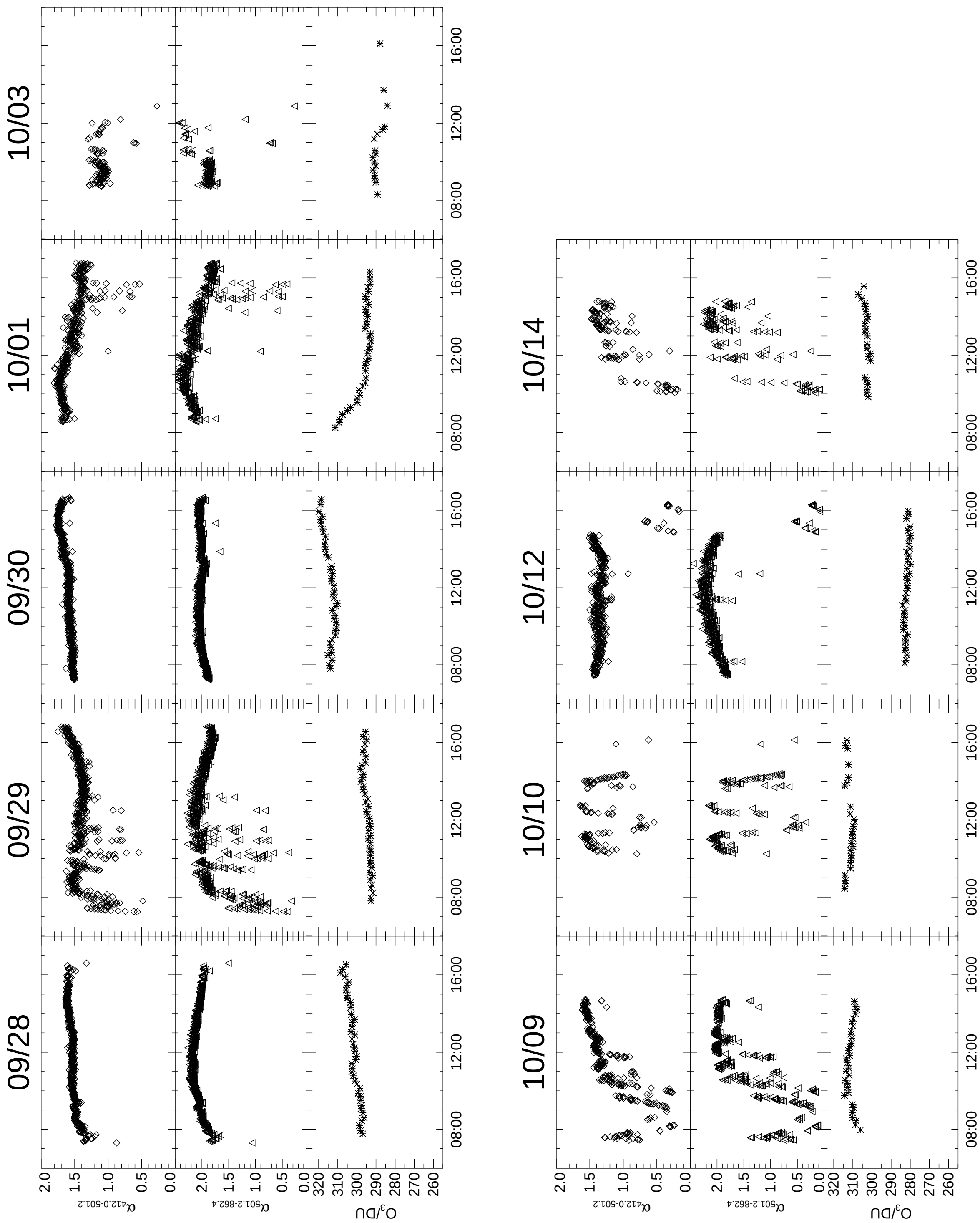

Ångström exponents (α) from PFR AOD data. Ozon (O_3) measured by the WRC Brewer #163.

4.4 Wind Speed

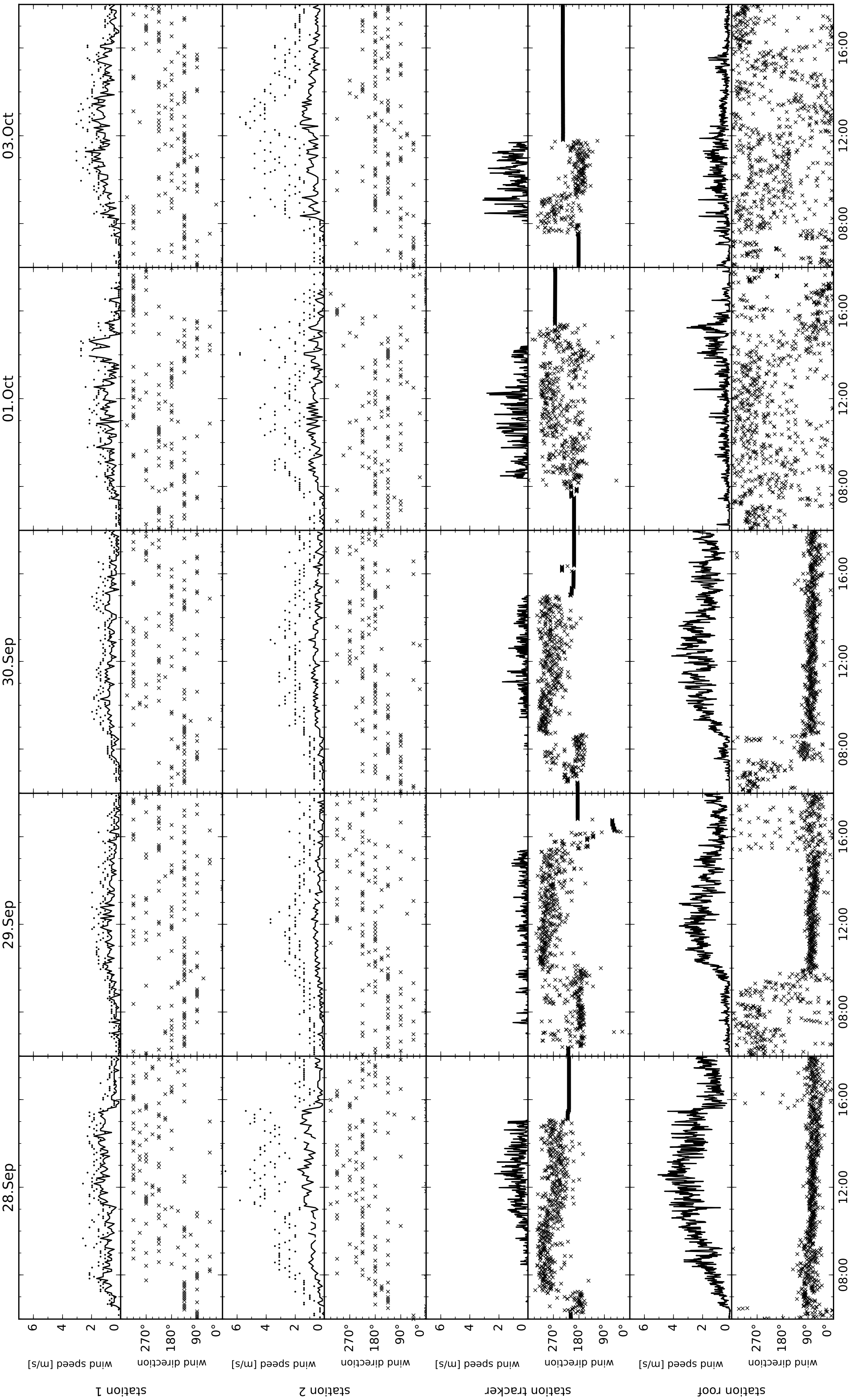

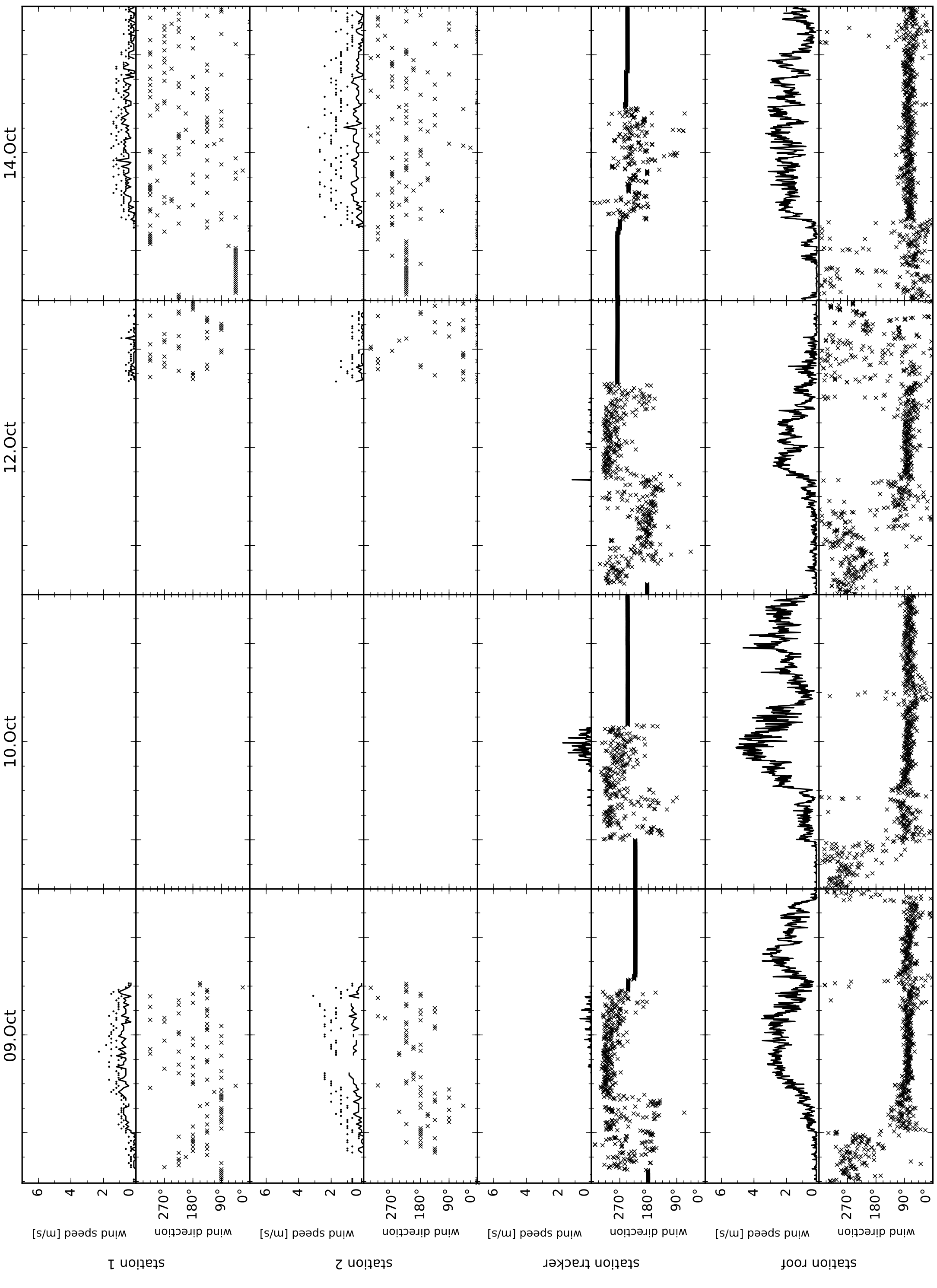

Wind speed and direction were measured near the southern (station 1) and northern (station 2) corners of the measurement field as well as by the WSG tracker and on the rooftop platform. The dots on the wind speed plots indicate gust velocity.

4.5 Meteorological Data

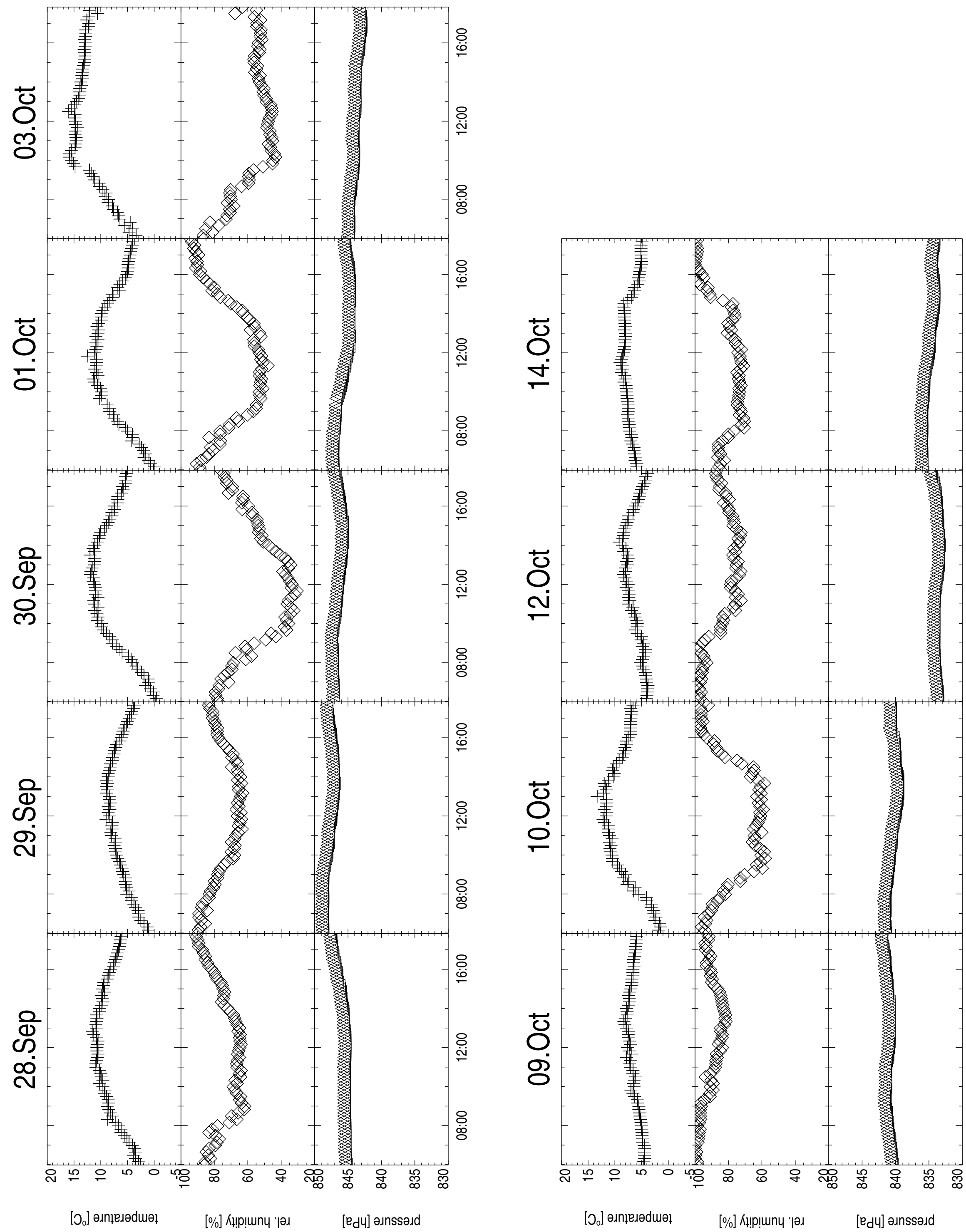

Meteorological parameters measured by the SwissMetNet Davos station of MeteoSwiss (adjacent to IPC-XII measuring field).

Chapter 5 Symposium

5.1 To Build and Share Knowledge

On cloudy, overcast, or rainy days when no measurements were possible the IPC-XII symposium was held. Radiation experts from PMOD/WRC as well as many IPC-XII participants presented their work and/or national radiation infrastructure in order to share and build knowledge. Manufacturers of radiation measurement equipment were given the opportunity to present their products.

Over the three weeks, more than 40 talks and presentations were given, most of which are available for download from the ftp site ftp://ftp.pmodwrc.ch/stealth/ipc-xii.

Chapter 6 Supplementary Information

6.1 Addresses of Participants

Anjit Anjan
INDIA METEOROLOGICAL DEPT
CentralL Radiation Lab ,Surface Instrument Division,IMD,Shivaji Nagar
411 005 Pune Maharashtra
India
phone: +91-20-25865425,25535411
email: anjit_anjan@yahoo.com

Naif Alsaheel
K.A.CARE
Akaria Plaza, Ulaya St., Riyadh 11451, Saudi Arabia
11451 Riyadh
Saudi Arabia
phone: 966543666963
email: n.saheel@energy.gov.sa

Afshin Andreas
NREL
15013 Denver West Blvd
Golden, Colorado 80401
USA
phone: 303-384-6383
email: afshin.andreas@nrel.gov

Alexander Baskis
Israel Meteorological Service
PoBox - 25
50250 Bet Dagan
ISRAEL
email: balex@ims.gov.il

Klaus Behrens
DWD Met. Obs. Lindenberg
Am Observatorium 12
D-15848 Tauche OT Lindenberg
Germany
phone: +49-69-8062-5860
email: klaus.behrens@dwd.de

Sumaman Buntoung
Silpakorn University
Department of Physics, Faculty of Science
73000 Nakhon Pathom
Thailand
email: s.buntoung@gmail.com

Akihito Akiyama
EKO Instruments Co.,Ltd.
1-21-8 Hatagaya, Shibuya-ku
151-0072 Tokyo
Japan
phone: +81-3-3469-6713
email: akiyama@eko.co.jp

Anne Andersson
SP Swedish Technical Research
Brinellgatan 4
50462 Borås
Sweden
phone: 46-105165403
email: anne.andersson@sp.se

Mike Baker
Met Office
Fitzroy Road
EX1 3PB Exeter Devon
United Kingdom
phone: 441392884034
email: mike.baker@metoffice.gov.uk

Ralf Becker
DWD Met. Obs. Lindenberg
Am Observatorium 12
D-15848 Tauche OT Lindenberg
Germany
phone: +49-69-8062-5867
email: ralf.becker@dwd.de

William Beuttell
EKO Instruments Co.,Ltd.
1-21-8 Hatagaya, Shibuya-ku
151-0072 Tokyo
Japan
phone: 14089777751
email: beuttell@eko-usa.com

Gerardo Carbajal Benítez
Servicio Meteorológico Nacion
Av. de los Constituyentes 3454
C1427BLS Ciudad Autónoma de Buenos Aires
Argentina
phone: + 54 11 5167 6767
email: gcarbajal@smn.gov.ar

Thomas Carlund
SMHI
Folkborgsvägen 1
60176 Norrköping
Sweden
email: thomas.carlund@pmodwrc.ch

André Chevalier
RMIB
3,Av.Circulaire
1180 Uccle B
Belgium
phone: 0032 2 373 0602
email: a.chevalier@oma.be

Pranomkorn Choosri
Silpakorn University
Department of Physics, Faculty of Science
73000 Nakhon Pathom
Thailand
phone: 6634270761
email: pranomkorn_aum@hotmail.com

Christian Conscience
RMIB
3,Av.Circulaire
1180 Uccle B
Belgium
phone: 0032 2 373 0729
email: cch@oma.be

Cristian Cortes
Fundacion Fraunhofer Chile Res
310 Av. Mariano Sanchez Fontecilla, of 1401
7550296 Santiago
Chile
email: cristian.cortes@fraunhofer.cl

Henri DIEMOZ
ARPA Valle d'Aosta
loc. Grande Charrière 44
11020 Saint-Christophe Aosta
Italy
phone: +39(0)165278576
email: h.diemoz@arpa.vda.it

THIERRY DUPRAT
METEO-FRANCE
785 CH DE L'HERMITAGE
84200 CARPENTRAS VAUCLUSE
FRANCE
phone: (33) 4 90 63 69 67
email: thierry.duprat@meteo.fr

Ana M. Díaz-Rodríguez
AEMET
c/Leonardo Prieto Castro, 8
28040 Madrid
Spain
phone: +34-915819625
email: adiazr@aemet.es

Frederick Denn
NASA Langley / SSAI
1 Enterprise parkway
Hampton, Virginia 23666
USA
phone: 757 951 1636/or 757 865 7518
email: frederick.m.denn@nasa.gov

Steven Dewitte
RMIB
3,Av.Circulaire
1180 Uccle B
Belgium
phone: 0032 2 373 0624
email: Steven.Dewitte@oma.be

Rodrigo Escobar
Fundacion Fraunhofer Chile Res
310 Av. Mariano Sanchez Fontecilla, of 1401
7550296 Santiago
Chile
email: rodrigo.escobar@fraunhofer.cl

Hector Estevez
Universidad Nacional Autonoma
Av Universidad 3000
4350 México DF
México
phone: +52(55)56224139
email: hectorh@geofisica.unam.mx

Bryan Fabbri
NASA Langley / SSAI
1 Enterprise parkway
Hampton, Virginia 23666
USA
phone: 757 951 1639
email: bryan.e.fabbri@nasa.gov

Wei Fang
Chinese Academy of Sciences
Dong Nanhu Road 3888, Changchun 130033, China
130033 Changchun
China
phone: 86-0431-86176883
email: fangw@ciomp.ac.cn

Bruce Forgan
Bureau of Meteorology
700 Collins St
3008 Docklands Vic
Australia
phone: +61 39669 4111
email: b.forgan@bom.gov.au

Dirk Friedrich
PTB
Bundesallee 100
38116 Braunschweig
Deutschland
phone: +49 531 592 4141
email: dirk.friedrich@ptb.de

Dmitrii Frolov
Voeikov MGO
7, Karbyshev st
194021 St-Petersburg -
Russia
phone: (812) 297-43-90
email: tveynkrolkrol@rambler.ru

Eric HOEKSEMA
Hukseflux Thermal Sensors
Delftechpark 31
2628XJ Delft The Netherlands
The Netherlands
phone: 31-15-2142669
email: eric@hukseflux.com

Emiel Hall
NOAA/ESRL/GMD
325 Broadway
Boulder, Colorado 80305
USA
phone: 303 497-4264
email: emiel.hall@noaa.gov

Guy Harrison-Roberts
Met Office
Fitzroy Road
EX1 3PB Exeter Devon
United Kingdom
phone: 441392885533
email: guy.harrison-roberts@metoffice.gov.uk

John Hickey
The Eppley Laboratory, Inc.
12 Sheffield Avenue
Newport, RI 2840
USA
email: johnh@eppleylab.com

Kees Hoogendijk
EKO Instruments Co.,Ltd.
1-21-8 Hatagaya, Shibuya-ku
151-0072 Tokyo
Japan
phone: 31703050117
email: kees.hoogendijk@eko-eu.com

Osamu Ijima
Japan Meteorological Agency
1-3-4 Otemachi, Chiyoda-ku
100-8122 Tokyo
Japan
phone: +81-29-851-2572
email: ijima@met.kishou.go.jp

Keiji Ishikawa
ISHIKAWA TRADING CO., LTD.
4-6-10, Shinkawa
181-0004 Mitaka-shi Tokyo
Japan
phone: 81-422-44-5501
email: k.ishikawa@ishikawa-sangyo.co.jp

Serm Janjai
Silpakorn University
Department of Physics, Faculty of Science
73000 Nakhon Pathom
Thailand
email: Serm.janjai@gmail.com

Somchit Janjai
Silpakorn University
Department of Physics, Faculty of Science
73000 Nakhon Pathom
Thailand

Joachim Jaus
Black Photon Instrument
Emmy-Noether-Str.
79110 Freiburg
Germany
phone: 497614791466
email: joachim.jaus@black-photon.de

Stefan Källberg
SP Swedish Technical Research
Brinellgatan 4
50462 Borås
Sweden
phone: 46-105165626
email: stefan.kallberg@sp.se

Wael Khaled
Egyptian Meteorological Auth.
Koubry El Quobba
P.O. Box 11784 Cairo
Egypt
phone: +2 01006072166
email: wael.khaled@ema.gov.eg

Tom Kirk
The Eppley Laboratory, Inc.
12 Sheffield Avenue
Newport, RI 2840
USA
phone: 14018471020
email: info@eppleylab.com

Wouter Knap
KNMI
Utrechtseweg 297
3731 GA De Bilt
The Netherlands
phone: ++31 30 2206 469
email: knap@knmi.nl

Mohamed Korany
Egyptian Meteorological Auth.
Koubry El Quobba
P.O. Box 11784 Cairo
Egypt
phone: +2 01010404566
email: m_korany2002@yahoo.com

Marc Korevaar
Kipp & Zonen
Delftechpark 36
2628XH Delft
The Netherlands
email: marc.korevaar@kippzonen.com

Ingo Kröger
PTB
Bundesallee 100
38116 Braunschweig
Deutschland
phone: +49 531 592 4147
email: ingo.kroeger@ptb.de

Ding Lei
CMA
Meteorological Observation Centre, China Meteorological Administration, No.46, Zhongguancun Nandajie, Haidian District, Beijing, China 100081
100081 Beijing
China
phone: 86-10-68406936
email: dlaoc@cma.gov.cn

Yang Luo
Chinese Academy of Sciences
Dong Nanhu Road 3888, Changchun 130033, China
130033 Changchun
China
email: nickclarck@163.com

DARIUS MIKALAJUNAS
Lithuanian Hydrometeorological
Rudnios str. 6
LT-09300 Vilnius
LITHUANIA
phone: 37064806329
email: darius.mikalajunas@meteo.lt

Brighton Mabasa
South African Weather Service
Private Bag X097
1 Pretoria Gauteng
South Africa
phone: +27 12 367 6088
email: Brighton.Mabasa@weathersa.co.za

Duncan Maciver
Atlas-DSET Laboratories
45601 N 47th Avenue
Phoenix, Arizona 85087
USA
phone: 623 201 1026
email: duncan.maciver@ametek.com

Martin Mair
ZAMG
Hohe Warte 38
1190 Vienna
Austria
phone: +43/1/36026-2706
email: martin.mair@zamg.ac.at

Kotaro Makino
ISHIKAWA TRADING CO., LTD.
4-6-10, Shinkawa
181-0004 Mitaka-shi Tokyo
Japan
phone: 81-422-44-5501
email: kmakino@ishikawa-sangyo.co.jp

Pierre Malcorps
RMIB
3,Av.Circulaire
1180 Uccle B
Belgium
phone: 0032 2 373 0604
email: Pierre.Malcorps@oma.be

Tiemo Mathijssen
KNMI
Utrechtseweg 297
3731 GA De Bilt
The Netherlands
email: tiemo.mathijssen@knmi.nl

Irene Melero-Asensio
AEMET
c/Leonardo Prieto Castro, 8
28040 Madrid
Spain
phone: +34-9158190259
email: imeleroa@aemet.es

Michael Milner
Bureau of Meteorology
700 Collins St
3008 Docklands Vic
Australia
phone: 61 39669 4122
email: m.milner@bom.gov.au

Svetlana Morozova
VNIIOFI
46, Ozernaya str
119361 Moscow
Russia
phone: (..7 495) 437 37 00
email: morozova-m4@vniiofi.ru

Erik Naranen
ISO-CAL North America, LLC
36610 N 20th Street
Phoenix, Arizona 85086
USA
phone: +1(480) 336-8133
email: enaranen@isocalnorthamerica.com

Donald Nelson
NOAA/ESRL/GMD
325 Broadway
Boulder, Colorado 80305
USA
phone: 303 775-0443
email: donald.w.nelson@noaa.gov

Kristjan Nurmela
Estonian Environment Agency
Toravere Station
EE-61602 Toravere Tartumaa
Estonia
phone: +372 5513389
email: kristjan.nurmela@envir.ee

Kazuhiko Ohkubo
ISHIKAWA TRADING CO., LTD.
4-6-10, Shinkawa
181-0004 Mitaka-shi Tokyo
Japan
phone: 81-422-44-5501
email: ohkubo@ishikawa-sangyo.co.jp

Marc Olefs
ZAMG
Hohe Warte 38
1190 Vienna
Austria
phone: +43/1/36026-2233
email: marc.olefs@zamg.ac.at

Juan R. Moreta-González
AEMET
c/Leonardo Prieto Castro, 8
28040 Madrid
Spain
phone: +34-915819773
email: jmoretag@aemet.es

Sophie Mulaudzi
GeoSUN Africa
Unit 1, CS Africa Building, 1 Meson Street, Techno Park
7600 Stellenbosch Western Cape
South Africa

Katlego Ncongwane
South African Weather Service
Private Bag X097
1 Pretoria Gauteng
South Africa
phone: +27 12 367 6010
email: Katlego.Ncongwane@weathersa.co.za

Lucky Ntsangwane
South African Weather Service
Private Bag X097
1 Pretoria Gauteng
South Africa
phone: +27 12 367 6239
email: Lucky.Ntsangwane@weathersa.co.za

Nozomu Ohkawara
Japan Meteorological Agency
1-3-4 Otemachi, Chiyoda-ku
100-8122 Tokyo
Japan
phone: +81-3-3212-8341
email: ohkawara@met.kishou.go.jp

Olatokunbo Okulaja
Nigerian Meteorological Agency
Bill Clinton Drive, Nnamdi Azikiwe International Airport
9001 Abuja FCT
NIGERIA
phone: +234 816 0964048
email: olatokunbo.okulaja@gmail.com

Yong-June PARK
korea Meteorologica administra
61 Yeouidaebang-ro 16-gil Dongjak-gu seoul 156-720
AsI/KR/KS013/seoul seoul
Korea
phone: +82-2-2181-0719
email: juni8207@korea.kr

Somjet Pattarapanitchai
Silpakorn University
Department of Physics, Faculty of Science
73000 Nakhon Pathom
Thailand

Alexander Pavlov
Voeikov MGO
7, Karbyshev st
194021 St-Petersburg -
Russia
phone: (812) 297-43-90
email: aleksandrvpavlov@gmail.com

Mariia Pavlovich
VNIIOFI
46, Ozernaya str
119361 Moscow
Russia
phone: (..7 495)437 29 92, 781 86 54
email: pavlovitch-m4@vniiofi.ru

Matthew Perry
Campbell Scientific, Inc.
815 W 1800 N
Logan, UT 94321
USA
phone: 435-227-9622
email: mperry@campbellsci.com

Alan Pino
Fundacion Fraunhofer Chile Res
310 Av. Mariano Sanchez Fontecilla, of 1401
7550296 Santiago
Chile
phone: 56223781660
email: alan.pino@fraunhofer.cl

Fabian Plag
PTB
Bundesallee 100
38116 Braunschweig
Deutschland
phone: +49 531 592 4148
email: fabian.plag@ptb.de

Jiri Pokorny
Czech Hydromet. Institute
Zamecek 456
500 08 Hradec Kralove
Czech Republic
phone: +420 495 279 263
email: jiri.pokorny@chmi.cz

Krunoslav Premec
DHMZ
Gric 3
HR-10000 Zagreb
Croatia
phone: +385 1 4565 607
email: krunoslav.premec@cirus.dhz.hr

Anna Pribullova
SHMI
ARC SHMI
058 01 Poprad-Ganovce
Slovakia
email: anna.pribullova@shmu.sk

Jin Qi
NSMC,CMA
No. 46, South Street of Zhong-Guan-Cun
100081 Beijing
China
email: qijin@cma.gov.cn

Karthik Ramanathan
NIWE
Velachery- Tambaram Main Road, Pallikaranai,
600100 Chennai Tamil Nadu
India
phone: 91-44-22463996
email: karthik.niwe@nic.in

Ibrahim Reda
NREL
15013 Denver West Blvd
Golden, Colorado 80401
USA
phone: 303-384-6385
email: ibrahim.reda@nrel.gov

David Riveros
Universidad Nacional Autonoma
Av Universidad 3000
4350 México DF
México
phone: +52(55)56224141
email: driveros@geofisica.unam.mx

Adrián Jorge Roldán
Universidad Nacional de Luján
Ruta 5 y Av.Constitución
6700 Luján Buenos Aires
Argentina
email: roldanadrian@gmail.com

Kazunori Shibayama
EKO Instruments Co.,Ltd.
1-21-8 Hatagaya, Shibuya-ku
151-0072 Tokyo
Japan

Hussain Shibli
K.A.CARE
Akaria Plaza, Ulaya St., Riyadh 11451, Saudi Arabia
11451 Riyadh
Saudi Arabia
phone: 966504697298
email: h.shibli@energy.gov.sa

Ajay Singh
Campbell Scientific, Inc.
815 W 1800 N
Logan, UT 94321
USA
phone: 435-227-9677
email: asingh@campbellsci.com

Patrick Smith
Atlas-DSET Laboratories
45601 N 47th Avenue
Phoenix, Arizona 85087
USA
phone: 623 465 7356 Ext 162
email: patrick.smith@ametek.com

Ilja Staupe
Kipp & Zonen
Delftechpark 36
2628XH Delft
The Netherlands
email: ilja.staupe@kippzonen.com

Jonathan Tamlyn
Met Office
Fitzroy Road
EX1 3PB Exeter Devon
United Kingdom
phone: 441392886289
email: jonathan.tamlyn@metoffice.gov.uk

Viktar Tatsiankou
COFOVO Energy
800 King Edward Avenue, Suite 3014
K1N 6N5 Ottawa ON
Canada
phone: 613 562 5800 x1032
email: viktar.tatsiankou@cofovo.com

Cristhian Timoté
Universidad Los Libertadores
Carrera 16 # 63A - 68
110821 Bogotá Cundinamarca
Colombie
email: timote13@gmail.com

Bill To
Black Photon Instrument
Emmy-Noether-Str.
79110 Freiburg
Germany
phone: 497614791466
email: bill.to@black-photon.de

Kees VAN DEN BOS
Hukseflux Thermal Sensors
Delftechpark 31
2628XJ Delft The Netherlands
The Netherlands
phone: 31-15-2142669
email: kees@hukseflux.com

Dorine VAN DER VLIES
Hukseflux Thermal Sensors
Delftechpark 31
2628XJ Delft The Netherlands
The Netherlands
phone: 31-15-2142669
email: dorine@hukseflux.com

Luis Valdés
Dirección Meteorológica Chile
Avenida Portales 3450
9170018 Santiago Estación Central
Chile
phone: (56)(2)24364560
email: lvaldes@meteochile.cl

Mauro Valdes
Universidad Nacional Autonoma
Av Universidad 3000
4350 México DF
México
phone: +52(55)56224139
email: mauro@geofisica.unam.mx

Yupeng Wang
Chinese Academy of Sciences
Dong Nanhu Road 3888, Changchun 130033, China
130033 Changchun
China
email: wangyp@ciomp.ac.cn

Hongrui Wang
Chinese Academy of Sciences
Dong Nanhu Road 3888, Changchun 130033, China
130033 Changchun
China
email: wanghongrui@ciomp.ac.cn

Sheng-Hsiang Wang
National Central University
No. 300, Zhongda Rd., Zhongli District
32001 Taoyuan City
Taiwan
phone: +886-972881003
email: shenghsiang.wang@gmail.com

Craig Webb
Argonne Natiotional Lab
109596 Coal Road
Billings, Oklahoma 74630
USA
phone: 001-331-318-3354
email: craigw@ops.sgp.arm.gov

Chong Wei
CMA
Meteorological Observation Centre, China Meteorological Administration, No.46, Zhongguancun Nandajie, Haidian District, Beijing, China 100081
100081 Beijing
China
phone: 86-10-68406936
email: chongwei@cma.gov.cn

Jim Wendell
NOAA/ESRL/GMD
325 Broadway
Boulder, Colorado 80305
USA
phone: 303 497-6994
email: jim.wendell@noaa.gov

Stefan Winter
PTB
Bundesallee 100
38116 Braunschweig
Deutschland
phone: +49 531 592 4140
email: stefan.winter@ptb.de

Yanqun Xue
ISHIKAWA TRADING CO., LTD.
4-6-10, Shinkawa
181-0004 Mitaka-shi Tokyo
Japan
email: yanqun.xue@ni.aist.go.jp

Yang Yun
CMA
Meteorological Observation Centre, China Meteorological Administration, No.46, Zhongguancun Nandajie, Haidian District, Beijing, China 100081
100081 Beijing
China
phone: 86-10-68408949
email: yyaoc@cma.gov.cn

Il-sung ZO
korea Meteorologica administra
61 Yeouidaebang-ro 16-gil Dongjak-gu seoul 156-720
AsI/KR/KS013/seoul seoul
Korea
phone: +82-33-640-2397
email: zoilsung@gwnu.ac.kr

Willem Zaaiman
European Commission - DG-JRC
Via Fermi, 2749
I-21028 Ispra Varese
Italy
phone: + 39 0332 785750
email: willem.zaaiman@jrc.ec.europa.eu

Ren Zhihua
CMA
Meteorological Observation Centre, China Meteorological Administration, No.46, Zhongguancun Nandajie, Haidian District, Beijing, China 100081
100081 Beijing
China
phone: 86-10-68406235
email: rzh@cma.gov.cn

Anro le Roux
GeoSUN Africa
Unit 1, CS Africa Building, 1 Meson Street, Techno Park
7600 Stellenbosch Western Cape
South Africa
phone: +27 21 250 0585
email: anro.leroux@geosun.co.za

Cor van Oort
KNMI
Utrechtseweg 297
3731 GA De Bilt
The Netherlands
phone: ++31 30 2206 417
email: oortvan@knmi.nl

Bart van der Meer
Hukseflux Thermal Sensors
Delftechpark 31
2628XJ Delft The Netherlands
The Netherlands
email: bart@hukseflux.com

Appendices

Appendix A Corrigendum

A.1 Tables

Table A.1: IPC-XII Participation: *Various Institutions and Manufacturers* (correction of Table 1.2)

Country	*Institution*	*Participant(s)*	*Instrument(s)*
Japan	AIST, Tsukuba	Yanqun Xue	

Table A.2: The new WRR factors for the participating instruments (correction of Table 2.2)

Instrument	C_1	C_2	R_n Ω	**WRR Factor**	σ ppm	*N*	*Country/ Owner*
NIP-35356E6	7.70			**1.011018**	2691	234	CIEMAT Spain

A.2 Addresses of Participants

Jose L. Balenzategui
CIEMAT
Avda. Complutense, 40
28040 Madrid
Spain
phone: +34 91 496 2509
email: jl.balenzategui@ciemat.es